

Prepared in cooperation with the Northeast Ohio Regional Sewer District

# Circulation, Mixing, and Transport in Nearshore Lake Erie in the Vicinity of Villa Angela Beach and Euclid Creek, Cleveland, Ohio, June 10–12, 2019, and August 19–21, 2019



Autonomous Underwater Vehicle

Scientific Investigations Report 2021–5122



**Front cover.** Autonomous Underwater Vehicle survey in Nearshore Lake Erie in the Vicinity of Villa Angela Beach and Euclid Creek, Cleveland, Ohio, on June 12, 2019. Photograph by Justin Boldt, U.S. Geological Survey.

**Back cover.** Mouth of Euclid Creek, June 12, 2019. Photograph by Justin Boldt, U.S. Geological Survey.



# **Circulation, Mixing, and Transport in Nearshore Lake Erie in the Vicinity of Villa Angela Beach and Euclid Creek, Cleveland, Ohio, June 10–12, 2019, and August 19–21, 2019**

By Justin A. Boldt and P. Ryan Jackson

Prepared in cooperation with the Northeast Ohio Regional Sewer District

Scientific Investigations Report 2021–5122

**U.S. Department of the Interior  
U.S. Geological Survey**



## U.S. Geological Survey, Reston, Virginia: 2022

For more information on the USGS—the Federal source for science about the Earth, its natural and living resources, natural hazards, and the environment—visit <https://www.usgs.gov> or call 1–888–ASK–USGS.

For an overview of USGS information products, including maps, imagery, and publications, visit <https://store.usgs.gov/>.

Any use of trade, firm, or product names is for descriptive purposes only and does not imply endorsement by the U.S. Government.

Although this information product, for the most part, is in the public domain, it also may contain copyrighted materials as noted in the text. Permission to reproduce copyrighted items must be secured from the copyright owner.

### Suggested citation:

Boldt, J.A., and Jackson, P.R., 2022, Circulation, mixing, and transport in nearshore Lake Erie in the vicinity of Villa Angela Beach and Euclid Creek, Cleveland, Ohio, June 10–12, 2019, and August 19–21, 2019:

U.S. Geological Survey Scientific Investigations Report 2021–5122, 78 p., <https://doi.org/10.3133/sir20215122>.

### Data associated with this report:

Boldt, J.A., 2021, Velocity surveys and three-dimensional point measurements of basic water-quality constituents in nearshore Lake Erie in the vicinity of Villa Angela Beach and Euclid Creek, Cleveland, Ohio, June 10–12, 2019, and August 19–21, 2019: U.S. Geological Survey data release, <https://doi.org/10.5066/P9630H6M>.

ISSN 2328-0328 (online)



## Acknowledgments

The authors acknowledge the Northeast Ohio Regional Sewer District for their continued support of these studies. The authors would like to thank Dennis Kumfer and Ed Puckett of the U.S. Geological Survey for their assistance in organizing and completing the field work, and Brandon Vonins of the U.S. Geological Survey for assistance in processing the acoustic Doppler velocity meter data.





## Contents

Acknowledgments .....	iii
Abstract .....	1
Introduction.....	1
Purpose and Scope .....	2
Description of the Study Area .....	2
Combined Sewer Overflows .....	2
Previous Work .....	5
Data Collection .....	5
Meteorological Data.....	5
Continuous Monitoring of Nearshore Currents .....	5
Synoptic Surveys .....	7
Description of the Autonomous Underwater Vehicle .....	7
Manned Boat Deployments .....	9
Data Processing.....	10
Meteorological Data.....	10
Acoustic Doppler Velocity Meter Data .....	10
Acoustic Doppler Current Profiler Data .....	10
Multiparameter Sonde Data .....	11
Autonomous Underwater Vehicle Data .....	11
Observations.....	11
Meteorological Data.....	11
Euclid Creek Inflow.....	16
Water within Wildwood Marina and the Easterly Wastewater Treatment Plant.....	16
Nearshore Circulation.....	19
Magnitude and Direction of Observed Currents near Villa Angela Beach, Cleveland, Ohio, for Summer 2019 .....	19
Longshore Currents .....	21
Using Specific Conductance in Combination with Velocity Mapping.....	40
Spatial Distribution of Water-Quality Constituents .....	48
Depth Profiles of Water-Quality Constituents .....	48
Water Density Distribution .....	48
Water Temperature Distribution.....	49
Specific Conductance Distribution.....	57
pH Distributions.....	65
Dissolved Oxygen Distributions.....	65
Turbidity Distributions .....	66
Summary.....	66
References Cited.....	68
Appendix 1. Supplemental Photographs .....	69



## Figures

1. Figure showing coastal Lake Erie in the vicinity of Villa Angela Beach and Euclid Creek, Cleveland, Ohio, April 2017 .....	3
2. Image showing an aerial of the shoreline in the vicinity of Villa Angela Beach showing the, <i>A</i> , before and, <i>B</i> , after the construction of the Euclid Beach Park pier .....	4
3. Figure showing the schematic of the autonomous underwater vehicle.....	8
4. Image showing manned boat and onboard equipment used in the coastal Lake Erie surveys .....	9
5. Graphs showing, <i>A</i> , Wind-direction and <i>B</i> , wind-speed characteristics observed at the Lakefront Nature Preserve, Cleveland, Ohio, for the period June 1–September 30, 2019 .....	12
6. Graph showing wind-rose diagram of the wind-direction and wind-speed characteristics observed at the Lakefront Nature Preserve, Cleveland, Ohio, for the period June 1–September 30, 2019 .....	13
7. Observations of <i>A</i> , wind speed, <i>B</i> , wind direction, and <i>C</i> , air temperature for June 10–12, 2019, at Lakeshore Nature Preserve, Cleveland, Ohio .....	14
8. Graphs showing observations of <i>A</i> , wind speed, <i>B</i> , wind direction, and <i>C</i> , air temperature for August 19–21, 2019, at Lakeshore Nature Preserve, Cleveland, Ohio, and <i>D</i> , daily rainfall for August 10–21, 2019, at the Northeast Ohio Regional Sewer District Easterly Wastewater Treatment Plant rain gauge.....	15
9. Graphs showing hydrographs of streamflow for <i>A</i> , June 6–16, 2019, and <i>B</i> , August 15–25, 2019.....	17
10. Graphs showing characteristics of nearshore currents measured by the acoustic Doppler velocity meter mounted to the northwest side of the southwest caisson in front of the Wildwood Marina near Villa Angela Beach .....	21
11. Graphs showing characteristics of nearshore currents measured by the acoustic Doppler velocity meter mounted to the southeast side of the northeast caisson in front of the Wildwood Marina near Villa Angela Beach.....	22
12. Graphs showing current-rose diagrams of the current direction and current speed characteristics measured by <i>A</i> , the acoustic Doppler velocity meter and <i>B</i> , the acoustic Doppler velocity meter.....	23
13. Graphs showing monthly characteristics of nearshore currents measured by <i>A</i> , the acoustic Doppler velocity meter and <i>B</i> , the acoustic Doppler velocity meter near Villa Angela Beach .....	25
14. Graph showing hourly characteristics of nearshore currents measured by <i>A</i> , the acoustic Doppler velocity meter and <i>B</i> , the acoustic Doppler velocity meter near Villa Angela Beach .....	26
15. Figure showing depth-averaged currents in coastal Lake Erie in the vicinity of Villa Angela Beach and Euclid Creek, Cleveland, Ohio, morning of June 10, 2019.....	27
16. Figure showing depth-averaged currents in coastal Lake Erie in the vicinity of Villa Angela Beach and Euclid Creek, Cleveland, Ohio, afternoon of June 10, 2019.....	28
17. Figure showing depth-averaged currents in coastal Lake Erie in the vicinity of the Easterly Wastewater Treatment Plant, Cleveland, Ohio, June 11, 2019.....	29
18. Figure showing depth-averaged currents in coastal Lake Erie in the vicinity of Villa Angela Beach and Euclid Creek, Cleveland, Ohio, morning of June 12, 2019.....	30
19. Figure showing depth-averaged currents in coastal Lake Erie in the vicinity of Villa Angela Beach and Euclid Creek, Cleveland, Ohio, afternoon of June 12, 2019.....	31

20.	Figure showing depth-averaged currents in coastal Lake Erie in the vicinity of Villa Angela Beach and Euclid Creek, Cleveland, Ohio, morning of August 19, 2019 .....	32
21.	Figure showing depth-averaged currents in coastal Lake Erie in the vicinity of Villa Angela Beach and Euclid Creek, Cleveland, Ohio, afternoon of August 19, 2019.....	33
22.	Figure showing depth-averaged currents in coastal Lake Erie in the vicinity of the Easterly Wastewater Treatment Plant, Cleveland, Ohio, morning of August 20, 2019.....	34
23.	Figure showing depth-averaged currents in coastal Lake Erie in the vicinity of the Easterly Wastewater Treatment Plant, Cleveland, Ohio, afternoon of August 20, 2019.....	35
24.	Figure showing depth-averaged currents in coastal Lake Erie in the vicinity of Villa Angela Beach and Euclid Creek, Cleveland, Ohio, morning of August 21, 2019 .....	36
25.	Figure showing depth-averaged currents in coastal Lake Erie in the vicinity of Villa Angela Beach and Euclid Creek, Cleveland, Ohio, later morning of August 21, 2019.....	37
26.	Figure showing depth-averaged currents in coastal Lake Erie in the vicinity of the Easterly Wastewater Treatment Plant, Cleveland, Ohio, afternoon of August 21, 2019.....	38
27.	Figure showing depth-averaged currents and distribution of near-surface specific conductance in coastal Lake Erie in the vicinity of Villa Angela Beach and Euclid Creek, Cleveland, Ohio, June 10, 2019 .....	41
28.	Figure showing depth-averaged currents and distribution of near-surface specific conductance in coastal Lake Erie in the vicinity of the Easterly Wastewater Treatment Plant, Cleveland, Ohio, June 11, 2019.....	42
29.	Figure showing depth-averaged currents and distribution of near-surface specific conductance in coastal Lake Erie in the vicinity of Villa Angela Beach and Euclid Creek, Cleveland, Ohio, June 12, 2019 .....	43
30.	Figure showing depth-averaged currents and distribution of near-surface specific conductance in coastal Lake Erie in the vicinity of Villa Angela Beach and Euclid Creek, Cleveland, Ohio, August 19, 2019 .....	44
31.	Figure showing depth-averaged currents and distribution of near-surface specific conductance in coastal Lake Erie in the vicinity of the Easterly Wastewater Treatment Plant, Cleveland, Ohio, August 20, 2019.....	45
32.	Figure showing depth-averaged currents and distribution of near-surface specific conductance in coastal Lake Erie in the vicinity of Villa Angela Beach and Euclid Creek, Cleveland, Ohio, August 21, 2019 .....	46
33.	Graphs showing depth profiles of water-quality constituents <i>A</i> , water density; <i>B</i> , water temperature; <i>C</i> , specific conductance; <i>D</i> , pH; and <i>E</i> , dissolved oxygen compiled from the autonomous underwater vehicle surveys of coastal Lake Erie in the vicinity of Villa Angela Beach, Euclid Creek, and the Easterly Wastewater Treatment Plant, Cleveland, Ohio.....	49
34.	Maps showing spatial distributions of near-surface basic water-quality constituents: <i>A</i> , water density; <i>B</i> , water temperature; <i>C</i> , specific conductance; <i>D</i> , pH; <i>E</i> , dissolved oxygen; and <i>F</i> , turbidity for coastal Lake Erie in the vicinity of Villa Angela Beach and Euclid Creek, Cleveland, Ohio, June 10, 2019 .....	50
35.	Maps showing spatial distributions of near-surface basic water-quality constituents: <i>A</i> , water density; <i>B</i> , water temperature; <i>C</i> , specific conductance; <i>D</i> , pH; <i>E</i> , dissolved oxygen; and <i>F</i> , turbidity for coastal Lake Erie in the vicinity of the Easterly Wastewater Treatment Plant, Cleveland, Ohio, June 11, 2019 .....	51



36.	Maps showing spatial distributions of near-surface basic water-quality constituents: <i>A</i> , water density; <i>B</i> , water temperature; <i>C</i> , specific conductance; <i>D</i> , pH; <i>E</i> , dissolved oxygen; and <i>F</i> , turbidity for coastal Lake Erie in the vicinity of Villa Angela Beach and Euclid Creek, Cleveland, Ohio, June 12, 2019 .....	52
37.	Maps showing spatial distributions of near-surface basic water-quality constituents: <i>A</i> , water density; <i>B</i> , water temperature; <i>C</i> , specific conductance; <i>D</i> , pH; <i>E</i> , dissolved oxygen; and <i>F</i> , turbidity for coastal Lake Erie in the vicinity of Villa Angela Beach and Euclid Creek, Cleveland, Ohio, August 19, 2019.....	53
38.	Maps showing spatial distributions of near-surface basic water-quality constituents: <i>A</i> , water density; <i>B</i> , water temperature; <i>C</i> , specific conductance; <i>D</i> , pH; <i>E</i> , dissolved oxygen; and <i>F</i> , turbidity for coastal Lake Erie in the vicinity of the Easterly Wastewater Treatment Plant, Cleveland, Ohio, August 20, 2019 .....	54
39.	Maps showing spatial distributions of near-surface basic water-quality constituents: <i>A</i> , water density; <i>B</i> , water temperature; <i>C</i> , specific conductance; <i>D</i> , pH; <i>E</i> , dissolved oxygen; and <i>F</i> , turbidity for coastal Lake Erie in the vicinity of Villa Angela Beach and Euclid Creek, Cleveland, Ohio, August 21, 2019.....	55
40.	Figures showing cross sections of basic water-quality constituents: <i>A</i> , water density; <i>B</i> , water temperature; <i>C</i> , specific conductance; <i>D</i> , pH; and <i>E</i> , dissolved oxygen for 18 sections of coastal Lake Erie in the vicinity of Villa Angela Beach and Euclid Creek, Cleveland, Ohio, June 10, 2019 .....	56
41.	Figures showing cross sections of basic water-quality constituents: <i>A</i> , water density; <i>B</i> , water temperature; <i>C</i> , specific conductance; <i>D</i> , pH; and <i>E</i> , dissolved oxygen for 21 sections of coastal Lake Erie in the vicinity of the Easterly Wastewater Treatment Plant, Cleveland, Ohio, June 11, 2019.....	58
42.	Figures showing cross sections of basic water-quality constituents: <i>A</i> , water density; <i>B</i> , water temperature; <i>C</i> , specific conductance; <i>D</i> , pH; and <i>E</i> , dissolved oxygen for 18 sections of coastal Lake Erie in the vicinity of Villa Angela Beach and Euclid Creek, Cleveland, Ohio, June 12, 2019 .....	60
43.	Figures showing cross sections of basic water-quality constituents: <i>A</i> , water density; <i>B</i> , water temperature; <i>C</i> , specific conductance; <i>D</i> , pH; and <i>E</i> , dissolved oxygen for 18 sections of coastal Lake Erie in the vicinity of Villa Angela Beach and Euclid Creek, Cleveland, Ohio, August 19, 2019 .....	61
44.	Figures showing cross sections of basic water-quality constituents: <i>A</i> , water density; <i>B</i> , water temperature; <i>C</i> , specific conductance; <i>D</i> , pH; and <i>E</i> , dissolved oxygen for 22 sections of coastal Lake Erie in the vicinity of the Easterly Wastewater Treatment Plant, Cleveland, Ohio, August 20, 2019.....	62
45.	Figures showing cross sections of basic water-quality constituents: <i>A</i> , water density; <i>B</i> , water temperature; <i>C</i> , specific conductance; <i>D</i> , pH; and <i>E</i> , dissolved oxygen for 7 sections of coastal Lake Erie in the vicinity of Villa Angela Beach and Euclid Creek, Cleveland, Ohio, August 21, 2019 .....	64

## Tables

1.	Combined sewer overflows near Villa Angela Beach, Cleveland, Ohio, June 1–12, 2019, and August 10–21, 2019 (data provided by the Northeast Ohio Regional Sewer District).....	6
2.	Manufacturer's specifications for the water-quality sensors aboard the autonomous underwater vehicle .....	8

3. Point measurements of water-quality characteristics in Euclid Creek, Wildwood Marina, and Easterly Wastewater Treatment Plant, Cleveland, Ohio, June 10–12, 2019, and August 19–21, 2019 .....	18
4. Summary of the acoustic Doppler velocity meter data collected during summer 2019 near Villa Angela Beach, Cleveland, Ohio .....	20
5. Prevalence of the orientation of the longshore current component of observed currents, sorted by bin, measured by the acoustic Doppler velocity meter and the acoustic Doppler velocity meter near Villa Angela Beach .....	24
6. Prevalence of the orientation of the longshore current component of observed currents, sorted by month, measured by the acoustic Doppler velocity meter and the acoustic Doppler velocity meter near Villa Angela Beach .....	24

## Conversion Factors

### U.S. customary units to International System of Units

Multiply	By	To obtain
Length		
inch (in.)	2.54	centimeter (cm)
inch (in.)	25.4	millimeter (mm)
foot (ft)	0.3048	meter (m)
mile (mi)	1.609	kilometer (km)
Area		
acre	4,047	square meter (m <sup>2</sup> )
square mile (mi <sup>2</sup> )	2.590	square kilometer (km <sup>2</sup> )
Volume		
million gallons (Mgal)	3,785	cubic meter (m <sup>3</sup> )
cubic foot (ft <sup>3</sup> )	0.02832	cubic meter (m <sup>3</sup> )
Flow rate		
cubic foot per second (ft <sup>3</sup> /s)	0.02832	cubic meter per second (m <sup>3</sup> /s)
million gallons per day (Mgal/d)	0.04381	cubic meter per second (m <sup>3</sup> /s)
Velocity		
foot per second (ft/s)	0.3048	meter per second (m/s)
knots	0.51444	meter per second (m/s)
mile per hour (mi/h)	1.609	kilometer per hour (km/h)
Mass		
pound, avoirdupois (lb)	0.4536	kilogram (kg)
Density		
pound per cubic foot (lb/ft <sup>3</sup> )	16.02	kilogram per cubic meter per second (kg/m <sup>3</sup> )

Temperature in degrees Celsius (°C) may be converted to degrees Fahrenheit (°F) as follows:

$$^{\circ}\text{F} = (1.8 \times ^{\circ}\text{C}) + 32.$$

## Datum

Vertical coordinate information is referenced to the North American Vertical Datum of 1988 (NAVD 88).

Horizontal coordinate information is referenced to the North American Datum of 1983 (NAD 83).

## Supplemental Information

Specific conductance is given in millisiemens per centimeter at 25 degrees Celsius (mS/cm).

Concentrations of chemical constituents in water are given in milligrams per liter (mg/L).

## Abbreviations

ADCP	acoustic Doppler current profiler
ADVM	acoustic Doppler velocity meter
AUV	autonomous underwater vehicle
CSO	combined sewer overflow
<i>E. coli</i>	<i>Escherichia coli</i>
GPS	global positioning system
NEORS	Northeast Ohio Regional Sewer District
NOAA	National Oceanic and Atmospheric Administration
USGS	U.S. Geological Survey
VMT	Velocity Mapping Toolbox
WWTP	wastewater treatment plant



# Circulation, Mixing, and Transport in Nearshore Lake Erie in the Vicinity of Villa Angela Beach and Euclid Creek, Cleveland, Ohio, June 10–12, 2019, and August 19–21, 2019

By Justin A. Boldt and P. Ryan Jackson

## Abstract

Villa Angela Beach, on the Lake Erie lakeshore near Cleveland, Ohio, is just west of the mouth of Euclid Creek, a small, flashy stream that drains approximately 23 square miles and is susceptible to periodic contamination from combined sewer overflows (CSOs; 190 and 189 events in 2018 and 2019, respectively). Concerns about high concentrations of *Escherichia coli* (*E. coli*) in water samples collected along this beach and subsequent frequent beach closures led to the collection of water-quality and water-velocity data in the nearshore area to gain insights into nearshore mixing processes, circulation, and the potential for transport of bacteria and other CSO-related contaminants from nearby sources to the beach. Synoptic surveys were completed by the U.S. Geological Survey on June 10–12, 2019, and August 19–21, 2019, to observe conditions during early and late periods of the summer season. This study follows several studies in this area. Data-collection methods for this study included deployment of an autonomous underwater vehicle and use of a manned boat equipped with an acoustic Doppler current profiler and a multiparameter sonde. Spatial distributions of water-quality constituents and nearshore currents indicated that the mixing zone near the mouth of Euclid Creek and Villa Angela Beach is dynamic and highly variable in spatial extent. Similar observations around the Easterly Wastewater Treatment Plant 1.5 miles to the southwest of Villa Angela Beach indicated a mixing zone that was likewise dynamic and highly variable in spatial extent. Observed circulation patterns during synoptic surveys in summer 2019 indicated that contaminants from CSOs in Euclid Creek and at CSO discharge points along the Lake Erie lakefront (as traced using specific conductance as a surrogate) tended to be transported differently depending on the magnitude and direction of winds and longshore currents. The southwesterly longshore current that was responsible for driving a recirculation pattern along the beach during a previous study in summer 2012 was not observed during the summer 2019 synoptic surveys. That was not surprising because continuous velocity data collected

near Villa Angela Beach indicated that longshore currents with a northeasterly component occurred most (65 percent) of the time from June 12 to August 28, 2019.

## Introduction

The Ohio Department of Health monitors beaches along the Lake Erie shoreline for *Escherichia coli* (*E. coli*) bacteria. *E. coli* is a member of the fecal coliform group, and its concentration is commonly used as an indicator of potential exposure to pathogens from fecal sources. Villa Angela Beach, a bathing beach in northeast Ohio on the southern shore of Lake Erie, is one of the monitored beaches. Water samples at Villa Angela Beach are collected daily during the summer recreational season (typically the last week in May through September) by a local cooperator—the Northeast Ohio Regional Sewer District (NEORS D). Elevated *E. coli* concentrations occur frequently in water samples collected at Villa Angela Beach, which was on advisory 41 percent of the 2019 recreational season (Jenifer Hassinger, Ohio Department of Health, written commun., March 10, 2021). When the sample results are greater than the recreational standard of 235 colony forming units, an advisory is posted to warn swimmers of the risk of illness associated with water contact. The sampling results for current and prior years are publicly available through the Ohio Department of Health Bathing Beach Monitoring website, specifically their BeachGuard system (Ohio Department of Health, 2021). The data indicate that Villa Angela Beach has been on advisory a consistently large part of each summer recreational season (average of about 40 percent from 2008 to 2019, Ohio Department of Health, 2021). A microbial source-tracking study at Villa Angela Beach during the 2007 recreational season indicated humans and gulls as the sources of the *E. coli* (Bushon and others, 2009).

To better understand potential sources and transport of *E. coli* and other bacteria near the beach, the NEORS D requires information on flow patterns in Lake Erie near the

beach under a variety of conditions. Numerous previous studies and monitoring efforts have been completed (Bushon and others, 2009; Jackson, 2013). The objective of this study was to collect a new set of data to see whether conditions documented by the U.S. Geological Survey (USGS) during a September 2012 study (Jackson, 2013) are representative of 2019 conditions. With multiple potential sources of contaminants surrounding Villa Angela Beach—including Euclid Creek, lakefront combined sewer overflow (CSO) discharge points, and the NEORSD Easterly Wastewater Treatment Plant (WWTP)—understanding the circulation, mixing, and transport in the nearshore in the vicinity of Villa Angela Beach is important for making management decisions that can improve beach health.

## Purpose and Scope

The purpose of this report is to present the results of synoptic surveys completed during summer 2019 in nearshore Lake Erie in the vicinity of Euclid Creek and Villa Angela Beach and to characterize circulation, mixing, and transport patterns in this area. This study is a followup to a similar study completed in 2012 (as described later in the “Previous Work” section) and incorporates an extension of the survey area 1.5 miles (mi) to the southwest to include the area around the Easterly WWTP. Quantification of bacterial concentrations was not done as in some previous studies. Instead, this study focused on examining pathways for contaminant transport between potential human sources in the area and Villa Angela Beach. Potential human sources in this study are limited to Euclid Creek, the lakefront CSO discharge points surrounding Villa Angela Beach, and the Easterly WWTP. Recognizing that a synoptic survey represents only one instance in time and circulation patterns change, the results of the synoptic surveys were compared to earlier synoptic surveys and to continuous current and wind data measured near Villa Angela Beach during summer 2019.

## Description of the Study Area

Villa Angela Beach, on the Lake Erie lakeshore, is 8.8 mi northeast of Cleveland, Ohio, adjacent to the mouth of Euclid Creek. Euclid Creek is a small, flashy stream that drains approximately 23 square miles and is susceptible to periodic contamination from CSOs (fig. 1A). The shoreline in the study reach is oriented southwest to northeast. The beach is partially protected by 6 breakwaters approximately 200 feet (ft) offshore and oriented parallel to the beach. These breakwaters reduce the open water connection to the lake to approximately 44 percent of its original, unaltered state (Jackson, 2013). The part of the beach behind the western-most two breakwaters is called Euclid Beach by locals. For simplicity, we will not make this distinction in this report and instead use the term “Villa Angela Beach” to refer to the entire reach protected by the breakwaters (fig. 1B).

A monitored CSO discharge point (fig. 1B, point 239) is on Euclid Creek (right bank) at Lakeshore Boulevard about 3,800 ft upstream from the mouth. Two other unmonitored CSO discharge points (points 209 and 210) are also on Euclid Creek. CSO point 209 is on the left bank across from CSO point 239 (fig. 1B). CSO point 210 is on Euclid Creek (left bank) at St. Clair Avenue about 9,100 ft upstream from the mouth (not shown). In addition, three other CSO discharge points are along the lakefront within 1,600 ft of the beach (two to the southwest [fig. 1B, points 206 and 207] and one to the northeast [fig. 1B, point 208]). The Easterly WWTP, which can treat as much as 400 million gallons per day (Mgal/d) of wastewater and had an average daily flow of 86 Mgal/d in 2018 and 89 Mgal/d in 2019, is approximately 1.5 mi to the southwest of Villa Angela Beach along with two more CSO discharge points (fig. 1B, points 242 and 002). Lake Erie is the effluent discharge point for the Easterly WWTP.

The mouth of Euclid Creek is bordered by Villa Angela Beach to the southwest and Wildwood Marina to the northeast. A short jetty (pier) separates the mouth of the creek from the beach and extends just beyond the breakwaters (about 250 ft offshore) protecting the beach. Wildwood Marina, to the northeast of the mouth of Euclid Creek, is protected by a sea wall (pier) and two large caissons near the harbor entrance (fig. 1C). The marina sea wall and harbor entrance protection protrude out into the lake approximately 800 ft from the natural shoreline. The caissons protecting the entrance to Wildwood Marina served as platforms for instrumentation for continuous monitoring of nearshore currents using acoustic Doppler velocity meters (ADVM) operated by the USGS and a meteorological station operated by the NEORSD.

The shoreline at the southwest end of Villa Angela Beach was altered beginning in 2018 and ending in May 2019 (fig. 2). Previously, the shoreline extended out ending in a rocky point with approximately a 50 ft gap between the rocky point and the final (southwest-most) breakwater. In summer 2018, the rocky point was removed, the shoreline was moved back inland, and a pier was constructed extending westward out into the lake with the end of the pier in line with the breakwaters. There is about a 90 ft gap between the end of the pier and the final breakwater and also a small gap between the end of the pier structure and the shoreline. Water can pass through both gaps into the protected area between the breakwaters and Villa Angela Beach.

## Combined Sewer Overflows

Villa Angela Beach, near Cleveland, Ohio, is surrounded by six CSO discharge points, three on the lakefront (206, 207, 208) and three on Euclid Creek (239, 209, 210; 210 not shown) upstream from the mouth (fig. 1B). Two additional CSO discharge points (242, 002) are at the Easterly WWTP to the southwest of Villa Angela Beach (fig. 1B). All of these discharge points are managed by the NEORSD. To aid in the interpretation of the synoptic data presented in this report,



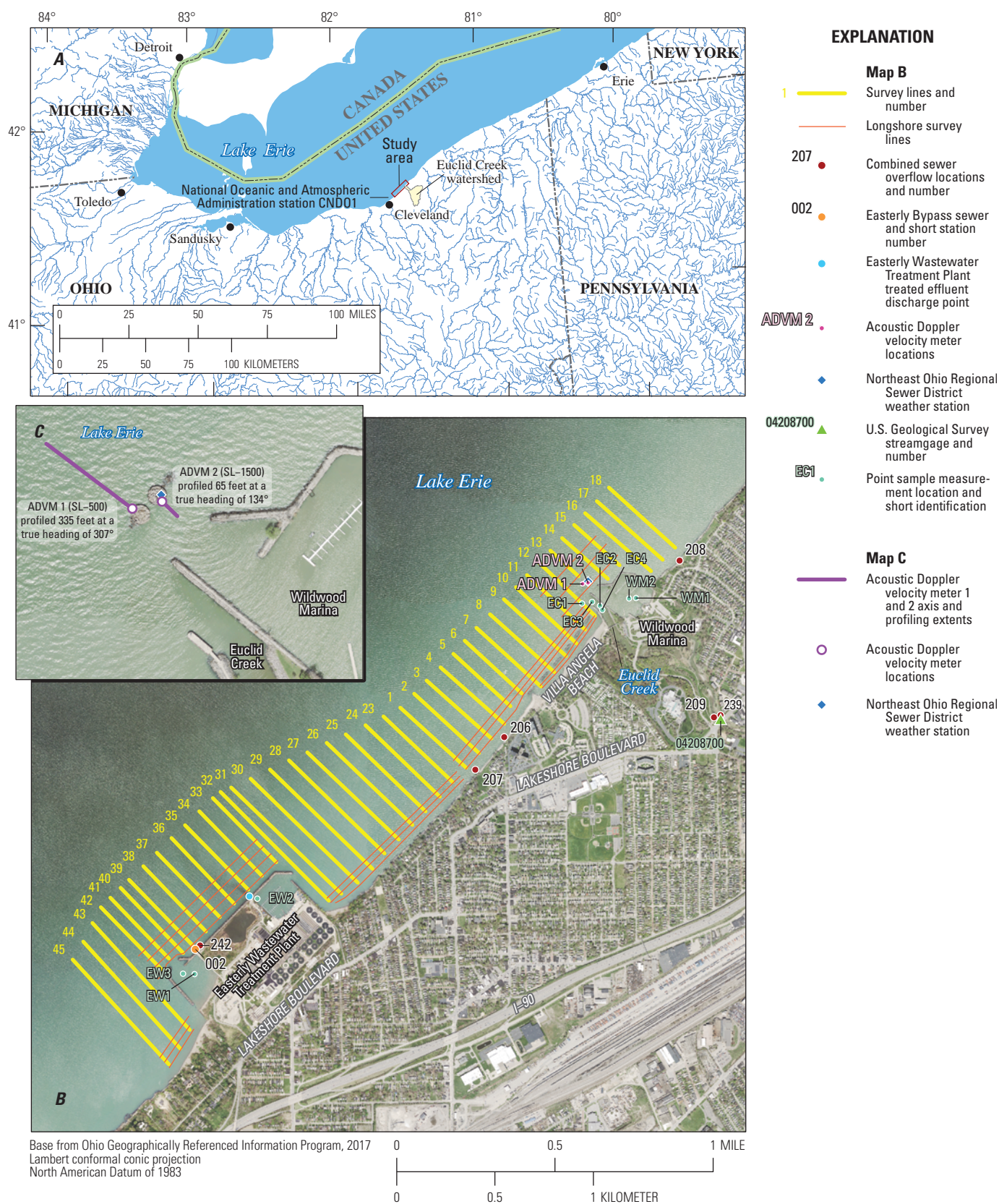


**Figure 1.** Coastal Lake Erie in the vicinity of Villa Angela Beach and Euclid Creek, Cleveland, Ohio, April 2017. *A*, Overview of the study area and Euclid Creek drainage basin. *B*, Survey domain with designated survey lines and combined sewer overflow permitted discharge points. *C*, Inset of acoustic Doppler velocity meter (ADVM) locations and measurement profiling extent.



#### 4 Circulation, Mixing, and Transport in Nearshore Lake Erie



Base map data from Google, 2021

#### EXPLANATION

— Modified shoreline area

**Figure 2.** Aerial imagery of the shoreline in the vicinity of Villa Angela Beach showing the, *A*, before (2017) and, *B*, after (2019) the construction of the Euclid Beach Park pier.



the NEORSRD provided the USGS with CSO discharges to Euclid Creek and Lake Erie for 2018–19 and for all the monitored and modelled outfalls for the 9-day period leading up to and including the synoptic surveys in summer 2019 (table 1)

Euclid Creek and the lakefront surrounding Villa Angela Beach are subject to a large number of CSO events throughout the year. Euclid Creek received approximately 213 million gallons (Mgal) of CSO in 2018 and 107 Mgal of CSO in 2019 (totals based on CSO points 239, 209, and 210), which is broadly similar to the Euclid Creek CSO volumes in 2010 and 2011 (Jackson, 2013). The Lake Erie lakefront around Villa Angela Beach received approximately 156 Mgal of CSO in 2018 and 58 Mgal of CSO in 2019 (totals based on CSO points 206, 207, and 208). The Lake Erie lakefront around the Easterly WWTP received approximately 1,488 Mgal of CSO in 2018 and 463 Mgal of CSO in 2019 (totals based on CSO point 242 and Easterly Bypass 002).

The Easterly Bypass is technically not a CSO, but it is still a potential source of contamination to Lake Erie. Three interceptors enter the Easterly WWTP from the collection system and split into nine channels. All nine channels have bar screens to remove rags, sticks, and other large solids from the flow as it enters the plant. Flows from the collection system into the plant more than 400 Mgal/d will overflow over top of these nine channels directly to Lake Erie via the Easterly Bypass (which used to be called CSO-001). The overflow typically happens downstream from the bar screens so the overflows are screened. There are occasions where the overflow can happen upstream from the bar screens and the overflow is unscreened (Scott Broski, NEORSRD, written commun., February 5, 2021).

In the 9 days before and including the June 2019 synoptic survey, Euclid Creek received 3 CSO events totaling approximately 7.95 Mgal of CSO (table 1). In addition, Lake Erie received approximately 2.61 Mgal of CSO from point 206 and approximately 2.52 Mgal of CSO from point 242. In the 9 days before and including the August 2019 synoptic survey, Euclid Creek received 3 CSO events totaling approximately 4.90 Mgal of CSO (table 1). In addition, Lake Erie received approximately 0.94 Mgal of CSO from point 206 and approximately 0.93 Mgal of CSO from point 242.

## Previous Work

The USGS completed an initial study in 2007 to measure and map nearshore currents in the vicinity of Villa Angela Beach. A second effort to map the nearshore circulation and mixing off Villa Angela Beach was completed in late August 2011 by the USGS in cooperation with the NEORSRD. The previous work in 2007 and 2011 are summarized in Jackson (2013).

A third study (Jackson, 2013) was completed by the USGS on September 11–12, 2012, after a high-flow event and a CSO discharge in Euclid Creek. Spatial distributions of specific conductance, water temperature, and nearshore currents

indicated that the mixing zone in the vicinity of Euclid Creek and Villa Angela Beach was dynamic and highly variable spatially and temporally. The study noted that currents were decoupled from local wind forcing, which was different from the observations from the 2011 study. The 2012 study also determined that the high specific conductance of Euclid Creek water relative to Lake Erie water provided an excellent tracer that could be used to visualize the transport and fate of Euclid Creek water in the nearshore environment. Finally, the study noted that circulation patterns indicate that Euclid Creek water and water discharged from nearby CSO discharge points along the shoreline, and the bacteria therein, may be mixing along Villa Angela Beach by interaction of nearshore currents and shoreline structures.

## Data Collection

This section describes the methods and instrumentation used to collect the meteorological data, continuous observations of nearshore currents, water-velocity data, and water-quality data in the vicinity of Villa Angela Beach, Euclid Creek, and the Easterly WWTP.

### Meteorological Data

Local meteorological data are collected during the summer months at the NEORSRD weather station mounted on the northern caisson at the entrance to Wildwood Marina (fig. 1B). The NEORSRD began operation of a meteorological station at the Wildwood Marina near Villa Angela Beach in May 2019. The NEORSRD provided 15-minute interval data for the period of record (May 31 to October 23, 2019) to the USGS for analysis of dominant wind characteristics; however, because of a technical problem, the wind-speed data were not usable. Consequently, meteorological data were obtained from the National Oceanic and Atmospheric Administration's (NOAA) National Data Buoy Center for station CND01 ([https://www.ndbc.noaa.gov/station\\_page.php?station=cnd01](https://www.ndbc.noaa.gov/station_page.php?station=cnd01)). Station CND01 is on Lake Erie near the Lakefront Nature Preserve in Cleveland, Ohio (fig. 1A), about 4.8 miles southwest of the mouth of Euclid Creek. Meteorological data for station CND01 were reported at 6-minute intervals for the entire 2019 calendar year.

### Continuous Monitoring of Nearshore Currents

In June 2019, the USGS began operation of two ADVMS near the entrance of the Wildwood Marina, just northeast of Villa Angela Beach. The first ADVMS (ADVMS 1) was mounted to the northwest side of the southwest caisson near the harbor entrance and was programmed to measure currents out approximately 360 ft into Lake Erie (fig. 1C). ADVMS 1 operated at a frequency of 500 kilohertz (kHz) and was mounted

**Table 1.** Combined sewer overflows near Villa Angela Beach, Cleveland, Ohio, June 1–12, 2019, and August 10–21, 2019 (data provided by the Northeast Ohio Regional Sewer District).

[CSO, combined sewer overflow; WWTP, wastewater treatment plant]

Discharge location name (CSO number)	Receiving body	Date	Volume <sup>1</sup> , in millions of gallons	Monitored or modelled discharge
West side of Euclid Creek at Lakeshore Boulevard (209)	Euclid Creek	June 2, 2019	0.60	Modelled.
Euclid Creek at St. Clair Avenue (210)	Euclid Creek	June 2, 2019	0.89	Modelled.
Lake Erie shoreline north of East 156th Street (206)	Lake Erie	June 2, 2019	0.14	Monitored.
West side of Euclid Creek at Lakeshore Boulevard (209)	Euclid Creek	June 5, 2019	1.56	Modelled.
Euclid Creek at St. Clair Avenue (210)	Euclid Creek	June 5, 2019	3.02	Modelled.
Lake Erie shoreline north of East 156th Street (206)	Lake Erie	June 5, 2019	1.13	Monitored.
Lake Erie northwest of Easterly WWTP (242)	Lake Erie	June 5, 2019	0.40	Monitored.
Lake Erie northwest of Easterly WWTP, Easterly Bypass (002)	Lake Erie	June 5, 2019	19.95	Monitored.
Lake Erie northwest of Easterly WWTP (242)	Lake Erie	June 6, 2019	0.43	Monitored.
Lake Erie northwest of Easterly WWTP, Easterly Bypass (002)	Lake Erie	June 6, 2019	1.49	Monitored.
West side of Euclid Creek at Lakeshore Boulevard (209)	Euclid Creek	June 10, 2019	0.68	Modelled.
Euclid Creek at St. Clair Avenue (210)	Euclid Creek	June 10, 2019	1.20	Modelled.
Lake Erie shoreline north of East 156th Street (206)	Lake Erie	June 10, 2019	1.34	Monitored.
Lake Erie northwest of Easterly WWTP (242)	Lake Erie	June 10, 2019	1.69	Monitored.
Lake Erie northwest of Easterly WWTP, Easterly Bypass (002)	Lake Erie	June 10, 2019	28.20	Monitored.
Total from all CSO locations (not including Easterly Bypass) near Villa Angela Beach, June 1–12, 2019			13.08	
Lake Erie shoreline north of East 156th Street (206)	Lake Erie	August 13, 2019	0.02	Monitored.
West side of Euclid Creek at Lakeshore Boulevard (209)	Euclid Creek	August 15, 2019	0.46	Modelled.
Euclid Creek at St. Clair Avenue (210)	Euclid Creek	August 15, 2019	0.83	Modelled.
Lake Erie shoreline north of East 156th Street (206)	Lake Erie	August 16, 2019	0.02	Monitored.
West side of Euclid Creek at Lakeshore Boulevard (209)	Euclid Creek	August 17, 2019	0.92	Modelled.
Euclid Creek at St. Clair Avenue (210)	Euclid Creek	August 17–18, 2019	2.06	Modelled.
West side of Euclid Creek at Lakeshore Boulevard (209)	Euclid Creek	August 18, 2019	0.25	Modelled.
Lake Erie shoreline north of East 156th Street (206)	Lake Erie	August 18, 2019	0.49	Monitored.
Lake Erie northwest of Easterly WWTP (242)	Lake Erie	August 18, 2019	0.93	Monitored.
Lake Erie northwest of Easterly WWTP, Easterly Bypass (002)	Lake Erie	August 18, 2019	0.02	Monitored.
West side of Euclid Creek at Lakeshore Boulevard (209)	Euclid Creek	August 19, 2019	0.12	Modelled.
Euclid Creek at St. Clair Avenue (210)	Euclid Creek	August 19, 2019	0.26	Modelled.
Lake Erie shoreline north of East 156th Street (206)	Lake Erie	August 19, 2019	0.41	Monitored.
Total from all CSO locations (not including Easterly Bypass) near Villa Angela Beach, August 10–21, 2019			6.76	

<sup>1</sup>Approximate volume.

about 8 ft above the bed (approximately middepth at the time of installation) at a true heading of 307 degrees and measured the currents parallel and perpendicular to the face of the meter (which was approximately parallel with the shoreline) with a sampling volume northwest of the caisson and discretized in bins of about 33 ft width (10 bins total with a 6.6-ft blanking zone). The second ADVN (ADVN 2) was mounted to the southeast side of the northeast caisson near the harbor entrance and was programmed to measure currents out about 60 ft into Wildwood Marina (fig. 1C). ADVN 2 operated at a frequency of 1500 kHz and was mounted about 8 ft above the bed (approximately middepth at the time of installation) at a true heading of 134 degrees and measured the currents parallel and perpendicular to the face of the meter with a sampling volume southeast of the caisson and discretized in bins of about 6 ft width (10 bins total with a 5-ft blanking zone). Each ADVN averaged 5 minutes of data in each bin during every 15-minute period and recorded the values. ADVN 1 logged data from June 12 to August 28, 2019, and ADVN 2 logged data from June 8 to July 23, 2019. The end date for ADVN 2 was earlier than planned because of an equipment issue.

## Synoptic Surveys

Synoptic surveys that integrated measurements of bathymetry, basic water-quality constituents, water velocity, and side-scan sonar were completed by using a combination of an AUV and a manned boat. Surveys were completed on June 10–12, 2019 (survey 1), and August 19–21, 2019 (survey 2), by using the manned boat and the AUV simultaneously in the mornings and early afternoons. The primary objective was to complete one simultaneous AUV and manned boat survey each day, which typically started midmorning and lasted 3–6 hours. If there was any extra time in the afternoon, additional velocity surveys were completed with only the manned boat. The AUV was used to complete synoptic surveys of the spatial distributions of basic water-quality constituents, bathymetry, and water velocity. In addition, side-scan sonar imagery (not presented in this report) was collected by the vehicle along the primary transects of the survey. The basic water-quality constituents collected by the instrument include water temperature, specific conductance, pH, dissolved oxygen, turbidity, total chlorophyll, and blue-green algae concentrations. The manned boat was used to deploy and recover the AUV, collect independent water-velocity and water-quality data, and complete general observations of nearshore mixing. Manned boat survey lines coincided with the programmed AUV mission lines, which were generally perpendicular to the shoreline and spaced 328 ft (100 meters) apart (fig. 1B). Additional benefits and limitations of synoptic surveys are described in Jackson and Reneau (2014).

A total of five synoptic surveys were completed during June 10–12, 2019. Three of the surveys (one per day) were simultaneous AUV and manned boat surveys, and the remaining two surveys were velocity surveys with only the manned

boat. A total of seven synoptic surveys were completed during August 19–21, 2019. Three of the surveys (one per day) were simultaneous AUV and manned boat surveys, and the remaining four surveys were velocity surveys with only the manned boat. The purpose of the additional velocity surveys (which were done with any extra time each day) was to better capture the temporal aspect of changing current conditions. With the exception of longshore surveys, all surveys were carried out according to the onshore-offshore transects depicted in figure 1B. Longshore surveys followed three to five survey lines that paralleled the shoreline at Villa Angela Beach (two lines inside the breakwaters and three lines outside the breakwaters), that paralleled the remaining shoreline in the study area, and that paralleled the Wildwood Marina and Easterly WWTP structures (fig. 1B). The onshore-offshore surveys were completed with the AUV by using an undulating dive pattern (between 6 ft above bottom and the surface), and the longshore surveys were completed with the AUV at the surface because these areas were not deep enough for diving missions. The undulating dive pattern used a 15-degree dive angle and resulted in approximately 12 profiles of the water column along a 1,200 ft transect. In all simultaneous surveys, the manned boat stayed ahead of the AUV, which was programmed to move at a constant speed of 2 knots (3.4 feet per second [ft/s]). The manned boat started each transect after the AUV had surfaced for the final time on the previous transect. The manned boat stayed ahead of the AUV to avoid collisions with the AUV and to maintain an optimal boat speed for the velocity surveys (about 5 ft/s). Because the manned boat completed transects faster than the AUV, the manned boat would typically wait a few minutes at the end of each transect, but this time was often useful for directing other boat traffic out of the survey area. The velocity-only surveys (the extra surveys in some afternoons) typically consisted of repeat transects on each of the survey lines (one offshore transect and one onshore transect). Repeat transect surveys provide additional data to permit averaging, thereby reducing variability in the measurements.

## Description of the Autonomous Underwater Vehicle

The AUV used in the 2019 surveys is 69.0 inches in length, 6.0 inches in diameter, weighs approximately 65 pounds in air (fig. 3), and is built by YSI, Inc. (EcoMapper AUV, IVER2 base vehicle). The AUV consists of a carbon-fiber hull with aluminum nose and tail sections. The nose of the AUV houses a 6600 V2-4 YSI sonde bulkhead with four optical ports and temperature/conductivity and pH ports. A pressure sensor also is integrated into the sonde bulkhead for measurement of the sample depth. Aft of the sensor suite on the nose of the vehicle is the Doppler velocimetry log (DVL) instrument. The DVL is a 10-beam system for underwater navigation (bottom tracking) and includes vertical beams (uplooking and downlooking) for altitude and

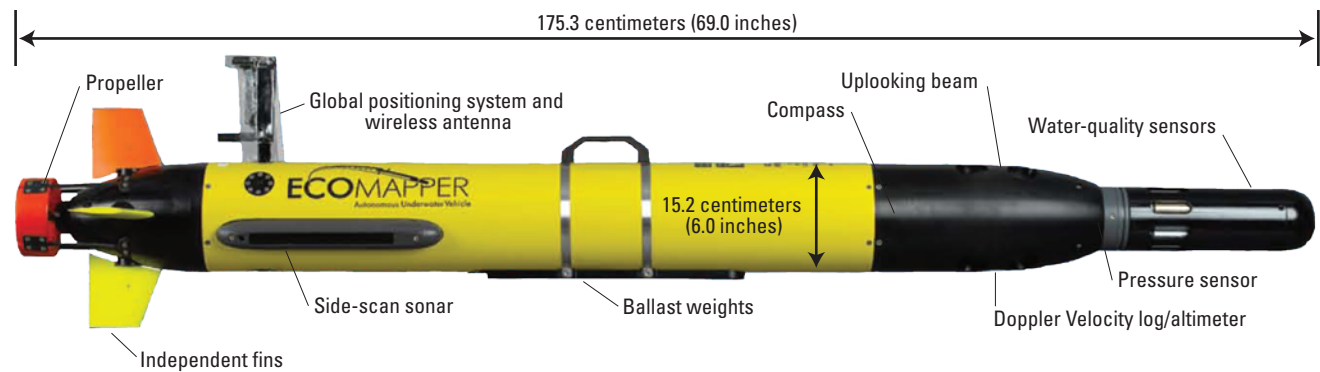


Figure 3. Schematic of the autonomous underwater vehicle.

depth measurement. Additionally, the DVL provides current-profiling capabilities below and above the instrument. The tail consists of four independent control fins and a three-blade propeller. Atop the vehicle near the tail section is the antennae mast, which houses the differential GPS antenna (Wide Area Augmentation System corrected), the 2.4 gigahertz 802.11g wireless radio antenna, navigation lights, and an external power plug for vehicle charging. All communication with the vehicle is through the wireless Ethernet radio link. Onboard electronics include an embedded computer running Windows XP and an 80-gigabyte hard drive for data storage. The aft section of the body also houses the integrated StarFish side-scan sonar transducers, mounted on the port and starboard sides of the vehicle just forward of the tail section. The

calibration procedures for the AUV, instrument operation, handling of data files, and data-processing routines are described in detail in appendix 1 of Jackson (2013). The water-quality sensor suite consists of a YSI 6600 V2-4 bulkhead equipped with a YSI 6560FR fast response temperature/conductivity probe, a YSI 6589FR fast response pH sensor, a YSI 6150FR fast response ROX optical dissolved oxygen sensor, a YSI 6136 turbidity sensor (not operational for this study), a YSI 6025 chlorophyll sensor, and a YSI 6131 BGA-PC Phycocyanin (blue-green algae) sensor. Manufacturer’s specifications for each of the probes are given in table 2. All water-quality sensors are sampled at a rate of 1 hertz.

Table 2. Manufacturer’s specifications for the water-quality sensors aboard the autonomous underwater vehicle.

[mS/cm, millisiemens per centimeter; %, percent; °C, degree Celsius; ft, foot; m, meter; ppt, parts per thousand; mg/L, milligram per liter; NTU, Nephelometric turbidity units; µg/L, microgram per liter; cells/mL, cells per milliliter; R<sup>2</sup>, coefficient of determination; >, greater than; —, not specified]

Sensor	Range	Detection limit	Resolution	Accuracy	Linearity	Estimated lag, in seconds
Conductivity	0 to 100 mS/cm	—	0.001 to 0.1 mS/cm	±0.5% or ± 0.001 mS/cm	—	0.5
Temperature	-5 to 50 °C	—	0.01 °C	±0.15 °C	—	2.1
Depth	0 to 656 ft (200 m)	—	0.001 ft	±1 ft (±0.3 m)	—	—
Salinity	0 to 70 ppt	—	0.01 ppt	±1% or 0.1 ppt	—	—
pH	0 to 14 units	—	0.01 units	±0.2 units	—	<sup>a</sup> 7.1
Dissolved oxygen	0 to 50 mg/L	—	0.01 mg/L	±0.1 mg/L or 1%	—	5.5
Turbidity	0 to 1,000 NTU	—	0.01 NTU	±2% or 0.3 NTU	—	2.1
Chlorophyll <sup>b</sup>	0 to 400 µg/L	0.1 µg/L	0.1 µg/L	—	R <sup>2</sup> > 0.9999	2.1
Phycocyanin <sup>c</sup>	0 to 280,000 cells/mL	220 cells/mL	1 cell/mL	—	R <sup>2</sup> > 0.9999	2.1

<sup>a</sup>Can vary with age of sensor.  
<sup>b</sup>Total chlorophyll fluorescence (estimated as concentration).  
<sup>c</sup>Phycocyanin fluorescence (estimated as blue-green algae cell density).



The additional components of the AUV, including the DVL, compass, acoustic pinger, and side-scan sonar are discussed in detail in Jackson (2013); however, the AUV used during the summer 2019 surveys was a slightly different model, and as such, has a few notable differences. The DVL was a 10-beam system (four additional up-looking transducers), the acoustic pinger operated at a frequency of 71 kHz, and the side-scan sonar was a single frequency of 450 kHz with a range of as much as 328 ft (100 meters) on each side.

## Manned Boat Deployments

The manned boat used in the synoptic surveys was a Defender-class boat, a 25-ft aluminum-hulled vessel with a rigid foam-filled flotation collar built by SAFE Boats International. The boat was equipped with a Teledyne RD Instruments 1200 kHz RiverPro ADCP mounted on a rigid mount on the starboard side of the vessel between the

midpoint and the stern (fig. 4). A Trimble Ag 132 (for survey 1, June 10–12, 2019) or Hemisphere A222 (for survey 2, August 19–21, 2019) differential GPS receiver was mounted directly above the ADCP and was used to georeference the ADCP data. In addition, the GPS feed was used in conjunction with the HYPACK software suite (HYPACK, Inc., 2019) for precise navigation along planned lines during the survey (fig. 1B). Boat speeds were optimized during the survey to allow enough time to complete the survey without compromising the quality of the data. When time allowed, repeat transects were obtained along survey lines to reduce the noise in the data. Because currents and wind patterns can change throughout the day, there is a constant tradeoff among survey speed, data quality, and trying to accurately capture changing environmental conditions. The depth of the transducers was set to 1.75 ft below the water surface on average, and the ADCP was operated in the manufacturer's automatic mode with adaptive bin sizes. In general, this consisted of three to five 0.39 ft



**Figure 4.** Manned boat and onboard equipment used in the coastal Lake Erie surveys in the vicinity of Villa Angela Beach and Euclid Creek, Cleveland, Ohio. Photograph by Justin Boldt, U.S. Geological Survey.



(12 cm) surface bins with either 0.79 ft (24 cm) bins (in shallower areas) or 1.57 ft (48 cm) bins (in deeper areas) below. Standard field procedures for ADCP data collection were followed to the extent necessary (Mueller and others, 2013). The ADCP data were postprocessed and visualized by using the Velocity Mapping Toolbox (VMT; Parsons and others, 2013). Independent water-quality point measurements were made throughout the survey by using a YSI 6920 multiparameter sonde equipped with a suite of sensors including water temperature, specific conductance, pH, dissolved oxygen, and turbidity. The multiparameter sonde was calibrated before survey 1 and survey 2 following standard USGS procedures (Gibs and others, 2012). The multiparameter sonde was deployed from the side of the boat inside a tube (for protection and stability) about 1 ft below the water surface, and data were logged continuously at 5-second intervals during the surveys.

## Data Processing

This section describes the techniques used for processing the meteorological, ADVM, ADCP, multiparameter sonde, and AUV data. Where possible, computer scripts were used to process the data for efficiency and consistency. All processed data are available for download through a data release at <https://doi.org/10.5066/P963OH6M> (Boldt, 2021).

## Meteorological Data

The meteorological data were processed by using custom scripts written in MATLAB, but first the raw data files obtained from the NEORS and NOAA were edited to the period from June 1 to September 30, 2019 (4 months total), to correspond with most of the summer recreational season. It was during data processing that the NEORS wind-speed data were discovered to be unusable. Time-series plots of wind speed, wind direction, and air temperature from the NEORS and NOAA weather stations were compared. It was observed that all data agreed well except for the wind-speed data during periods of higher winds, in which the NOAA station reported wind speeds 2–3 times higher than the NEORS station. During summer 2019, the maximum wind speed recorded at the NOAA weather station was 40.0 miles per hour (mi/h); however, the maximum wind speed recorded at the NEORS weather station was 16.1 mi/h. Reasons for the comparatively lower wind speeds at the NEORS station could include an equipment issue, the wind averaging methods, or a nearby obstruction. Given the suspect wind-speed data from the NEORS weather station and the availability of a suitable alternative (NOAA station CND01), it was decided to continue the meteorological data analysis with the data from the NOAA weather station. The meteorological data were processed by developing histograms of wind direction (10-degree

bins) and wind speed (1-mi/h bins). To compute a percentage of the record corresponding to each wind direction and speed, the number of observations in each bin was divided by the total number of 6-minute interval observations in the period of record ( $n = 26,571$ ). Wind directions are referenced to the direction (in heading from true north) from which the wind is originating (that is, the direction facing into the wind). This is an opposite convention to water currents, which are referenced to the direction the current is flowing.

## Acoustic Doppler Velocity Meter Data

Data from the ADVMs from June 12 to August 28, 2019 (ADVM 1), and from June 8 to July 23, 2019 (ADVM 2), were analyzed to aid in the interpretation of the synoptic data and provide insight into the repeatability of nearshore current patterns. Because of issues associated with boundaries or obstructions, only data from the first three bins from ADVM 1 (6.6–105 ft from instrument face) and the first seven bins from ADVM 2 (5–47 ft from instrument face) were considered valid. Data processing consisted of rotating the velocity data from a local X–Y coordinate system (X is parallel and Y is perpendicular to the face of the instrument) to a geographic coordinate system. The orientation of each ADVM (along the center of its acoustic beams or Y-axis) was measured after installation with a marine compass. This was necessary because the onboard compass in the ADVM did not provide accurate headings because of the presence of ferrous materials in the caisson's sheet pilings. A projection angle of 307 degrees from true north was used for computation as the Y-axis orientation of ADVM 1, and a projection angle of 134 degrees from true north was used for computation as the Y-axis orientation of ADVM 2. The rotated east and north components of velocity were then used to compute the magnitude and direction (in geographic coordinates) of the velocity vector for every sample in each of the bins. The magnitude of the rotated vector was compared to that reported by the ADVM to ensure no errors were made in the rotation. Lastly, histograms were generated for all the data with respect to current speed (by using 0.05 ft/s bins) and direction (by using 10-degree bins), and for each month of data (to determine whether the direction of the currents varied by month). The histograms were used to develop frequency plots showing the percentage of the period of record (or month) that the currents displayed a particular speed or direction.

## Acoustic Doppler Current Profiler Data

Processing of the manned boat ADCP data was completed by using the VMT by Parsons and others (2013). This software suite allows for transect averaging in addition to spatial averaging of the data to allow for the reduction of noise

in the velocity data. In addition, VMT allows for visualization of the velocity data in plan view and with depth for each cross section.

## Multiparameter Sonde Data

The multiparameter sonde data were processed by using custom scripts written in MATLAB. The primary purpose was to georeference the multiparameter sonde data by matching timestamps with the GPS logs. During the June 2019 surveys, the GPS log was made up of all the individual GPS log files that were recorded during ADCP transects; thus, all multiparameter sonde data that were recorded between ADCP transects were not able to be georeferenced, but there were still sufficient multiparameter sonde data available to generate the water-quality distribution maps. During the August 2019 surveys, a separate GPS log was recorded continuously each day, so all the multiparameter sonde data were able to be georeferenced. Boxplots and statistics were computed during processing to assist in the color categories used in the water-quality distribution maps.

## Autonomous Underwater Vehicle Data

Processing of the AUV data is discussed in detail in Jackson (2013). Output from data-processing routines was further refined using geographic information system software and graphics design software to generate the figures in this report. Jackson (2013) also discusses the method used to compute water density from measurements of temperature and specific conductance. A formal comparison between the multiparameter sonde data and the water-quality data from the AUV was not done because they were typically measuring different areas (spatially and temporally). However, there were locations during each survey where water-quality measurements from the multiparameter sonde and the AUV nearly coincided, and several of these were spot-checked to verify reasonable agreement between the two instruments.

## Observations

This section presents and discusses the observed meteorological, hydrodynamic, and water-quality conditions present near Villa Angela Beach, Euclid Creek, and the Easterly WWTP on June 10–12, 2019, and August 19–21, 2019. Distributions of individual constituents in time and space are compared and used to interpret interactions among atmospheric forcing, local lake circulation, and water-quality distributions in the vicinity of Villa Angela Beach and the mouth of Euclid Creek. The supporting data on which these observations are based can be obtained from the data release associated with this study (Boldt, 2021).

## Meteorological Data

Winds during summer 2019 were most frequently out of the northeast (50 to 60 degrees) at the Lake Erie lakefront about 5 miles southwest of Villa Angela Beach (fig. 5A). There was a secondary, broader peak in wind direction at 200–230 degrees (south-southwest to southwest). The histograms of wind direction from summer 2019 (fig. 5A) and summer 2012 (fig. 4 in Jackson, 2013) are similar. Wind speed during summer 2019 ranged from 0 to 40 mi/h with a typical wind speed (most frequent) of about 1–2 mi/h (fig. 5B). Based on the orientation of the shoreline (about 42 degrees from true north), the data indicate that offshore winds were present about 61 percent of the time and onshore winds occurred about 39 percent of the time during summer 2019. This is nearly the same as the results from the summer 2012 study (64 percent offshore and 36 percent onshore; Jackson, 2013).

Another way to visualize the wind data is with a wind-rose diagram. A wind-rose diagram shows the distribution of wind speed and wind direction in the same plot, presented in a circular format like a compass. The length of each bar shows the frequency of winds blowing from particular directions (in 10-degree bins), and the colors represent the wind speeds. The wind-rose diagram for the summer 2019 data (fig. 6) shows the same distribution by direction as figure 5A; however, figure 6 shows a clear distinction between offshore and onshore winds and shows that the winds blowing onshore are typically stronger (yellow colors) than the winds blowing offshore.

In the 12 hours leading up to the survey on June 10, 2019, the wind speeds were light (2.7 mi/h average), steady, and out of the south-southeast (fig. 7). During the survey on June 10, wind speeds were light and steady at the start (2.7 mi/h average) and then increased toward the end (20.3 mi/h average) while the wind direction shifted from south to west as a strong precipitation event (1.14 inches of rain in 7 hours) moved through the area. The change in wind direction was also observed in the longshore current data (shown later in the “Longshore Currents” section). In the 12 hours leading up to the survey on June 11, 2019, the wind speeds were moderate (11.8 mi/h average), decreasing, and out of the west-northwest (fig. 7). During the survey on June 11, wind speeds were moderate (7.8 mi/h average) and remained steady from the west. In the 12 hours leading up to the survey on June 12, 2019, the wind speeds were light (1.1 mi/h average), steady, and out of the south-southeast (fig. 7). During the survey on June 12, wind speeds were light (2.6 mi/h average) and remained steady from the south.

During the 3-day period of survey 1 (June 10–12, 2019), the air temperature ranged from 15.6 to 24.5 degrees Celsius (°C) at the NOAA weather station about 4.8 mi to the southwest of Villa Angela Beach and changed on average about 4 °C throughout each day’s survey (fig. 7). June 10 started out cloudy, but most of the survey was done in the rain with high winds. June 11 and 12 were sunny, dry, and relatively calm.

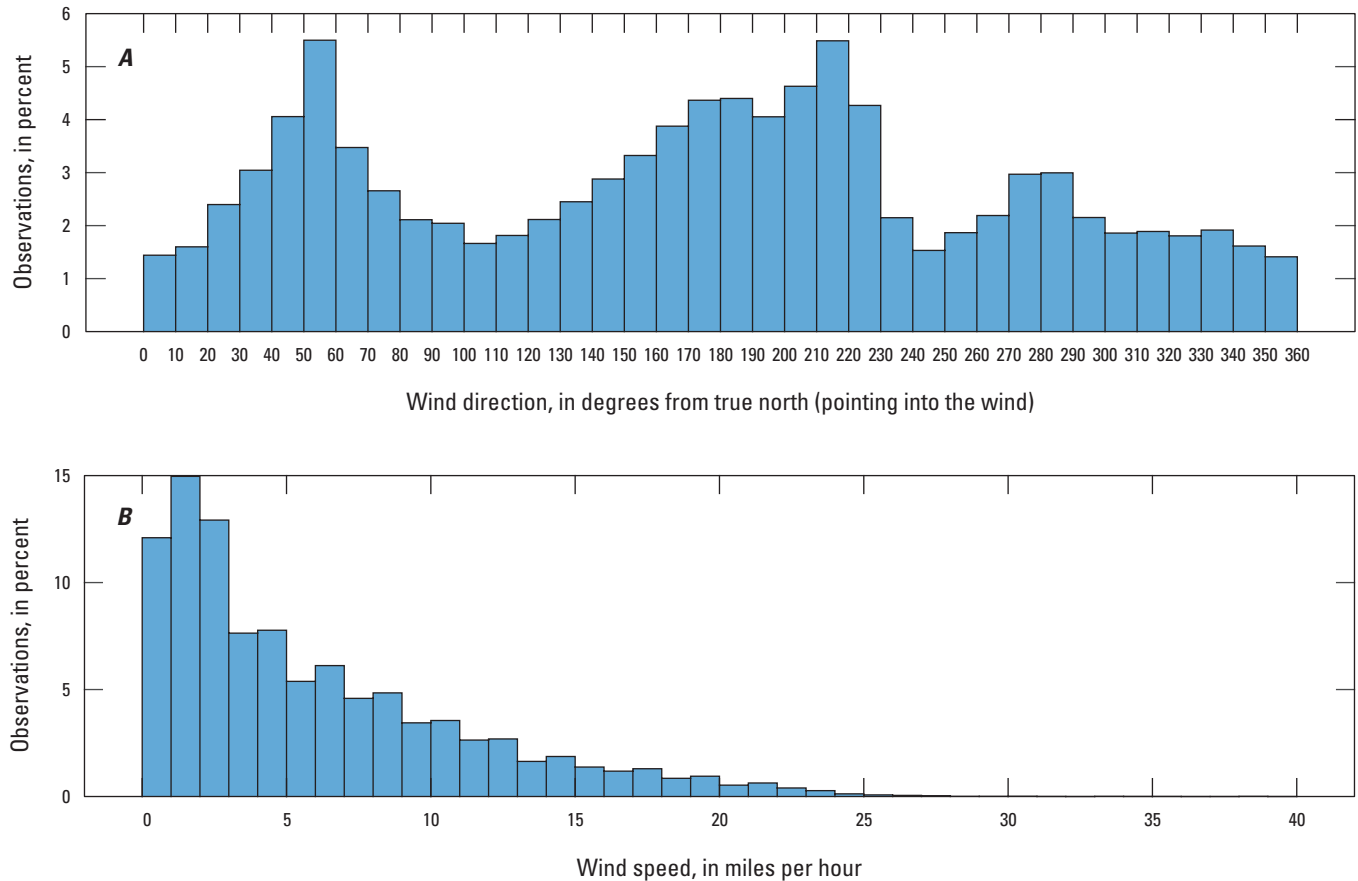


**Figure 5.** A, Wind-direction and B, wind-speed characteristics observed at the Lakefront Nature Preserve, Cleveland, Ohio, for the period June 1–September 30, 2019 (based on 6-minute interval data obtained from the National Oceanic and Atmospheric Administration station CND01; [https://www.ndbc.noaa.gov/station\\_page.php?station=cnd01](https://www.ndbc.noaa.gov/station_page.php?station=cnd01)).

In the 12 hours leading up to the survey on August 19, 2019, the wind speeds were strong overnight (25–35 mi/h) but then light (2.5 mi/h average), steady, and generally out of the south to southwest (fig. 8). During the survey on August 19, wind speeds were moderate (5.3 mi/h average) throughout while the wind direction shifted from west to north by the end of the survey. The change in wind direction was also observed in the water current data (shown later in the “Longshore Currents” section). In the 12 hours leading up to the survey on August 20, 2019, the wind speeds were light (0.6 mi/h average), steady, and out of the south-southeast (fig. 8). During the survey on August 20, wind speeds started out light (1.8 mi/h average) and from the south-southwest. About halfway through the survey, the wind speeds abruptly increased (8.9 mi/h average) and the wind direction changed from south-southwest to east-northeast. In the 12 hours leading up to the survey on August 21, 2019, the wind speeds were light (2.9 mi/h average), steady, and out of the south-southwest (fig. 8). During the survey on August 21, wind speeds started out light (4.5 mi/h average) and increased toward the end (12.3 mi/h average) while the wind direction shifted from southwest to west-northwest.

During the 3-day period of survey 2 (August 19–21, 2019), the air temperature ranged from 19.1 to 30.9 °C at the NOAA weather station about 4.8 mi to the southwest of Villa Angela Beach and changed on average about 3 °C throughout each day’s survey (fig. 8). August 19 and 20 were sunny, dry, and calm. A small weather system moved through the area the evening of August 20 and into the overnight (no recorded precipitation), and then August 21 was partly cloudy and dry.

In the previous study from summer 2012, the winds tended to be onshore during the day and offshore at night (Jackson, 2013). Wind speeds generally peaked in the midafternoon period at 10–20 mi/h and became calm overnight (0–10 mi/h). The pattern consisted of south winds before dawn followed by a clockwise rotation of the wind direction (south to west to north) through the afternoon (Jackson, 2013). Although this pattern was not as evident or not observed during the June 2019 and August 2019 surveys, it was observed on many other days during summer 2019. Another pattern commonly observed during summer 2019 was sustained winds from generally the same direction for a typical period of two to three days.

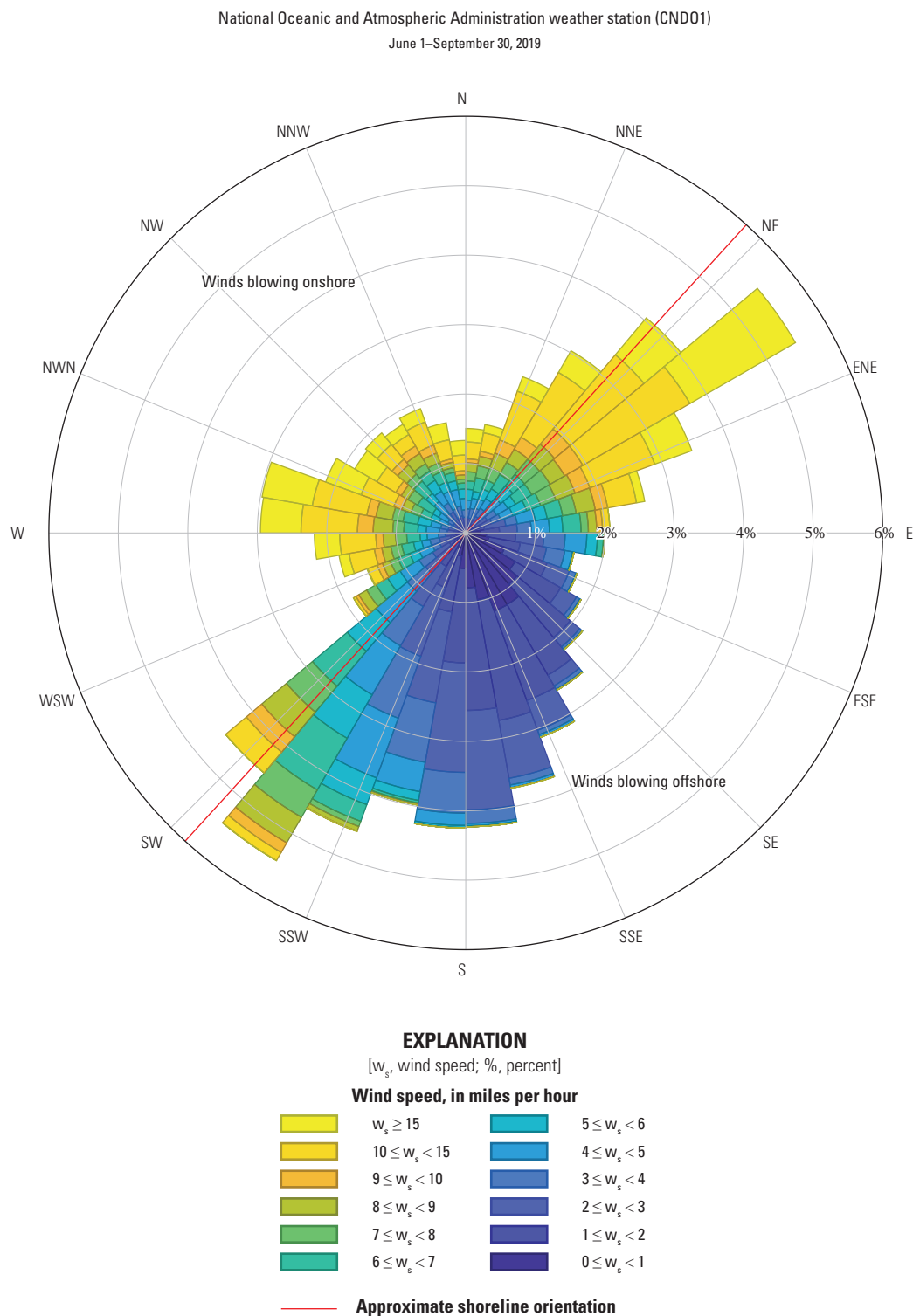


**Figure 6.** Wind-rose diagram of the wind-direction and wind-speed characteristics observed at the Lakefront Nature Preserve, Cleveland, Ohio, for the period June 1–September 30, 2019 (based on 6-minute interval data obtained from the National Oceanic and Atmospheric Administration station CND01; [https://www.ndbc.noaa.gov/station\\_page.php?station=cnd01](https://www.ndbc.noaa.gov/station_page.php?station=cnd01)).

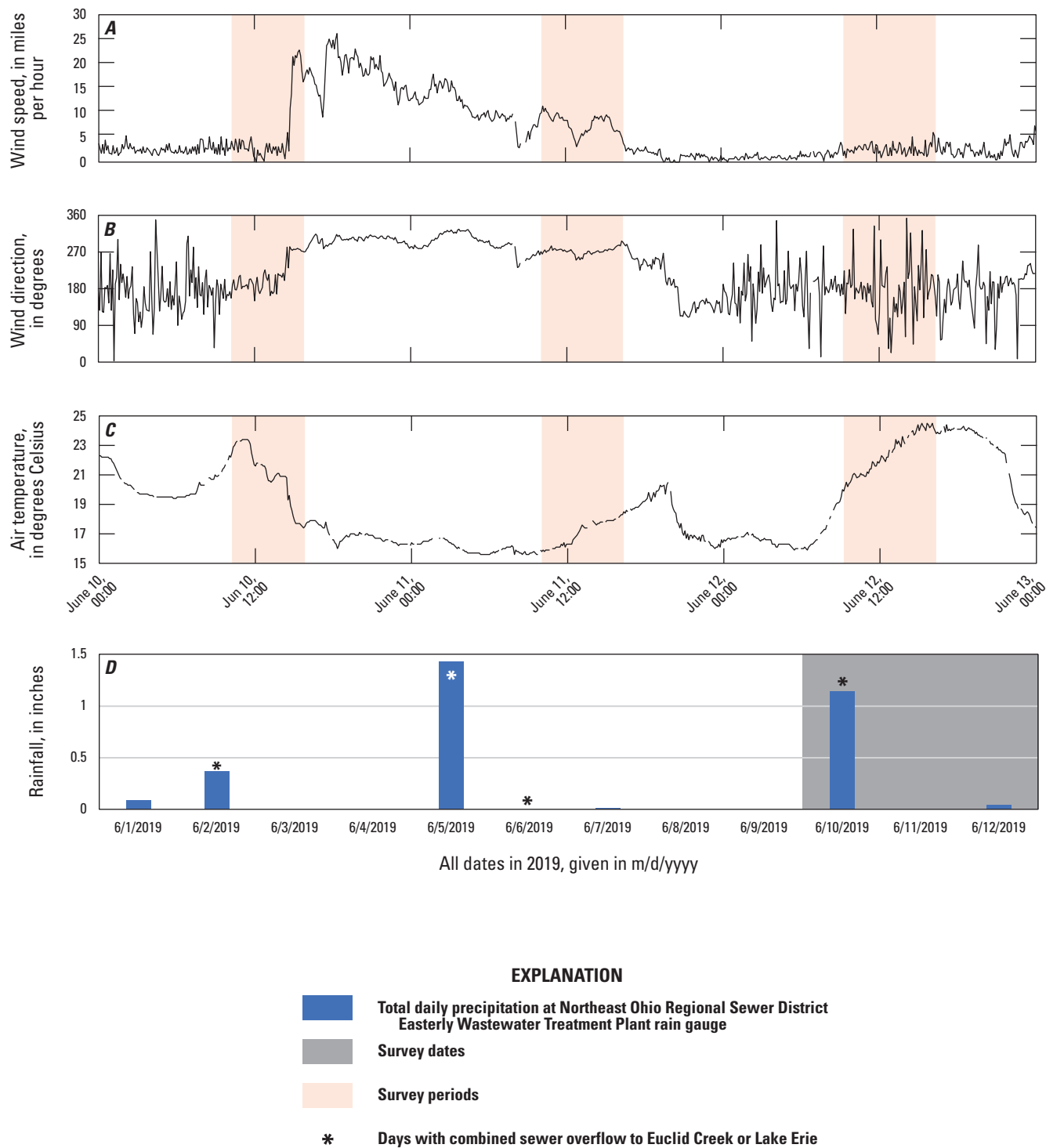
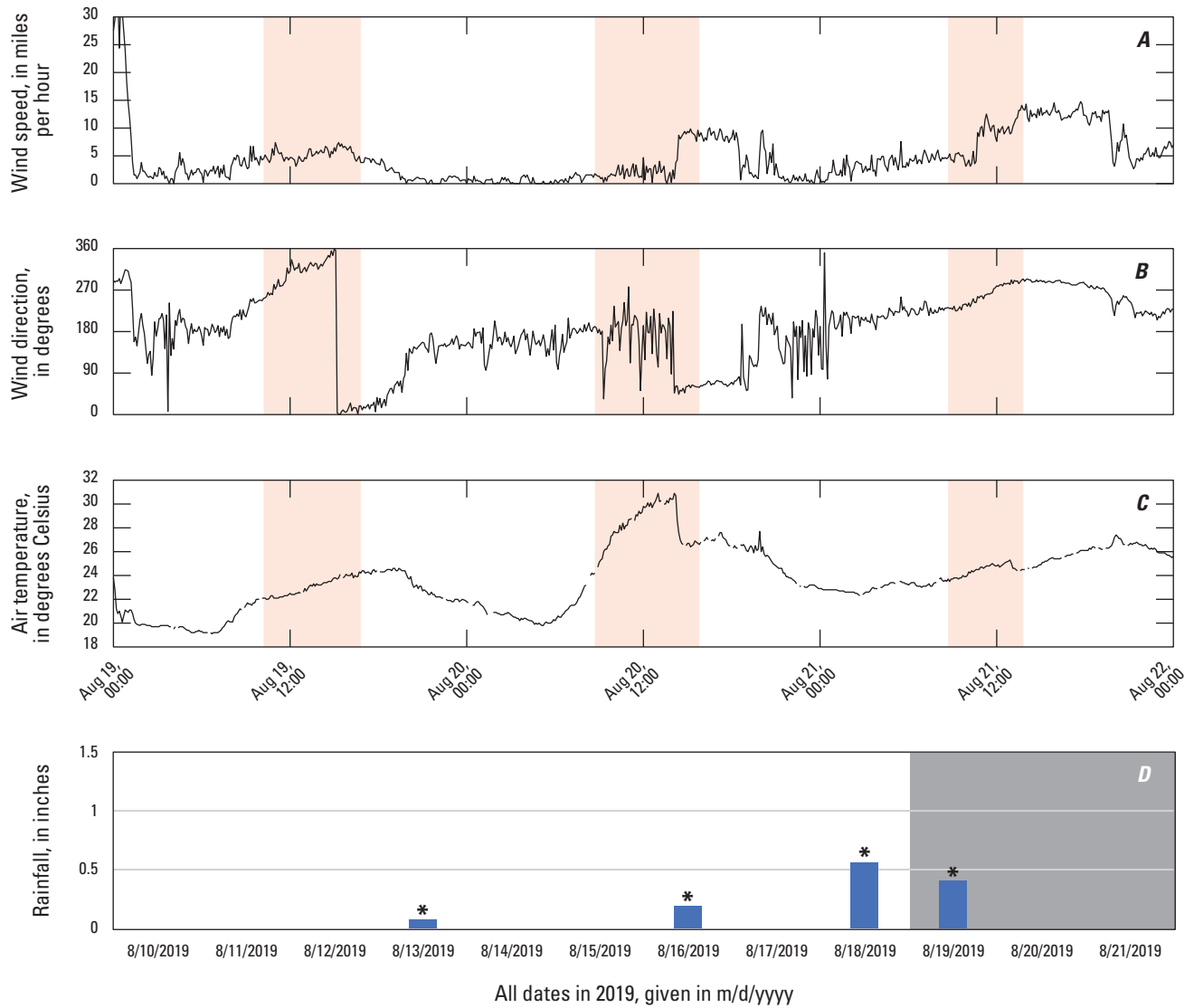


**Figure 7.** Observations of *A*, wind speed, *B*, wind direction (pointing into the wind), and *C*, air temperature for June 10–12, 2019, at Lakeshore Nature Preserve, Cleveland, Ohio (based on 6-minute interval data obtained from National Oceanic and Atmospheric Administration station CND01; [https://www.ndbc.noaa.gov/station\\_page.php?station=cndo1](https://www.ndbc.noaa.gov/station_page.php?station=cndo1)), and *D*, daily rainfall for June 1–12, 2019, at the Northeast Ohio Regional Sewer District Easterly Wastewater Treatment Plant rain gauge (Eric Soehnen, Northeast Ohio Regional Sewer District, written commun., March 16, 2021).



## EXPLANATION

- Total daily precipitation at Northeast Ohio Regional Sewer District Easterly Wastewater Treatment Plant rain gauge
- Survey dates
- Survey periods
- Days with combined sewer overflow to Euclid Creek or Lake Erie

**Figure 8.** Observations of *A*, wind speed, *B*, wind direction (pointing into the wind), and *C*, air temperature for August 19–21, 2019, at Lakeshore Nature Preserve, Cleveland, Ohio (based on 6-minute interval data obtained from National Oceanic and Atmospheric Administration station CND01; [https://www.ndbc.noaa.gov/station\\_page.php?station=cnd01](https://www.ndbc.noaa.gov/station_page.php?station=cnd01)), and *D*, daily rainfall for August 10–21, 2019, at the Northeast Ohio Regional Sewer District Easterly Wastewater Treatment Plant rain gauge (Eric Soehnlen, Northeast Ohio Regional Sewer District, written commun., March 16, 2021).



## Euclid Creek Inflow

Euclid Creek is a flashy stream, which means it responds quickly (a rapid increase in streamflow and return to normal) to precipitation events. In general, the runoff from a precipitation event may cause the streamflow in Euclid Creek to rapidly increase over several hours and decrease back to normal over a couple days; however, there is variation in these timeframes depending on the characteristics (such as intensity and duration) of each precipitation event. Euclid Creek ranged in flow from 18 to 700 cubic feet per second ( $\text{ft}^3/\text{s}$ ) at USGS streamgage 04208700 (U.S. Geological Survey, 2020) during these surveys. The first day of survey 1 (June 10, 2019) started at normal (base) flow conditions (about  $20 \text{ ft}^3/\text{s}$ ), but the precipitation event during the afternoon (1.14 inches of rain in 7 hours) caused a rapid increase in streamflow (over about 4 hours) to about  $700 \text{ ft}^3/\text{s}$  (fig. 9A). The surveys on June 11 (daily average flow of  $113 \text{ ft}^3/\text{s}$ ) and June 12 (daily average flow of  $36 \text{ ft}^3/\text{s}$ ) were on the receding limb of the hydrograph (as the streamflow was decreasing back to normal; U.S. Geological Survey, 2020). The August 2019 surveys were all on the receding limb of a much smaller hydrograph (fig. 9B). There was a precipitation event (0.62 inches total) the night before the first day of survey 2 (August 19, 2019) that caused the streamflow to increase from about  $7 \text{ ft}^3/\text{s}$  to  $300 \text{ ft}^3/\text{s}$ . The daily average flows on August 19–21, 2019, were  $56 \text{ ft}^3/\text{s}$ ,  $21 \text{ ft}^3/\text{s}$ , and  $12 \text{ ft}^3/\text{s}$ , respectively.

The higher-flow events on June 10, 2019 (peak of  $701 \text{ ft}^3/\text{s}$ ), and August 18, 2019 (peak of  $288 \text{ ft}^3/\text{s}$ ), and associated CSO discharges (1.88 Mgal on June 10 and 2.31 Mgal on August 18) were likely to deliver bacteria to the creek mouth that could discharge to the lake over time. This claim is supported by water sample results; Villa Angela Beach was under advisory June 11–12, 2019, and August 19, 2019, for elevated *E. coli* concentrations (Ohio Department of Health, 2021). Additionally, a previous study by Bushon and others (2009) detected the highest *E. coli* concentrations within Euclid Creek after recent rainfall. Higher-flow events occurred near the beginning of both surveys, which allowed for observation of water-quality characteristics in the days after.

Euclid Creek water-quality characteristics were measured on June 10 and 12, 2019, and August 19 and 21, 2019 (table 3). Although the water-quality characteristics are just a single point measurement near the water surface, they provide a basis for comparing Euclid Creek water with Lake Erie water measured during the synoptic surveys. Euclid Creek water was much warmer (by about  $2.5^\circ\text{C}$ ) during the June 2019 surveys and nearly the same temperature during the August 2019 surveys as the nearshore Lake Erie water in the vicinity of Villa Angela Beach. For the June and August 2019 surveys, Euclid Creek water had a higher specific conductance, a lower pH, and a lower dissolved oxygen than nearshore Lake Erie water in the vicinity of Villa Angela Beach. During the June 2019 surveys, the specific conductance in Euclid Creek was more than two times higher than that in the lake, providing the opportunity to use specific conductance

as a tracer to track the plume of Euclid Creek water after it entered the lake. During the August 2019 surveys, the specific conductance in Euclid Creek was lower than it was during the June 2019 surveys but still higher than that in the lake. Specific conductance is relatively high in raw sewage and septic tank water compared to lake water and is nearly conservative in this environment making it an excellent candidate for a tracer (Lalor and Pitt, 1999). Lastly, the Euclid Creek water was similar in density with the Lake Erie water so an underflow (or density current) as it entered the lake would have been unlikely during the June and August 2019 surveys.

A specific question that was raised before this study was to what extent does Euclid Creek water move through the gap in the pier near the northeast end of Villa Angela Beach. Although the deployment of continuous sondes would provide data to help answer this question, the data collected in this study can be used to answer this question to some extent. The reasoning behind this question is that the piers on either side of Euclid Creek help guide the water out into Lake Erie where the water is then directed by lake currents, and the gap in the pier may allow Euclid Creek water, and the bacteria therein, to more easily enter the nearshore area along Villa Angela Beach. Based on the data collected during this study, there is some evidence that Euclid Creek water is able to move through the gap in the pier into the water along the northeast end of Villa Angela Beach. During the four days of surveys around Euclid Creek and Villa Angela Beach in summer 2019, water of equal or even near-equal specific conductance to that of Euclid Creek was never detected on the Villa Angela Beach side of the gap in the pier. The observation made each of the four days was that there was a small area of water near the gap in the pier that had specific conductance values that were much lower than the Euclid Creek water but still slightly higher than the other water in the nearby area and these areas tended to align with the gap in the pier. Thus, the data seem to indicate that a transport path is likely through the gap in the pier, but other explanations may be possible. The possible transport path through the gap in the pier was not alarming based on observations from this study because the elevated specific conductance core of the Euclid Creek water tended to exit out into Lake Erie between the ends of the piers, but additional surveys and monitoring during other conditions, such as during a southwest longshore current, would provide additional insight.

## Water within Wildwood Marina and the Easterly Wastewater Treatment Plant

Water in the Wildwood Marina had little exchange with the lake because of the surrounding jetties (piers and [or] sea walls). The water-quality characteristics of the marina also were documented. The marina water was slightly warmer and had a slightly higher specific conductance, a lower pH, and a lower dissolved oxygen than nearshore Lake Erie water in the vicinity of Villa Angela Beach (table 3).

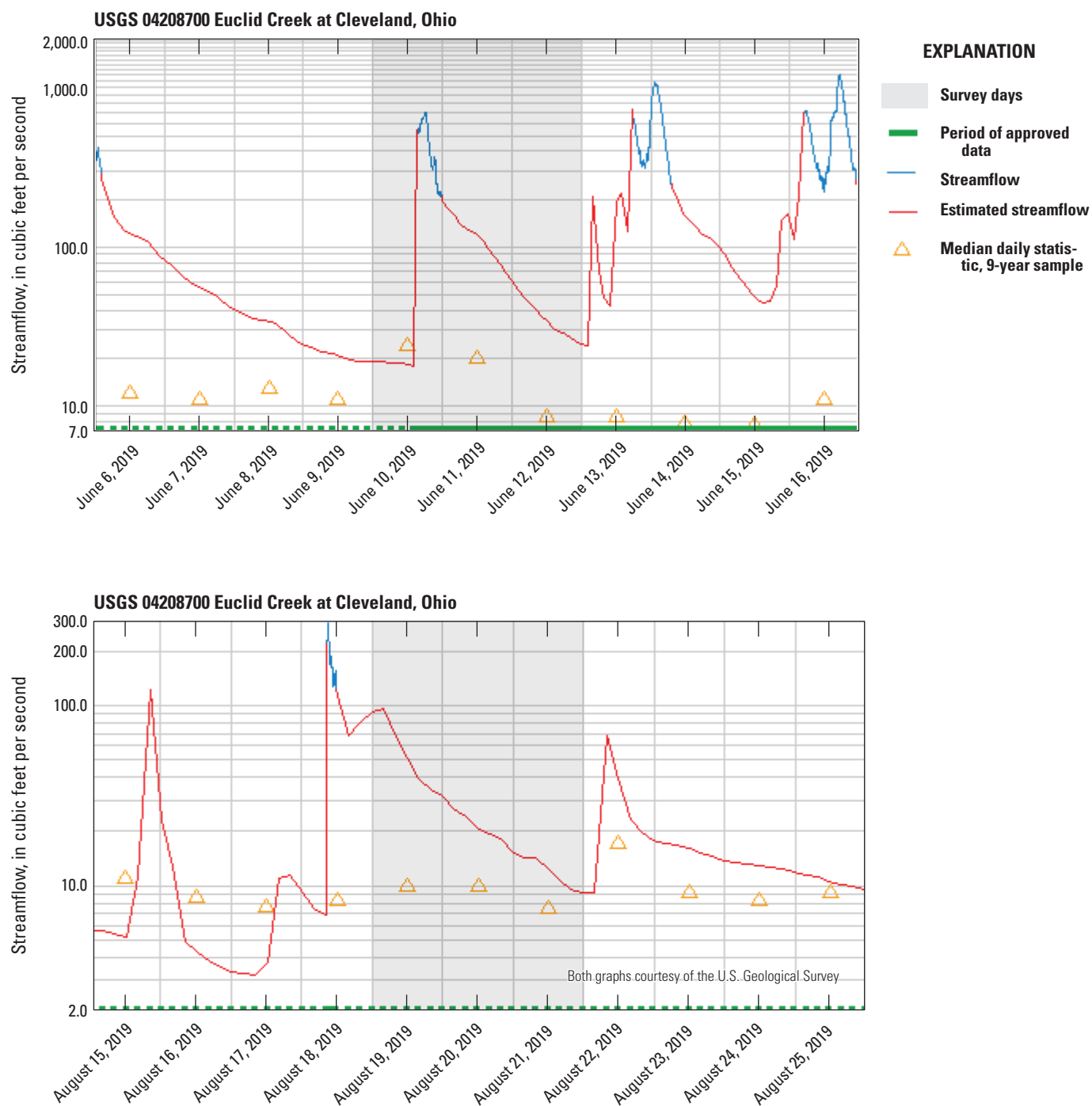


**Figure 9.** Hydrographs of streamflow for A, June 6–16, 2019 (an 11-day period centered on survey 1), and B, August 15–25, 2019 (an 11-day period centered on survey 2), recorded by the U.S. Geological Survey streamgage on Euclid Creek near Villa Angela Beach, Cleveland, Ohio (station number 04208700; U.S. Geological Survey, 2020).

**Table 3.** Point measurements of water-quality characteristics in Euclid Creek, Wildwood Marina, and Easterly Wastewater Treatment Plant, Cleveland, Ohio, June 10–12, 2019, and August 19–21, 2019.

[—, no measurement; m/dd/yyyy, date in month/day/year]

Site	Short ID <sup>a</sup>	Latitude (degrees)	Longitude (degrees)	Sample time (Eastern Daylight Time)	Sampling depth, in feet	Temperature, in degrees Celsius	Specific conductance, in millisiemens per centimeter	pH, in standard units	Dissolved oxygen, in milligrams per liter	Turbidity, in nephelometric turbidity units	Density, in kilograms per cubic meter
Euclid Creek	EC1	41.587592	-81.567260	6/10/2019 12:43	<sup>b</sup> 0.1	19.1	0.634	7.86	7.93	—	998.62
Euclid Creek	EC2	41.587482	-81.566164	6/12/2019 15:39	1	20.4	0.607	8.10	8.74	6	998.35
Euclid Creek	EC3	41.587651	-81.566631	8/19/2019 14:21	1	25.6	0.310	8.38	8.26	2	997.02
Euclid Creek	EC4	41.587275	-81.566015	8/21/2019 8:42	1	24.9	0.366	8.00	7.49	1	997.22
Wildwood Marina	WM1	41.587806	-81.563956	8/19/2019 16:54	1	27.3	0.312	8.08	7.77	1	996.55
Wildwood Marina	WM2	41.587801	-81.564388	8/21/2019 8:34	1	25.4	0.304	8.11	7.43	1	997.05
Easterly Wastewater Treatment Plant (lagoon)	EW1	41.570802	-81.591130	6/11/2019 14:07	1	19.4	0.296	8.26	9.40	22	998.43
Easterly Wastewater Treatment Plant (marina)	EW2	41.574223	-81.587264	8/20/2019 10:52	1	25.9	0.306	8.31	9.11	0	996.91
Easterly Wastewater Treatment Plant (lagoon)	EW3	41.570829	-81.591844	8/20/2019 12:33	1	26.1	0.299	8.30	8.12	7	996.86

<sup>a</sup>The specific locations of the point measurements are shown in [figure 1B](#).<sup>b</sup>This measurement was from the autonomous underwater vehicle; whereas, all the other measurements were from the multiparameter sonde.

There are two distinct areas of water within the surrounding jetties (piers and [or] sea walls) of the Easterly WWTP. One area is a marina on the eastern side of the Easterly WWTP, and the other area is a lagoon on the western side of the Easterly WWTP. The water within the surrounding jetties of the Easterly WWTP was slightly warmer and had a slightly higher specific conductance, lower pH, and lower dissolved oxygen than nearshore Lake Erie water away from the Easterly WWTP (table 3). One anomaly was that the dissolved oxygen was higher on the marina side of the WWTP than the lagoon side of the WWTP. A large amount of aquatic vegetation was observed within the marina, whereas little vegetation was observed outside the marina. This may explain the elevated dissolved oxygen (produced during photosynthesis).

## Nearshore Circulation

Circulation within Lake Erie in the vicinity of Villa Angela Beach and Euclid Creek, Ohio, is affected by the interaction of the longshore currents—which are driven primarily by regional wind patterns but also affected by seiche activity and inertial waves—with shoreline structures and the outflow from Euclid Creek (Jackson, 2013). This section examines the observed currents for summer 2019 by using ADVm data (table 4) and highly resolved circulation patterns from synoptic surveys for 3 days in June 2019 and 3 days in August 2019. Circulation patterns are compared with observations from previous surveys (Jackson, 2013).

## Magnitude and Direction of Observed Currents near Villa Angela Beach, Cleveland, Ohio, for Summer 2019

Based on the entire period of record for ADVm 1, the currents near Villa Angela Beach (measured offshore from the caissons at the marina entrance) are oriented to the north-northeast (20–30 degrees) about 20 percent of the time (fig. 10A). This is an offshore orientation with a longshore component to the northeast and does not align with the shoreline orientation (about 42 degrees). This misalignment may be because of the local flow disturbance by the caissons and (or) error in the measurement of the orientation of ADVm 1. A second dominant direction in currents is to the south-southwest at a heading of about 210–220 degrees, approximately aligned with the shoreline and consistent with the synoptic observations presented in this report (fig. 10A). The magnitude of these currents is small (fig. 10B), with most of the currents less than 0.2 ft/s and a range of 0–0.92 ft/s (table 4). Currents in bin 1 (6–39 ft from the meter) are generally smaller than currents in bin 2 (39–72 ft from the meter) and bin 3 (72–105 ft from the meter), possibly indicating that flow disturbance around the caisson is occurring (recall that ADVm 1 is mounted to the northwest side of the southwest caisson at the marina entrance and points out into the lake; fig. 1C). Overall,

the magnitude and direction of observed currents is similar to what was observed in summer 2012 (fig. 6 in Jackson, 2013); however, the most frequent direction of the current (the primary peak in current direction) has shifted counterclockwise by about 50 degrees (from a direction of 75 degrees in summer 2012 to a direction of 25 degrees in summer 2019). This change in direction may be because of the local flow disturbance by the caissons and the different placement of the ADVm (it was mounted on the northwest side of the northeast caisson in summer 2012 but some of the data were obstructed, so it was mounted on the northwest side of the southwest caisson in summer 2019).

Based on the entire period of record for ADVm 2, the currents near Villa Angela Beach (measured between the nearshore side of the caissons and the marina entrance) are oriented to the north-northeast (20–30 degrees) about 23 percent of the time (fig. 11A). This is an offshore orientation with a longshore component to the northeast and does not align with the shoreline orientation (about 42 degrees). This misalignment may be because of the local flow disturbance by the caissons and the marina jetties and (or) error in the measurement of the ADVm 2 orientation. A second dominant direction in currents is to the south-southwest at a heading of about 200–210 degrees, approximately aligned with the shoreline and consistent with the synoptic observations presented in this report (fig. 11A). The magnitude of these currents is small (fig. 11B), with most of the currents less than 0.2 ft/s and a range of 0–1.24 ft/s (table 4). Currents in bin 1 (5–11 ft from the meter) are generally less than currents in bins 2–7 (11–47 ft from the meter), indicating that flow disturbance around the caisson is occurring (recall that ADVm 2 was mounted to the southeast side of the northeast caisson at the marina entrance and oriented toward the marina; fig. 1C). There was not an ADVm measuring in this location during the summer 2012 study (Jackson, 2013).

Another way to visualize the current data is with a current-rose diagram (the current equivalent of a wind-rose diagram). A current-rose diagram shows the distribution of current speed and current direction (direction in which the current is flowing) in the same plot, presented in a circular format like a compass. The length of each bar shows the frequency of currents moving in particular directions (in 10-degree bins), and the colors represent the current speeds. The current-rose diagrams for the ADVm data (fig. 12A–B) show the same distribution by direction as in figures 10–11 and there is a clear distinction between northeast longshore orientation and southwest longshore orientation; however, figure 12 shows that for ADVm 1 and ADVm 2, the currents moving in the northeast longshore orientation are typically stronger (more orange and yellow colors) than the currents moving in the southwest longshore direction. Further analysis indicates that there is strong correlation between the dominant flow directions of ADVm 1 and ADVm 2. When the current measured by ADVm 1 was in the 20–30 degrees direction, the corresponding (same time) current measured by ADVm 2 was in the 10–40 degrees direction about 75 percent of the time.

**Table 4.** Summary of the acoustic Doppler velocity meter (ADVM) data collected during summer 2019 near Villa Angela Beach, Cleveland, Ohio.

[ADVM, acoustic Doppler velocity meter; ft/s, foot per second]

Period of record	ADVM 1	ADVM 2
	June 12–August 28, 2019	June 8–July 23, 2019
Manufacturer	SonTek	SonTek
Model	SL500	SL1500
Frequency, in kiloHertz	500	1500
True heading, in degrees	307	134
Blanking distance, in feet	6.6	5
Bin size, in feet	32.8	6
Number of bins	10	10
Minimum velocity, in ft/s	0	0
Maximum velocity, in ft/s	0.92	1.24
Mean velocity, in ft/s	0.17	0.22
Median velocity, in ft/s	0.12	0.15
Northeast longshore current component (percent of observations)	64.6	66.0
Southwest longshore current component (percent of observations)	35.4	34.0

Overall, by dividing these data into two groups based on the longshore current component, the data from ADVM 1 indicate that currents with a longshore component to the northeast occurred 64.6 percent of the time and currents with a longshore component to the southwest occurred 35.4 percent of the time (table 4). This is nearly the same percentage split as was observed in the summer 2012 data (69.5 percent northeast and 30.5 percent southwest; Jackson, 2013). The data from ADVM 2 indicate that currents with a longshore component to the northeast occurred 66.0 percent of the time, and currents with a longshore component to the southwest occurred 34.0 percent of the time (table 4).

The longshore current component percentages in table 4 are based on the average of all bins, but the same calculations can be made for each bin (table 5) to determine whether the currents are homogeneous within each ADVM's sampling volume (6–105 ft for ADVM 1 and 5–47 ft for ADVM 2). The percentage of observations in each longshore current component direction is nearly the same among the bins of each ADVM, thus indicating that the currents are homogeneous within each ADVM's sampling volume (table 5). Therefore, based on the data from ADVM 1, longshore currents in similar directions (to the southwest) to those associated with the observed recirculation patterns off Villa Angela Beach in the summer 2012 study (Jackson, 2013) occurred approximately 35 percent of the time during summer 2019. It should be noted, however, that not all southwest longshore currents will produce a recirculation, and some northeast longshore currents also may induce flow separation and recirculation off Villa Angela Beach because of flow disturbance caused by the marina jetties and other structures.

Although the early summer months (June and July) indicate a similar trend in current direction (dominant in the northeast longshore current component direction for ADVM 1 and ADVM 2), a departure from this pattern was observed in August for ADVM 1 (table 6 and fig. 13A). In August, the longshore current component split became much more equal and was even slightly more dominant in the southwest direction (55.5 percent). The summer 2012 data indicated that longshore currents to the northeast occurred more often in early summer (June), and although the frequency decreased slightly throughout the summer, the longshore currents remained dominant in the northeast longshore current component direction from June through September (table 4 and fig. 7 in Jackson, 2013). Therefore, based on the data from ADVM 1, longshore currents in similar directions (to the southwest) to those associated with the observed recirculation patterns off Villa Angela Beach occurred much more often in August 2019 (55.5 percent of the time) than in June and July 2019 (27.0 and 22.7 percent of the time, respectively). Based on the two summers of data where there was a subanalysis by month (2012 and 2019), it seems likely that longshore currents in similar directions (to the southwest) to those associated with the observed recirculation patterns off Villa Angela Beach in the summer 2012 study (Jackson, 2013) occurred more often in the latter half of summer. However, because the overall dataset is small (only two summers), it is not known with great certainty whether the observed trends are characteristic of typical conditions. Additional data collection in more summer periods (June through September) would be beneficial.



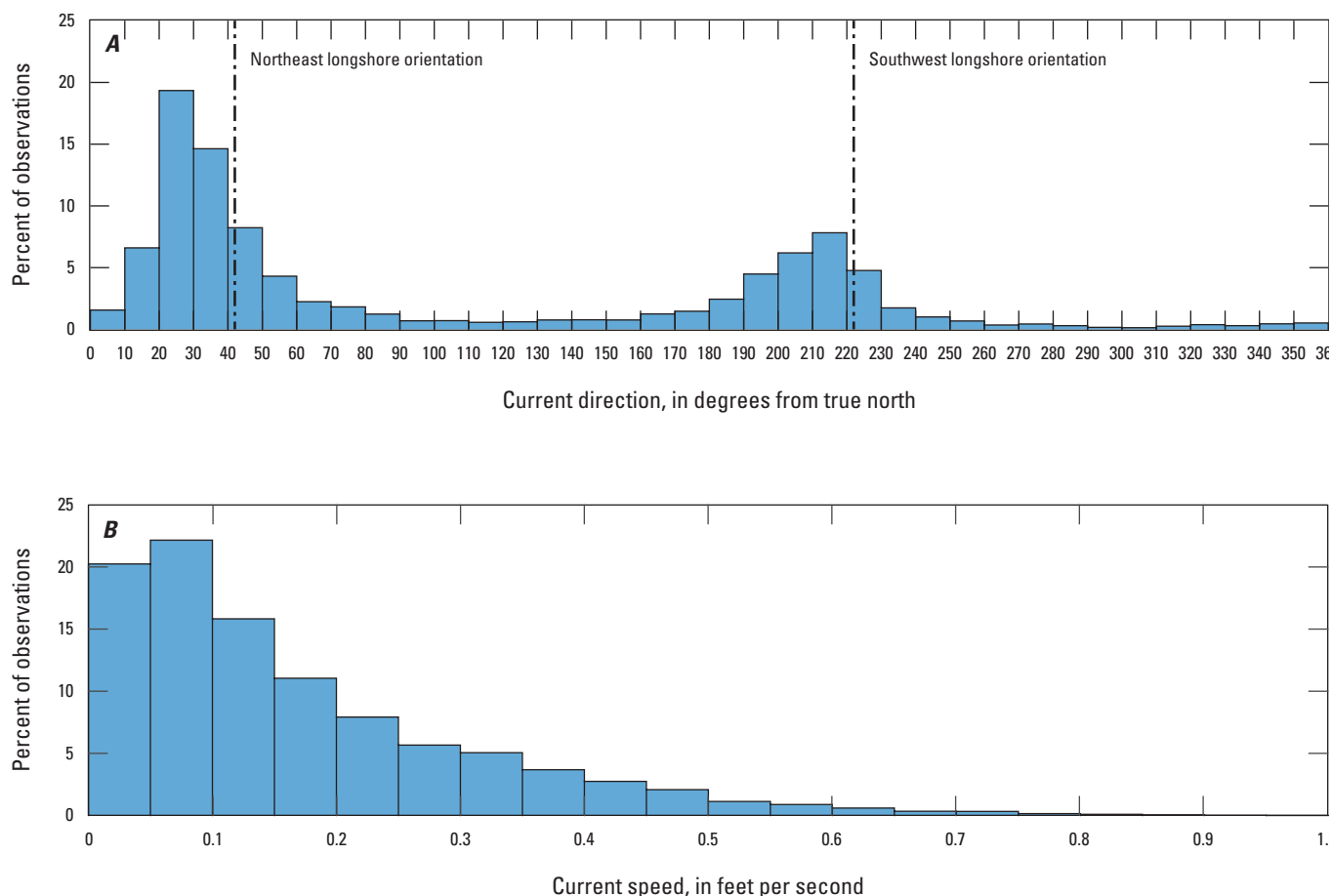


**Figure 10.** Characteristics of nearshore currents measured by the acoustic Doppler velocity meter (ADVM 1) mounted to the northwest side of the southwest caisson in front of the Wildwood Marina near Villa Angela Beach, Cleveland, Ohio. Currents were measured lakeside of the caisson from June 12 to August 28, 2019, at a height above bottom of approximately 8 feet.

Finally, the ADVM data were grouped and analyzed by time (hour of each day) to see whether any diurnal cycles were present (fig. 14). ADVM 1 and ADVM 2 showed slight peaks in the percent of observations around noon and midnight (hour window 12 and 24, respectively), indicating a weak diurnal cycle was present. This is consistent with the observation of daily repeatable wind patterns in the summer 2012 data (Jackson, 2013) and to a lesser extent in the summer 2019 data. Because of the finding that there was some relation between current direction and time, a more in-depth spectral analysis was done on the ADVM data (not shown). The current direction spectrum showed a distinct peak at 12.45 hours for ADVM 1 and 12.37 hours for ADVM 2. ADVM 2 also had a peak at 14.52 hours, which is very close to the observed period of the mode 1 longitudinal seiche in Lake Erie (14.38 hours, Platzman and Rao, 1964). ADVM 2 likely captured the mode 1 longitudinal seiche whereas ADVM 1 did

not because seiches will force water into and out of the marina as the lake level fluctuates, thus amplifying the signal for ADVM 2, which was pointed into Wildwood Marina (fig 1C).

## Longshore Currents

Throughout the entire synoptic survey period (June 10–12, 2019, and August 19–21, 2019), longshore currents as measured by the ADCP mounted on the manned boat were oriented approximately parallel to the shoreline but varied in direction either to the northeast or the southwest (figs. 15–26). The magnitude of the depth-averaged longshore currents generally ranged from 0.1 to 0.4 ft/s. The velocity colorbar is the same in all these figures to facilitate comparison among days and with previous data from summer 2012 (Jackson, 2013). Near-surface currents were generally larger than near-bed currents for most of the survey area. Each of



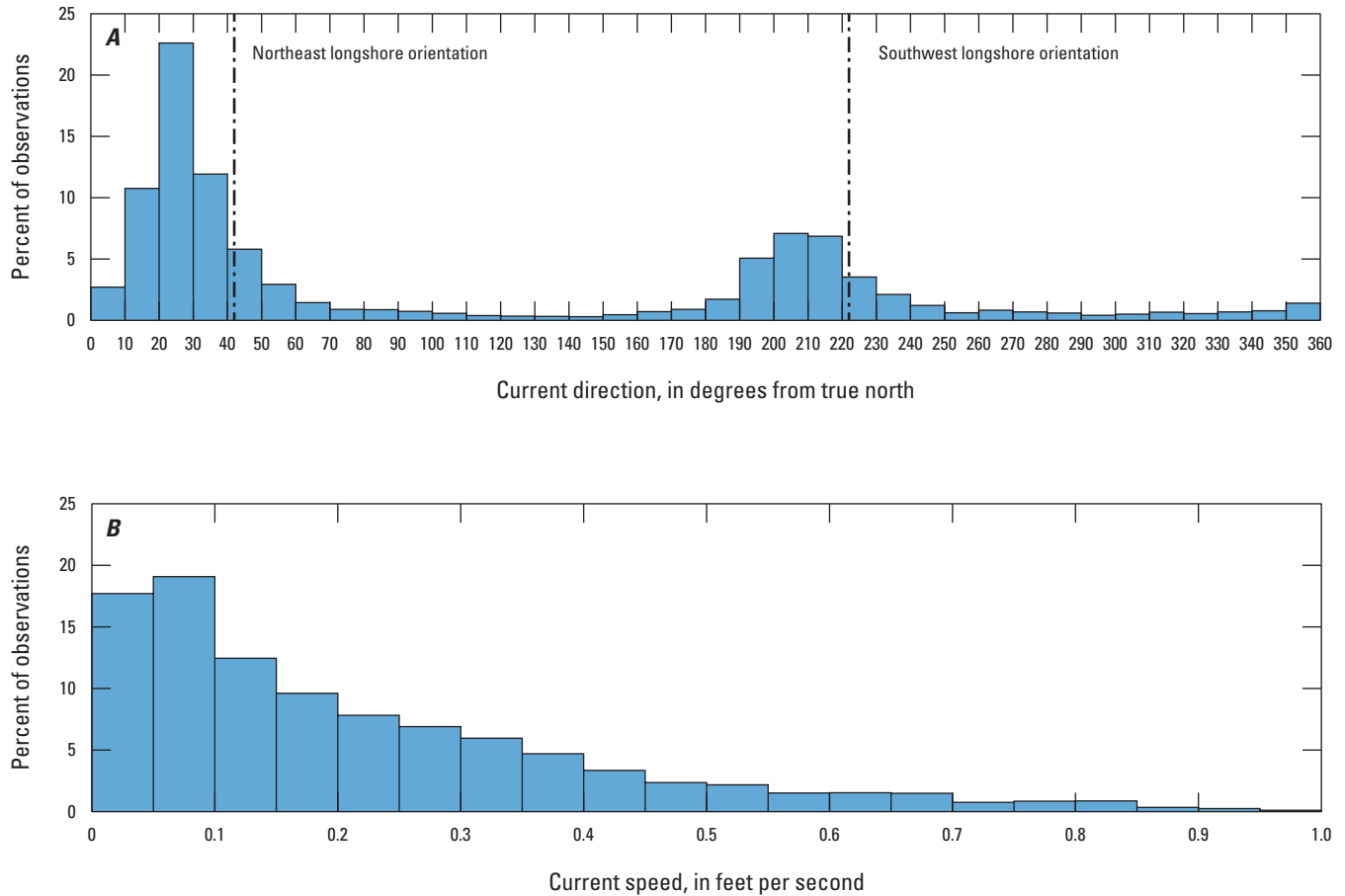


**Figure 11.** Characteristics of nearshore currents measured by the acoustic Doppler velocity meter (ADVM 2) mounted to the southeast side of the northeast caisson in front of the Wildwood Marina near Villa Angela Beach, Cleveland, Ohio. Currents were measured shoreside of the caisson from June 8 to July 23, 2019, at a height above bottom of approximately 8 feet.

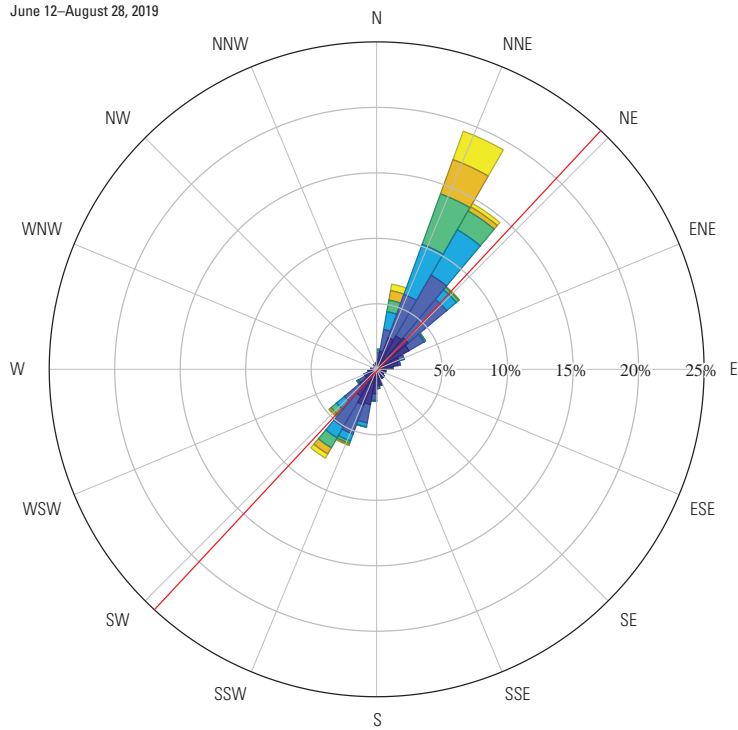
figures 15–26 includes an inset wind-rose diagram corresponding to the period between the overall start and end of the survey(s) each day. This allows for visual interpretation of any potential relation between wind and longshore current characteristics (direction and magnitude). However, because the surveys were not instantaneous (ranged from 3 to 6 hours), temporal changes commonly present as spatial variation, but there could also be true spatial variation as well. This can be difficult to separate. In addition to wind-driven longshore currents, seiches are well-documented within Lake Erie (Platzman and Rao, 1964) and can also complicate the interpretation of longshore currents.

On June 10, 2019, longshore currents were to the southwest at the start of the survey and the magnitude decreased as the survey progressed from line 1 to 18 (fig. 15). A reversal in direction to the northeast is evident starting around line 13 and onward. Recall that during the survey on June 10, a strong weather system was moving through the area, and the winds, which had been out of the south before and at the start of the

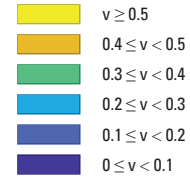
survey, were shifting to the west as the weather system moved through (fig. 7). By the time the ADCP survey was repeated in the afternoon, the longshore currents were strongly to the northeast (fig. 16). Note that the afternoon survey started at line 18 and proceeded until line 13 and then moved to line 1 and ended at line 10. If viewed in that order, an upward trend in velocity magnitude can be observed (fig. 16). Because of time constraints and safety reasons (the waves were getting too large for the boat), some lines near the end of the survey were selectively skipped while still covering the full extent of the survey area around Villa Angela Beach, but nevertheless, the overall characteristics of the longshore currents are evident. It is not entirely obvious how an approximately 90-degree shift in the wind could cause the longshore currents to reverse direction or if the response of the longshore currents to the wind happens that quickly. Between the start of the survey (fig. 15) and the end of the survey (fig. 16), the longshore currents changed direction over a period of 5.5 hours. The mode 3 longitudinal seiche for Lake Erie has a period of

**A. Acoustic Doppler velocity meter 1**

June 12–August 28, 2019

**EXPLANATION**

[v, current velocity; %, percent]

**Current velocity, in feet per second**

— Approximate shoreline orientation

**B. Acoustic Doppler velocity meter 2**

June 8–July 23, 2019

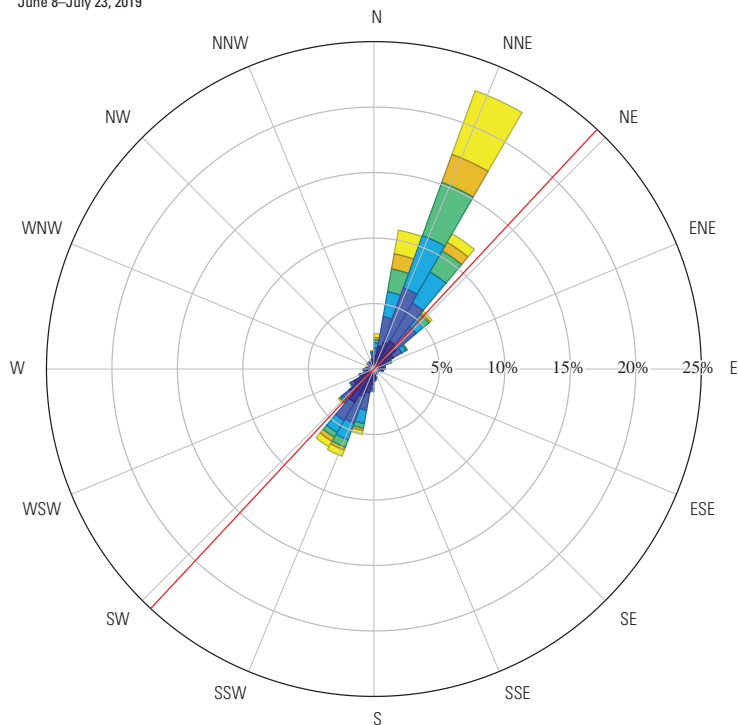


**Figure 12.** Current-rose diagrams of the current direction and current speed characteristics measured by *A*, the acoustic Doppler velocity meter (ADVM 1) mounted to the northwest side of the southwest caisson in front of the Wildwood Marina near Villa Angela Beach, Cleveland, Ohio, for the period June 12–August 28, 2019, and *B*, the acoustic Doppler velocity meter (ADVM 2) mounted to the southeast side of the northeast caisson in front of the Wildwood Marina near Villa Angela Beach, Cleveland, Ohio, for the period June 8–July 23, 2019.

**Table 5.** Prevalence of the orientation of the longshore current component of observed currents, sorted by bin, measured by the acoustic Doppler velocity meter (ADVM 1) mounted to the northwest side of the southwest caisson in front of the Wildwood Marina near Villa Angela Beach, Cleveland, Ohio, for the period June 12–August 28, 2019, and the acoustic Doppler velocity meter (ADVM 2) mounted to the southeast side of the northeast caisson in front of the Wildwood Marina near Villa Angela Beach, Cleveland, Ohio, for the period June 8–July 23, 2019, at a height above bottom of approximately 8 feet.

[ADVM, acoustic Doppler velocity meter; ft, foot]

ADVM	Bin	Bin range (ft from ADVM)	Northeast longshore current component (percent of observations)	Southwest longshore current component (percent of observations)
1	1	6–39	64.3	35.7
1	2	39–72	64.8	35.2
1	3	72–105	65.0	35.0
2	1	5–11	67.2	32.8
2	2	11–17	66.6	33.4
2	3	17–23	65.4	34.6
2	4	23–29	66.2	33.8
2	5	29–35	67.0	33.0
2	6	35–41	65.6	34.4
2	7	41–47	66.3	33.7

**Table 6.** Prevalence of the orientation of the longshore current component of observed currents, sorted by month, measured by the acoustic Doppler velocity meter (ADVM 1) mounted to the northwest side of the southwest caisson in front of the Wildwood Marina near Villa Angela Beach, Cleveland, Ohio, for the period June 12–August 28, 2019, and the acoustic Doppler velocity meter (ADVM 2) mounted to the southeast side of the northeast caisson in front of the Wildwood Marina near Villa Angela Beach, Cleveland, Ohio, for the period June 8–July 23, 2019, at a height above bottom of approximately 8 feet.

[ADVM, acoustic Doppler velocity meter]

ADVM	Month	Northeast longshore current component (percent of observations)	Southwest longshore current component (percent of observations)
1	June	73.0	27.0
1	July	77.3	22.7
1	August	44.5	55.5
2	June	67.1	32.9
2	July	65.0	35.0

5.9 hours (Platzman and Rao, 1964), so this is evidence that the longshore currents on June 10 may have been affected by seiche activity in addition to the wind.

On June 11, 2019, longshore currents were to the northeast throughout the survey; however, they were stronger at the start of the survey in the morning than at the end of the survey in the afternoon (fig. 17). There are several notable observations. First, the highest velocities (red arrows) occurred in a small area near the Easterly WWTP treated effluent discharge point. Given that the seawall is flat, local flow disturbance is unlikely, so it would seem most probable that the high velocities were caused by the effluent discharge. It seems that the same discharge point was in operation (note the dark color protruding out into the lake) on the date the

aerial photograph was taken (aerial imagery date: April 26, 2017; not the same day as the survey). Second, the Easterly WWTP structure seems to shield the nearshore area to the northeast of the WWTP and creates a recirculation zone there. This setup—a strong longshore current creating a recirculation zone on the leeward side of a structure protruding from the shoreline—was also observed in the summer 2012 surveys (fig. 9 in Jackson, 2013). Because of how the study area was split into two separate areas (lines 1–18 near Villa Angela Beach and lines 23–45 near the Easterly WWTP) which were surveyed on different days, it is not clear if the recirculation zone observed on June 11 extends all the way to Villa Angela Beach, but it seems to be lessening toward the northeastern extent of the survey (line 23). Roughly fitting a line to the

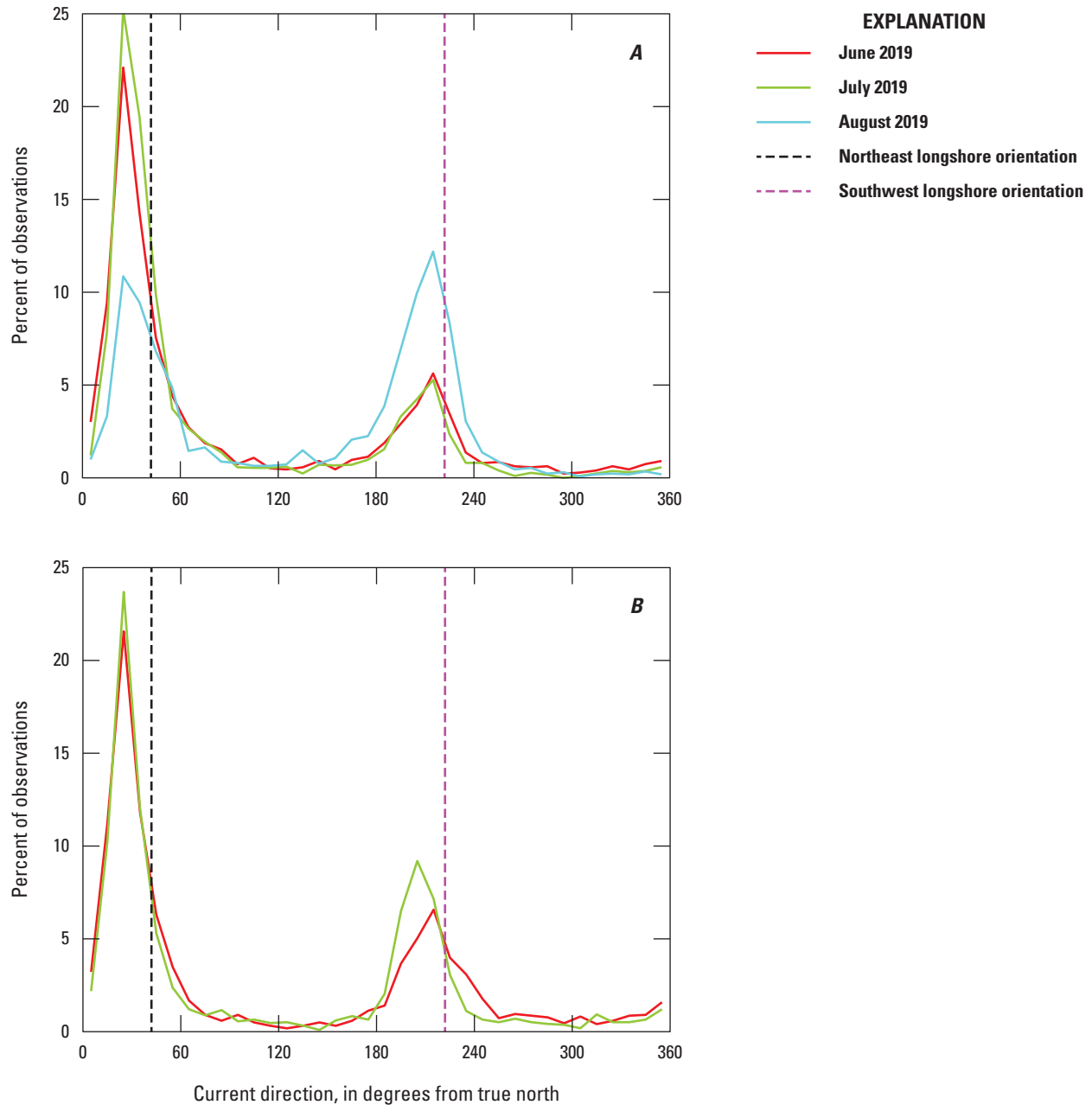


**Figure 13.** Monthly characteristics of nearshore currents measured by *A*, the acoustic Doppler velocity meter (ADVM 1) mounted to the northwest side of the southwest caisson in front of the Wildwood Marina near Villa Angela Beach, Cleveland, Ohio, for the period June 12–August 28, 2019, and *B*, the acoustic Doppler velocity meter (ADVM 2) mounted to the southeast side of the northeast caisson in front of the Wildwood Marina near Villa Angela Beach, Cleveland, Ohio, for the period June 8–July 23, 2019, at a height above bottom of approximately 8 feet. Histogram data are presented as a line plot (by connecting the top center of each bin with a line) to improve clarity.

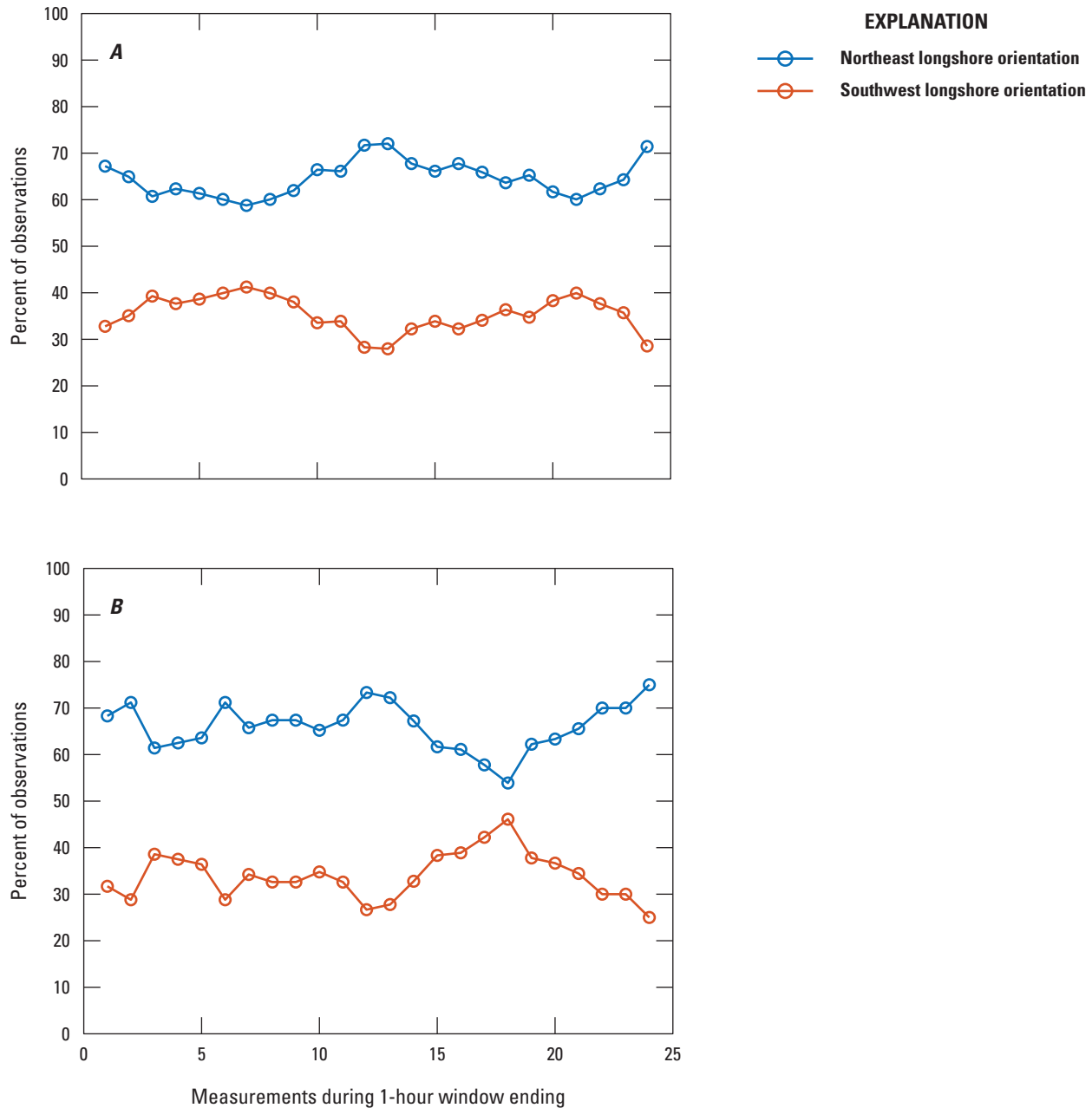
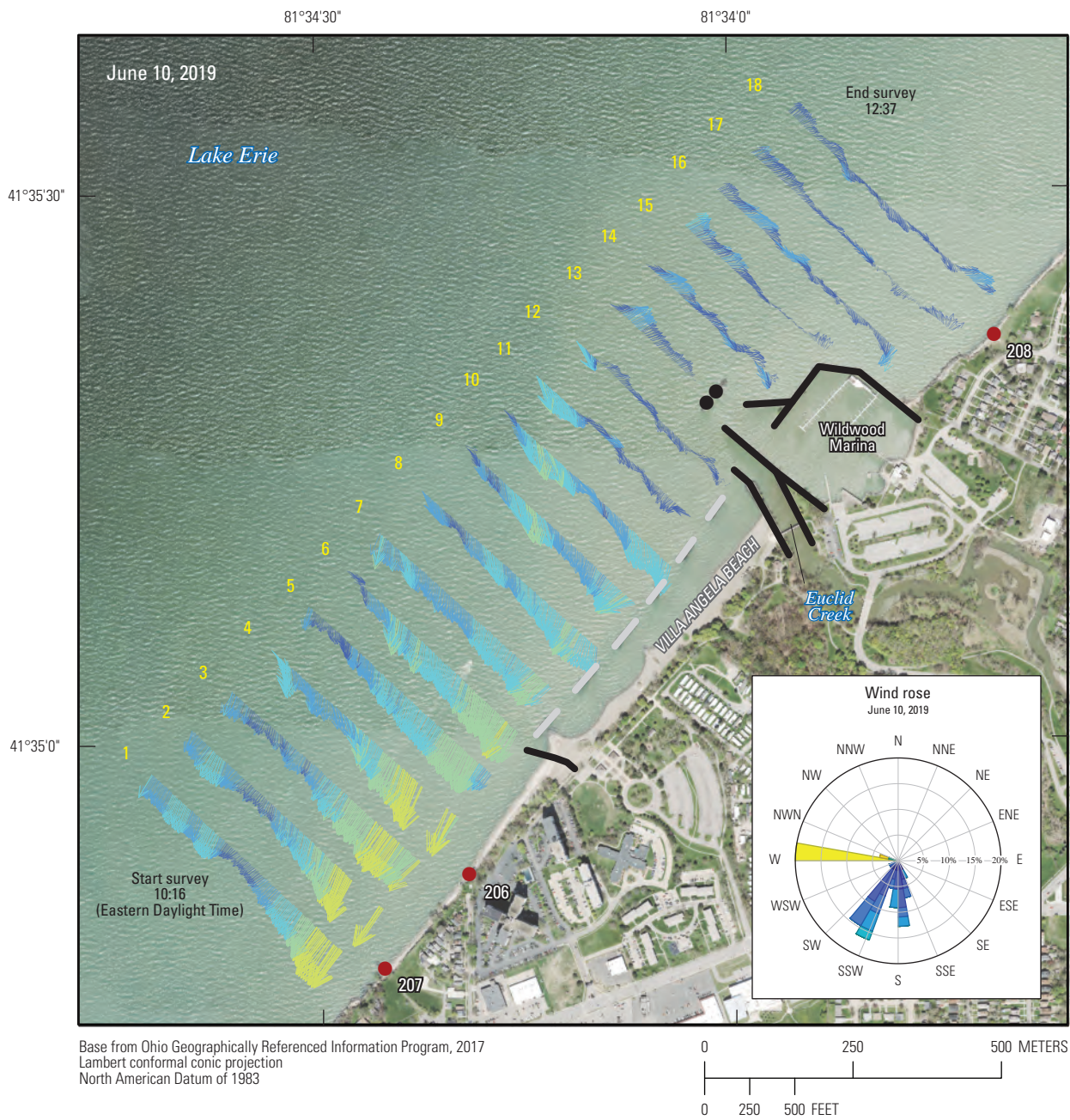


**Figure 14.** Hourly characteristics of nearshore currents measured by *A*, the acoustic Doppler velocity meter (ADVM 1) mounted to the northwest side of the southwest caisson in front of the Wildwood Marina near Villa Angela Beach, Cleveland, Ohio, for the period June 12–August 28, 2019, and *B*, the acoustic Doppler velocity meter (ADVM 2) mounted to the southeast side of the northeast caisson in front of the Wildwood Marina near Villa Angela Beach, Cleveland, Ohio, for the period June 8–July 23, 2019, at a height above bottom of approximately 8 feet. Histogram data are presented as a line plot (by connecting the top center of each bin with a line) to improve clarity.








### EXPLANATION


[w<sub>s</sub>, wind speed; %, percent]


**MAIN MAP**

 Survey line number

 Breakwaters

 Piers













 Caissons

 Combined sewer overflow locations and number

*207*

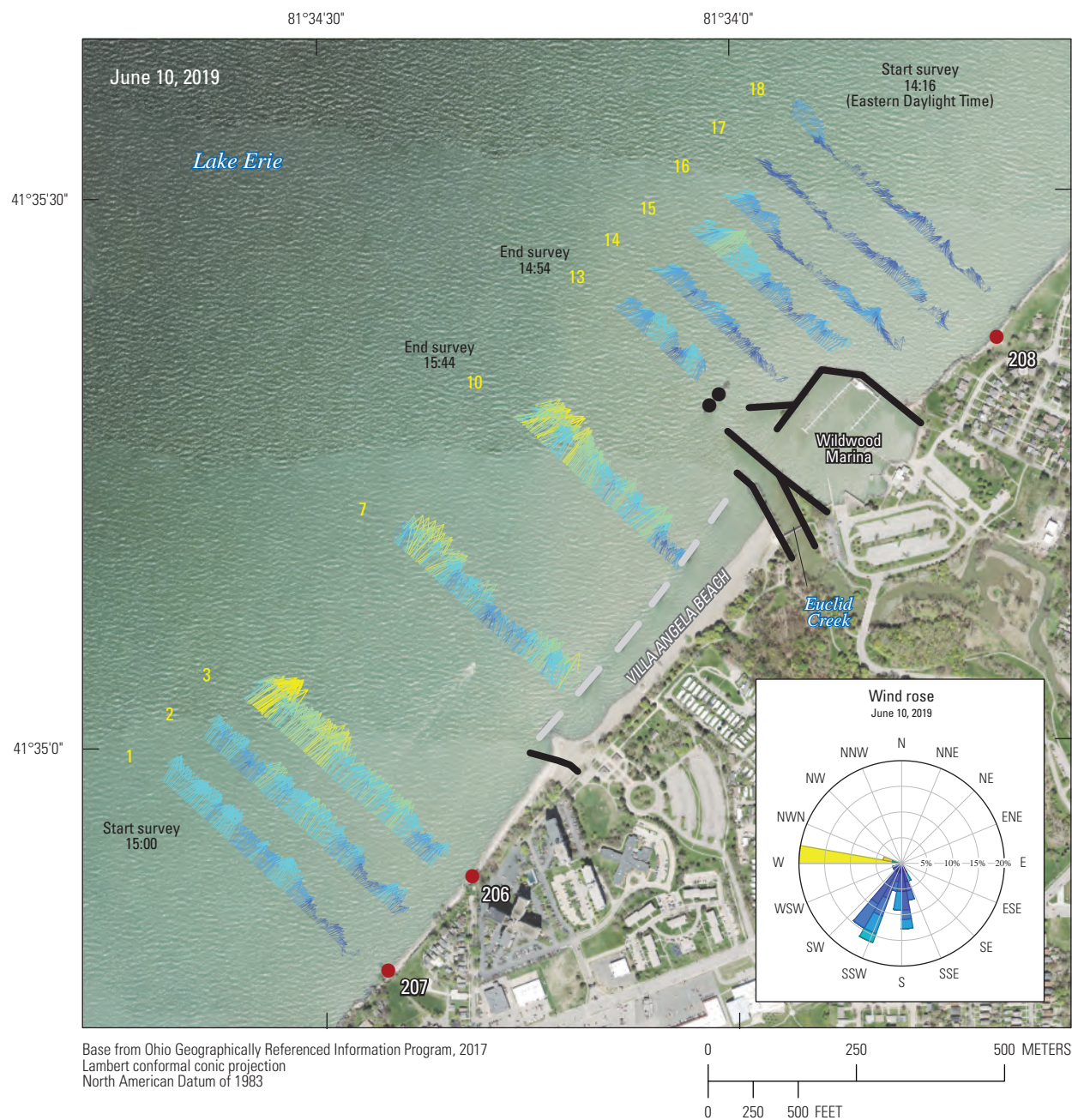
**WIND ROSE INSET**

Wind speed, in miles per hour

	$w_s \geq 15$		$5 \leq w_s < 6$
	$10 \leq w_s < 15$		$4 \leq w_s < 5$
	$9 \leq w_s < 10$		$3 \leq w_s < 4$
	$8 \leq w_s < 9$		$2 \leq w_s < 3$
	$7 \leq w_s < 8$		$1 \leq w_s < 2$
	$6 \leq w_s < 7$		$0 \leq w_s < 1$

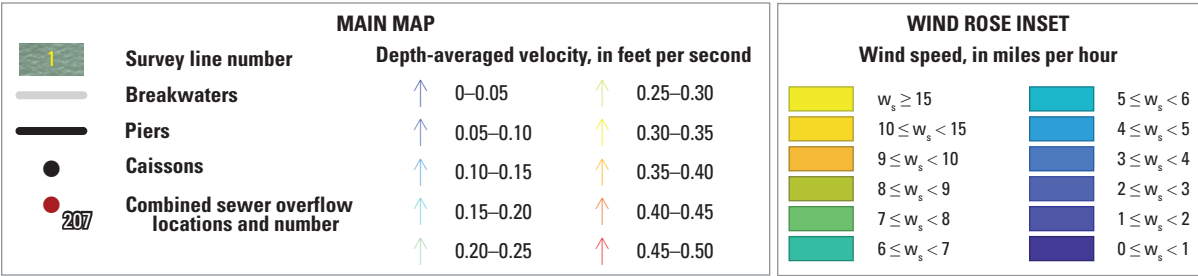
**Figure 15.** Depth-averaged currents in coastal Lake Erie in the vicinity of Villa Angela Beach and Euclid Creek, Cleveland, Ohio, morning of June 10, 2019.





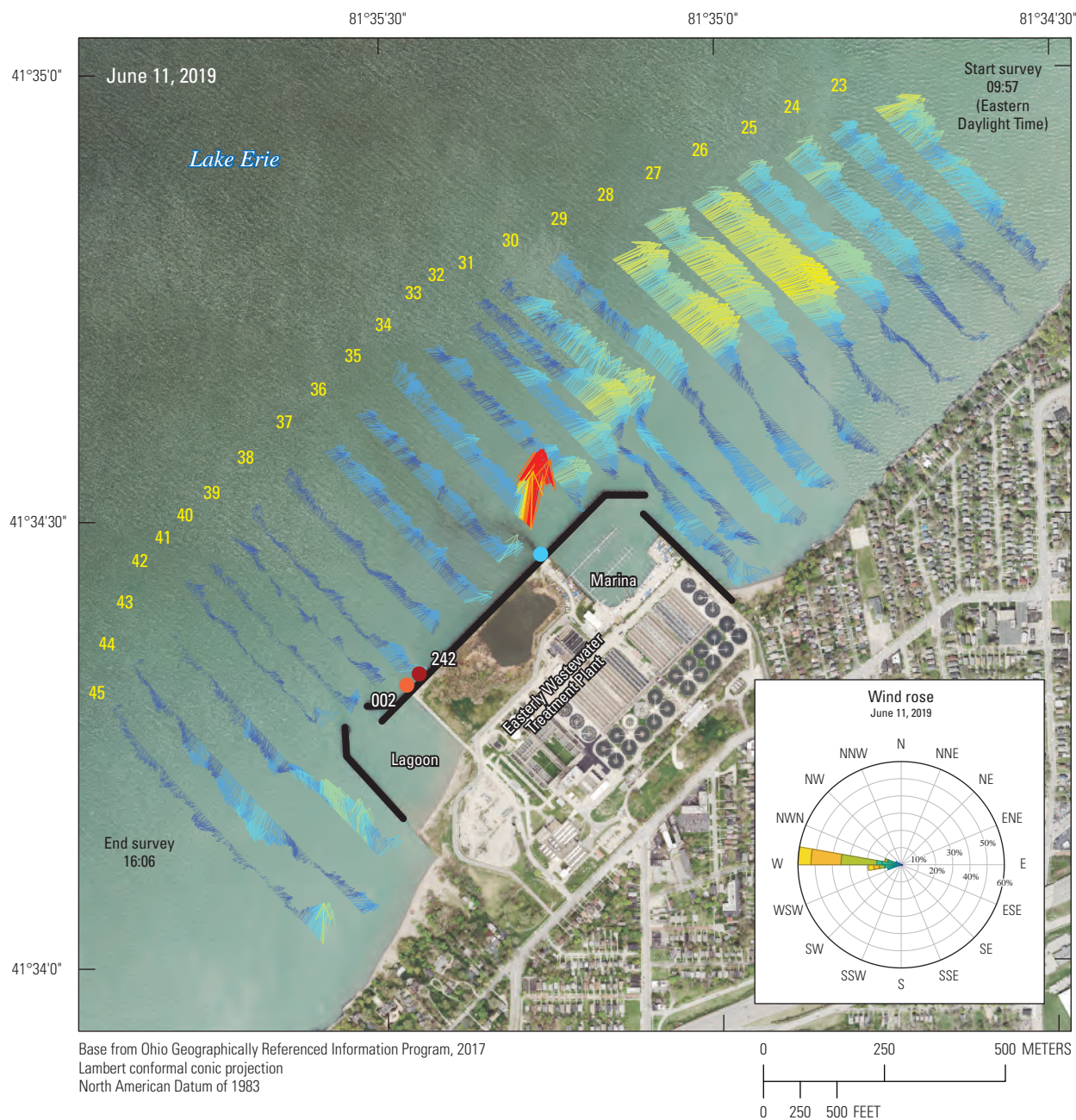
Base from Ohio Geographically Referenced Information Program, 2017  
Lambert conformal conic projection  
North American Datum of 1983

**EXPLANATION**  
[ $w_s$ , wind speed; %, percent]

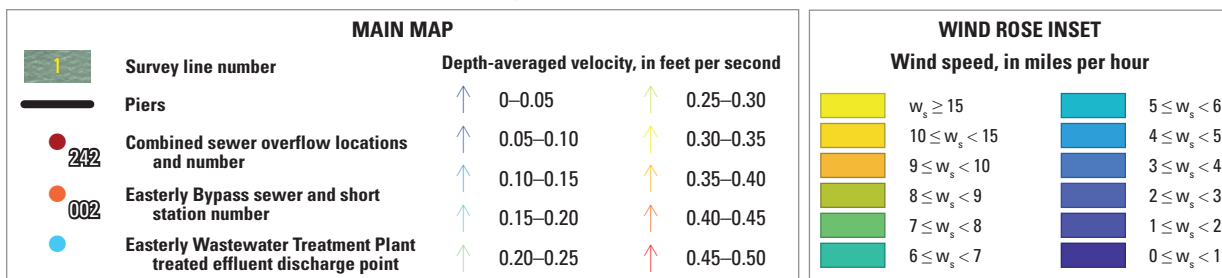


**Figure 16.** Depth-averaged currents in coastal Lake Erie in the vicinity of Villa Angela Beach and Euclid Creek, Cleveland, Ohio, afternoon of June 10, 2019.





## EXPLANATION

[ $w_s$ , wind speed; %, percent]

**Figure 17.** Depth-averaged currents in coastal Lake Erie in the vicinity of the Easterly Wastewater Treatment Plant, Cleveland, Ohio, June 11, 2019.



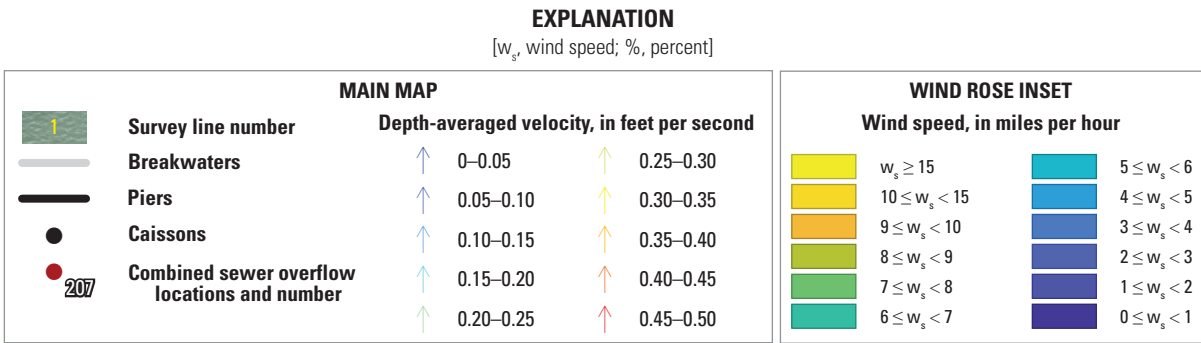
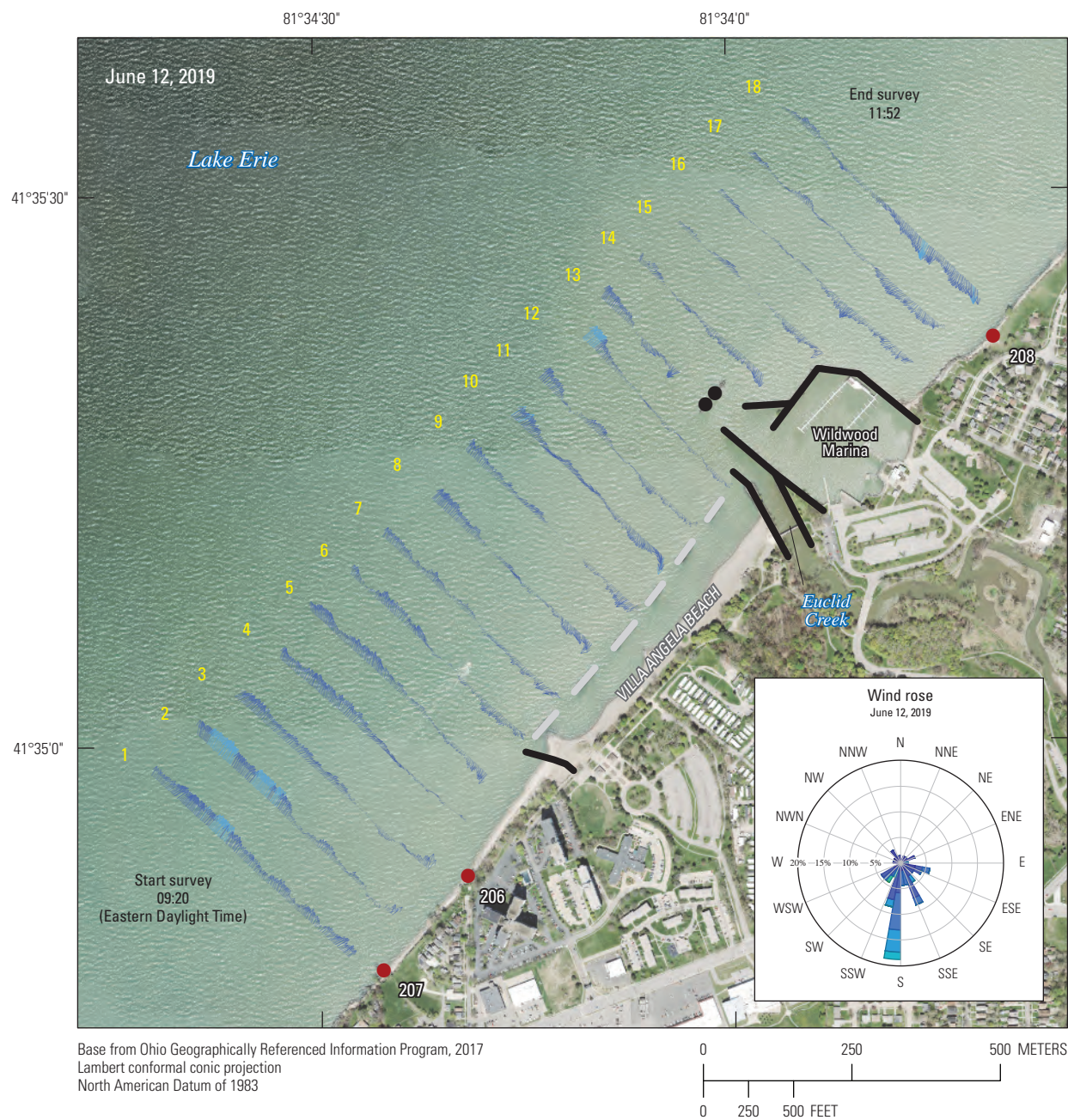
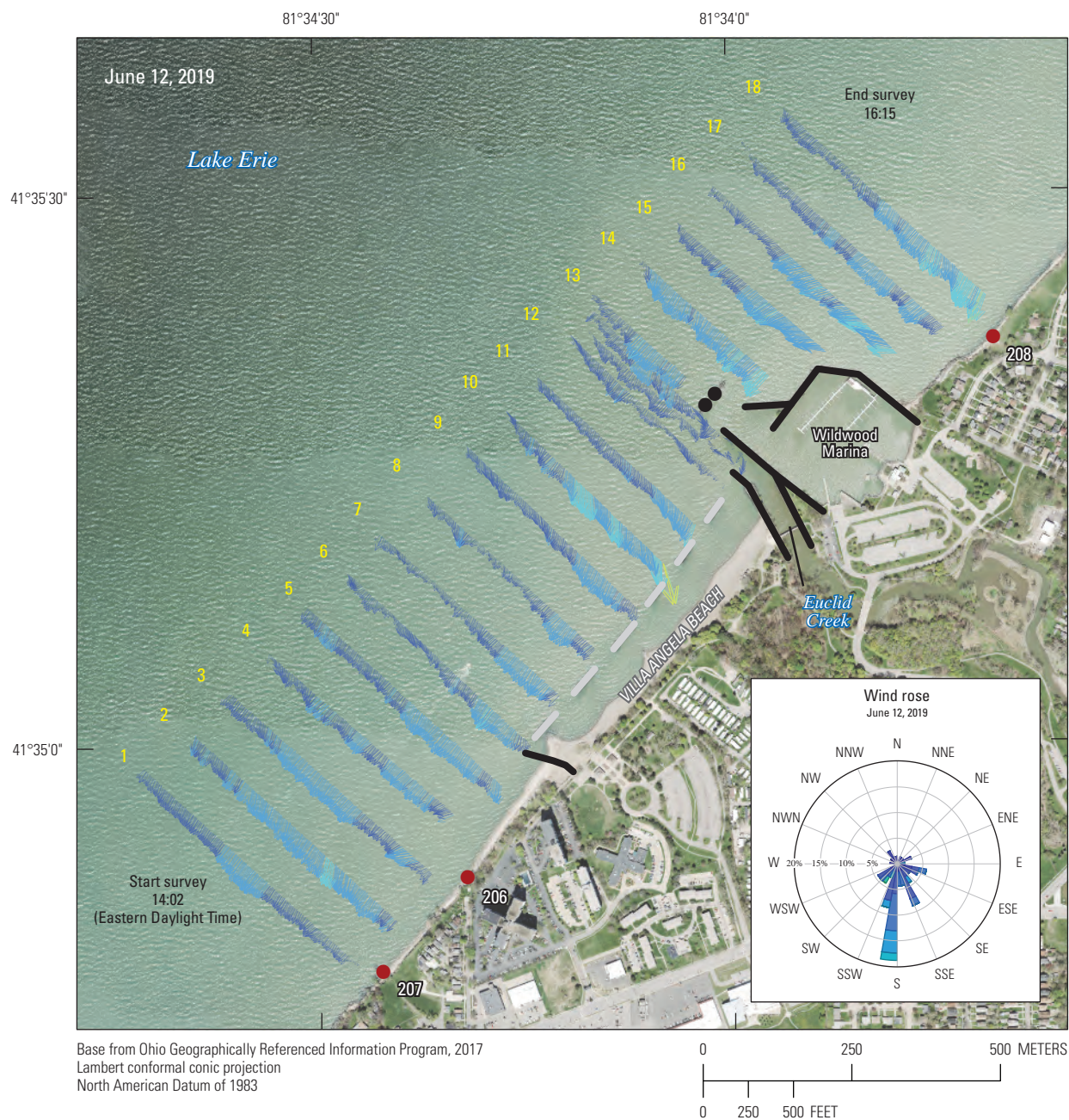


**Figure 18.** Depth-averaged currents in coastal Lake Erie in the vicinity of Villa Angela Beach and Euclid Creek, Cleveland, Ohio, morning of June 12, 2019.





# EXPLANATION

[ $w_s$ , wind speed; %, percent]

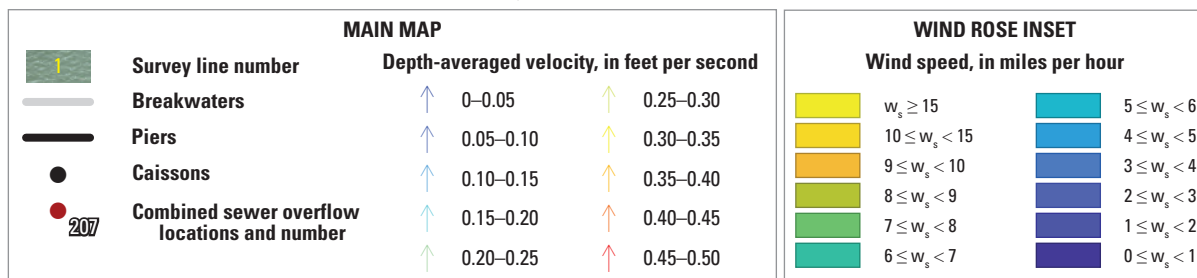
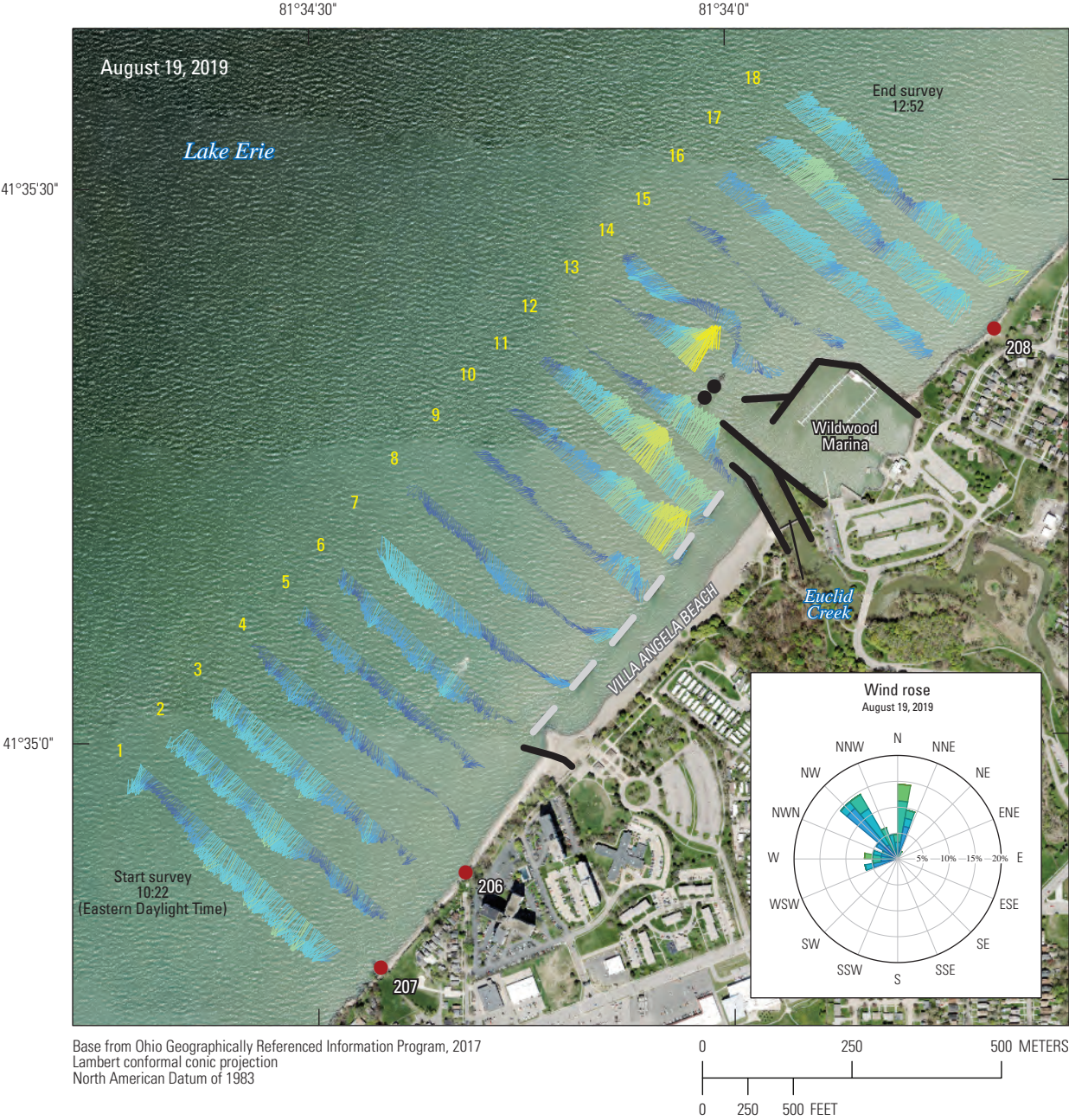


**Figure 19.** Depth-averaged currents in coastal Lake Erie in the vicinity of Villa Angela Beach and Euclid Creek, Cleveland, Ohio, afternoon of June 12, 2019.





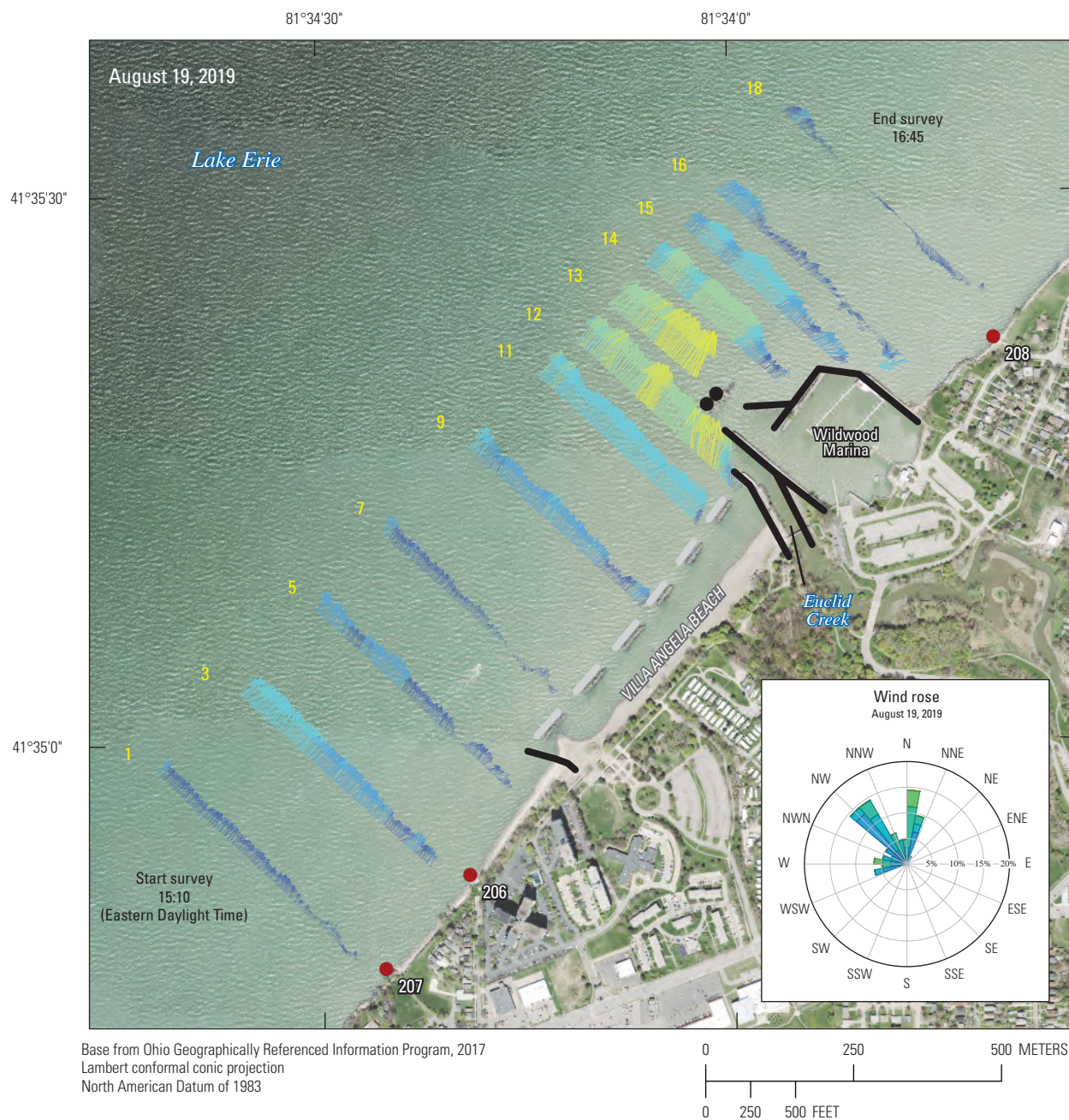
Base from Ohio Geographically Referenced Information Program, 2017  
Lambert conformal conic projection  
North American Datum of 1983

EXPLANATION  
[w<sub>s</sub>, wind speed; %, percent]

MAIN MAP			WIND ROSE INSET			
1	Survey line number	Depth-averaged velocity, in feet per second	Wind speed, in miles per hour			
	Breakwaters	↑ 0–0.05      ↑ 0.25–0.30	w <sub>s</sub> ≥ 15	5 ≤ w <sub>s</sub> < 6	4 ≤ w <sub>s</sub> < 5	3 ≤ w <sub>s</sub> < 4
	Piers	↑ 0.05–0.10      ↑ 0.30–0.35	10 ≤ w <sub>s</sub> < 15	4 ≤ w <sub>s</sub> < 5	3 ≤ w <sub>s</sub> < 4	2 ≤ w <sub>s</sub> < 3
	Caissons	↑ 0.10–0.15      ↑ 0.35–0.40	9 ≤ w <sub>s</sub> < 10	3 ≤ w <sub>s</sub> < 4	2 ≤ w <sub>s</sub> < 3	1 ≤ w <sub>s</sub> < 2
207	Combined sewer overflow locations and number	↑ 0.15–0.20      ↑ 0.40–0.45	8 ≤ w <sub>s</sub> < 9	2 ≤ w <sub>s</sub> < 3	1 ≤ w <sub>s</sub> < 2	0 ≤ w <sub>s</sub> < 1
		↑ 0.20–0.25      ↑ 0.45–0.50	7 ≤ w <sub>s</sub> < 8	1 ≤ w <sub>s</sub> < 2	0 ≤ w <sub>s</sub> < 1	
			6 ≤ w <sub>s</sub> < 7	0 ≤ w <sub>s</sub> < 1		

**Figure 20.** Depth-averaged currents in coastal Lake Erie in the vicinity of Villa Angela Beach and Euclid Creek, Cleveland, Ohio, morning of August 19, 2019.





### EXPLANATION

[ $w_s$ , wind speed; %, percent]

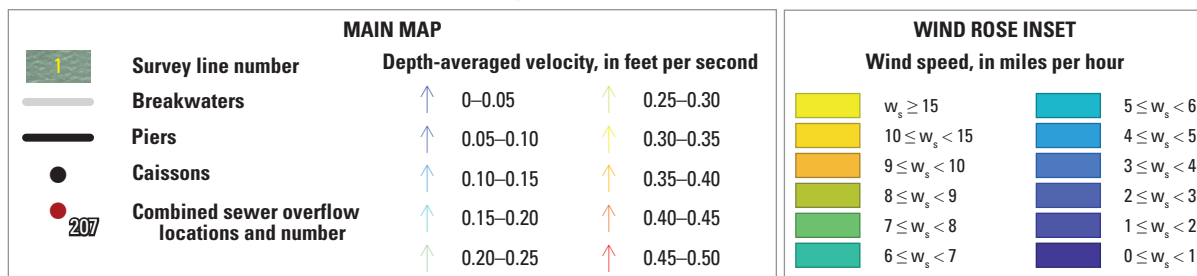
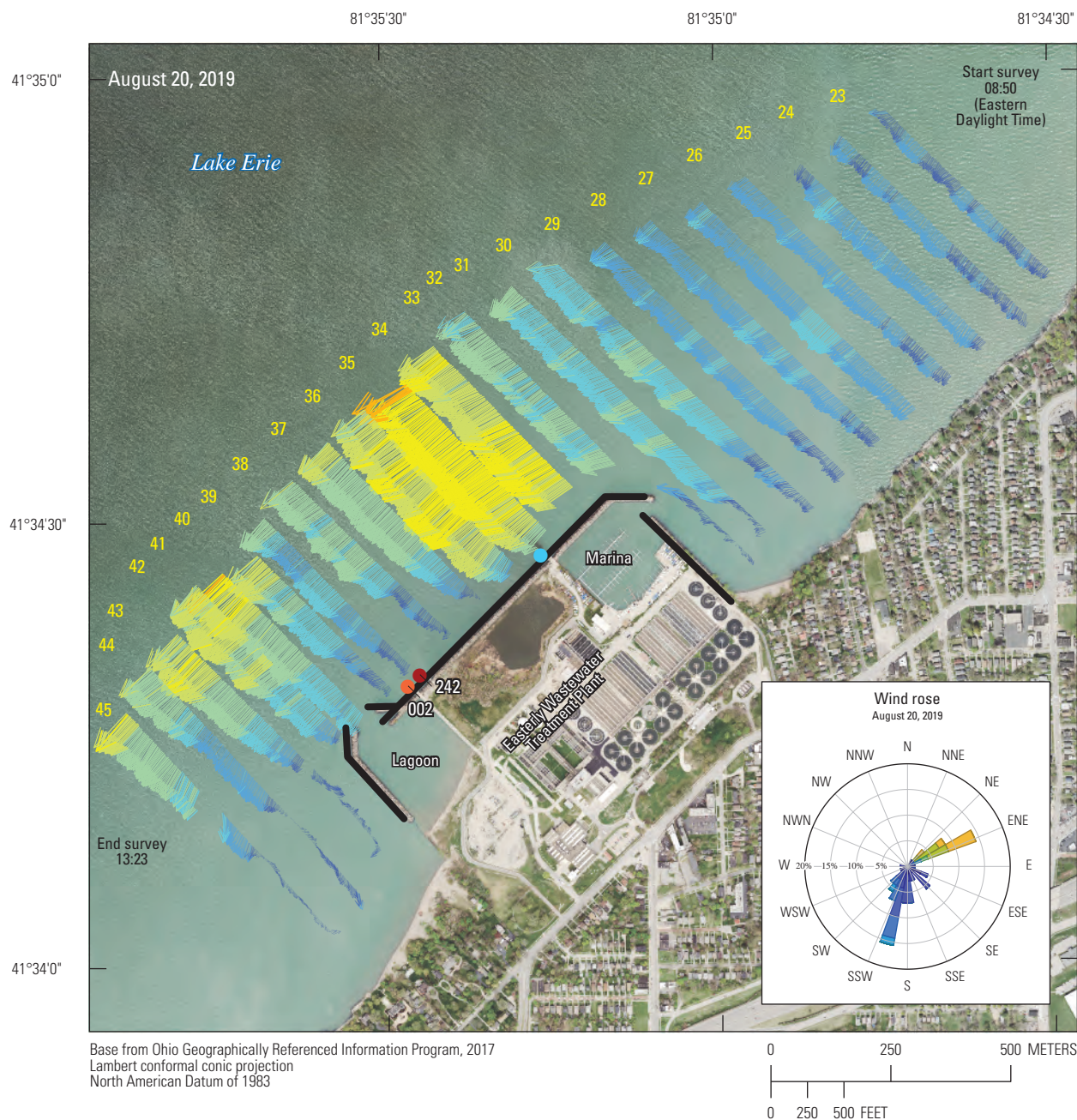


**Figure 21.** Depth-averaged currents in coastal Lake Erie in the vicinity of Villa Angela Beach and Euclid Creek, Cleveland, Ohio, afternoon of August 19, 2019.

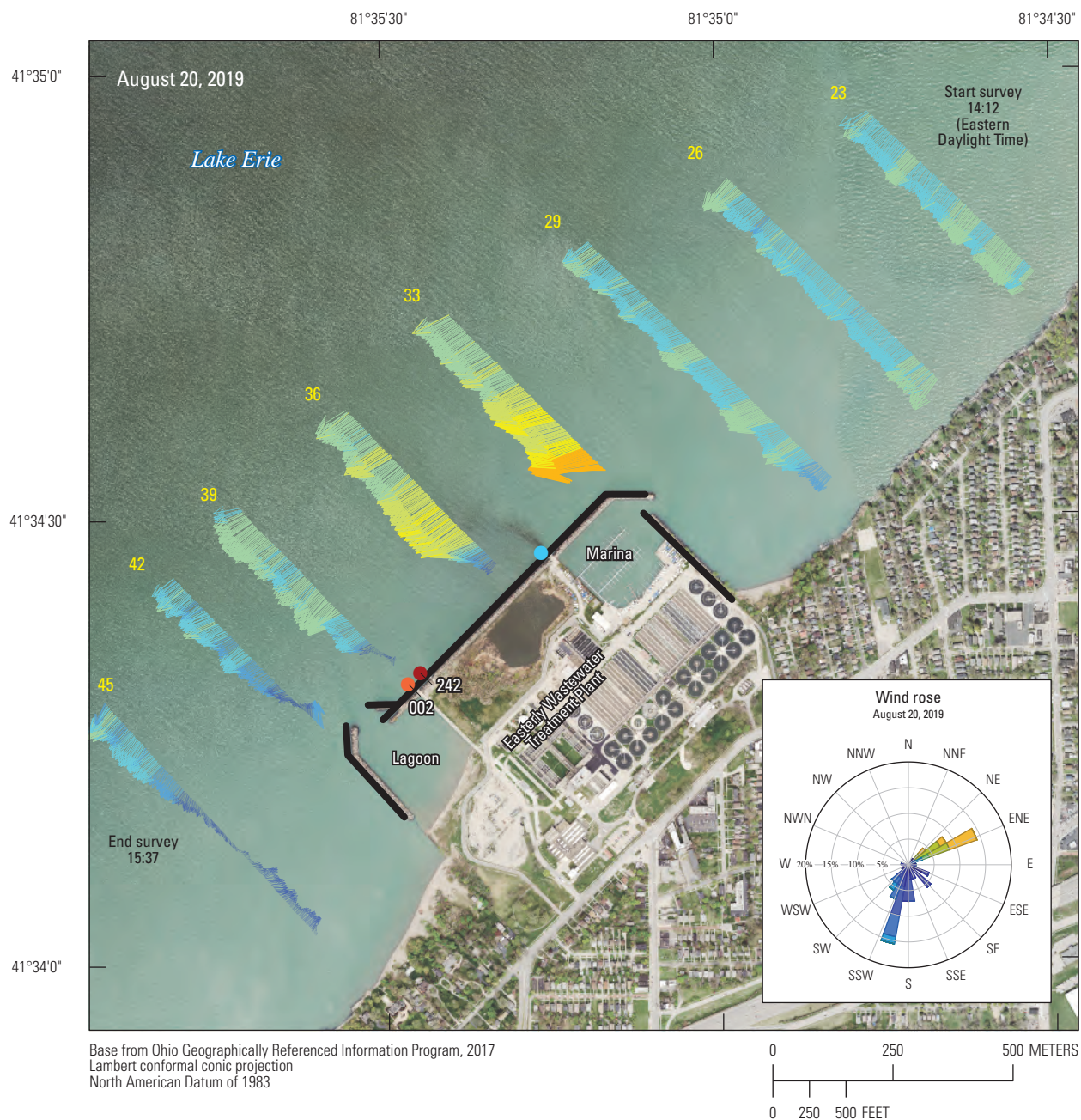




MAIN MAP			WIND ROSE INSET	
			Wind speed, in miles per hour	
1	Survey line number	Depth-averaged velocity, in feet per second	$w_s \geq 15$	$5 \leq w_s < 6$
—	Piers	0–0.05	$10 \leq w_s < 15$	$4 \leq w_s < 5$
242	Combined sewer overflow locations and number	0.05–0.10	$9 \leq w_s < 10$	$3 \leq w_s < 4$
002	Easterly Bypass sewer and short station number	0.10–0.15	$8 \leq w_s < 9$	$2 \leq w_s < 3$
●	Easterly Wastewater Treatment Plant treated effluent discharge point	0.15–0.20	$7 \leq w_s < 8$	$1 \leq w_s < 2$
		0.20–0.25	$6 \leq w_s < 7$	$0 \leq w_s < 1$
		0.25–0.30		
		0.30–0.35		
		0.35–0.40		
		0.40–0.45		
		0.45–0.50		

**Figure 22.** Depth-averaged currents in coastal Lake Erie in the vicinity of the Easterly Wastewater Treatment Plant, Cleveland, Ohio, morning of August 20, 2019.



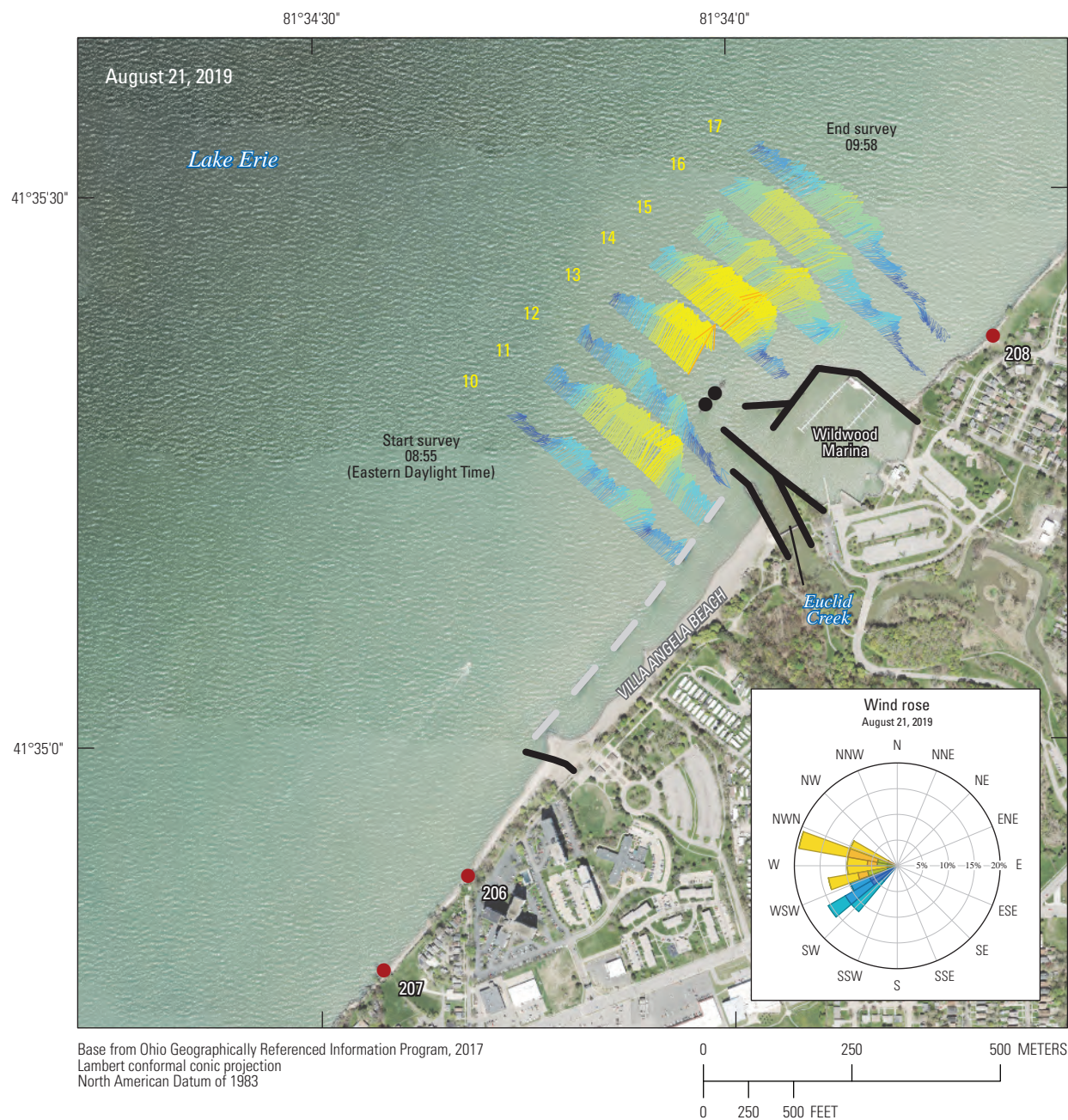


**EXPLANATION**  
[ $w_s$ , wind speed; %, percent]

MAIN MAP			WIND ROSE INSET	
	Survey line number	Depth-averaged velocity, in feet per second	Wind speed, in miles per hour	
1	Piers	0–0.05	$w_s \geq 15$	$5 \leq w_s < 6$
242	Combined sewer overflow locations and number	0.05–0.10	$10 \leq w_s < 15$	$4 \leq w_s < 5$
002	Easterly Bypass sewer and short station number	0.10–0.15	$9 \leq w_s < 10$	$3 \leq w_s < 4$
	Easterly wastewater treatment plant treated effluent discharge point	0.15–0.20	$8 \leq w_s < 9$	$2 \leq w_s < 3$
		0.20–0.25	$7 \leq w_s < 8$	$1 \leq w_s < 2$
		0.25–0.30	$6 \leq w_s < 7$	$0 \leq w_s < 1$
		0.30–0.35		
		0.35–0.40		
		0.40–0.45		
		0.45–0.50		

**Figure 23.** Depth-averaged currents in coastal Lake Erie in the vicinity of the Easterly Wastewater Treatment Plant, Cleveland, Ohio, afternoon of August 20, 2019.





Base from Ohio Geographically Referenced Information Program, 2017  
Lambert conformal conic projection  
North American Datum of 1983

EXPLANATION

[ $w_s$ , wind speed; %, percent]

MAIN MAP			WIND ROSE INSET	
Survey line number			Wind speed, in miles per hour	
Breakwaters			$w_s \geq 15$	
Piers			$10 \leq w_s < 15$	
Caissons			$9 \leq w_s < 10$	
Combined sewer overflow locations and number			$8 \leq w_s < 9$	
			$7 \leq w_s < 8$	
			$6 \leq w_s < 7$	
			$5 \leq w_s < 6$	
			$4 \leq w_s < 5$	
			$3 \leq w_s < 4$	
			$2 \leq w_s < 3$	
			$1 \leq w_s < 2$	
			$0 \leq w_s < 1$	

**Figure 24.** Depth-averaged currents in coastal Lake Erie in the vicinity of Villa Angela Beach and Euclid Creek, Cleveland, Ohio, morning of August 21, 2019.





MAIN MAP			WIND ROSE INSET	
	Survey line number	Depth-averaged velocity, in feet per second	Wind speed, in miles per hour	
	Breakwaters	0–0.05    0.20–0.25    0.35–0.40	$w_s \geq 15$	$5 \leq w_s < 6$
	Piers	0.05–0.10    0.25–0.30    0.40–0.45	$10 \leq w_s < 15$	$4 \leq w_s < 5$
	Caissons	0.10–0.15    0.30–0.35    0.45–0.50	$9 \leq w_s < 10$	$3 \leq w_s < 4$
	Combined sewer overflow locations and number	0.15–0.20    0.50–0.60	$8 \leq w_s < 9$	$2 \leq w_s < 3$
			$7 \leq w_s < 8$	$1 \leq w_s < 2$
			$6 \leq w_s < 7$	$0 \leq w_s < 1$

**Figure 25.** Depth-averaged currents in coastal Lake Erie in the vicinity of Villa Angela Beach and Euclid Creek, Cleveland, Ohio, later morning of August 21, 2019.



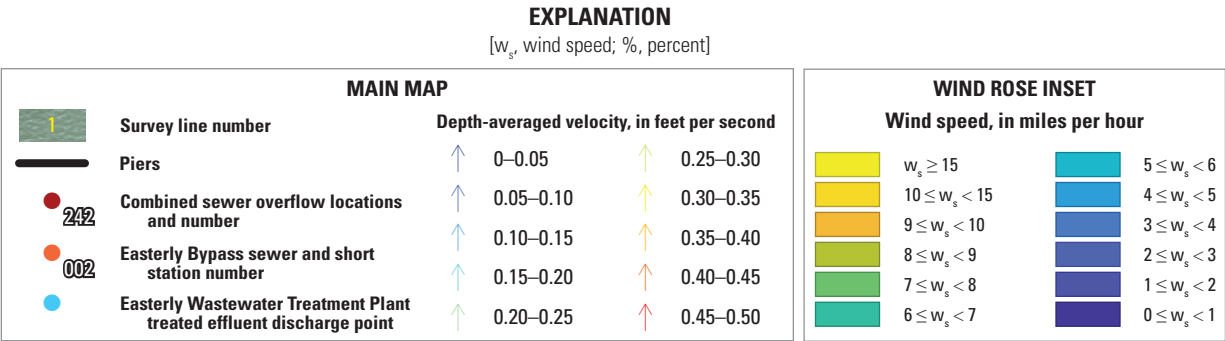
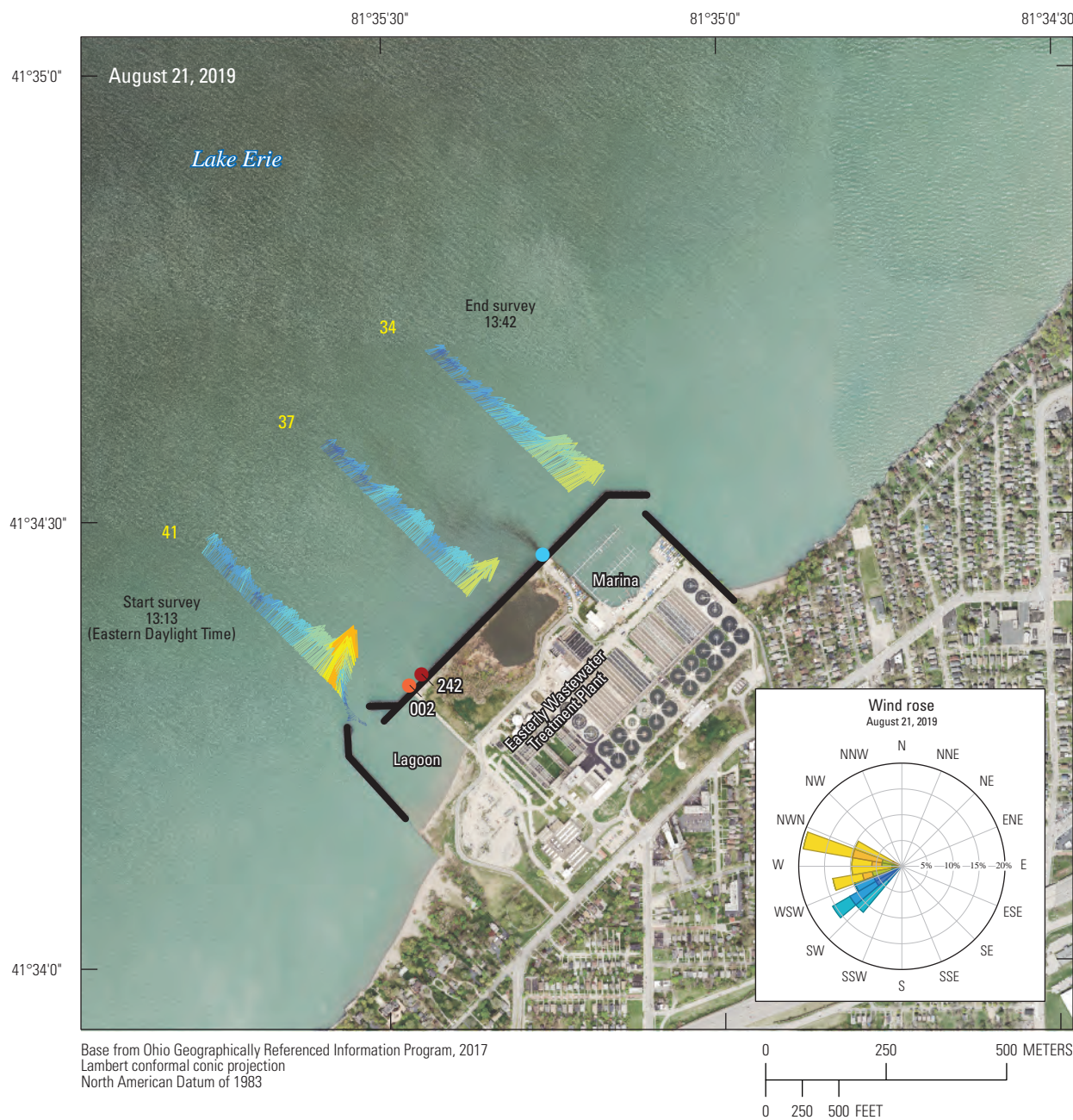


**Figure 26.** Depth-averaged currents in coastal Lake Erie in the vicinity of the Easterly Wastewater Treatment Plant, Cleveland, Ohio, afternoon of August 21, 2019.



high gradient zone bounding this recirculation (teal to blue vectors) intercepts the shoreline at about the new pier on the southwest end of Villa Angela Beach, so it is possible that the Easterly WWTP effluent discharge could be entrained into the nearshore current and transported to Villa Angela Beach. Finally, it seems that the longshore current may have been starting to reverse to the southwest toward the end of the survey and because of the interaction with the WWTP structure as described previously, created a small recirculation zone to the southwest of the WWTP in the nearshore area around lines 43–45. The winds on June 11 were moderate and steady from the west throughout the survey (fig. 7), which took about 6 hours to complete, so the variation and reversal of the longshore current may have been affected by the mode 3 longitudinal seiche (5.9 hours, Platzman and Rao, 1964).

On June 12, 2019, longshore currents were very weak and to the northeast at the start of the survey and nearly calm by the end of the survey (fig. 18). A reversal in direction to the southwest is possibly apparent starting around line 16 and onward; however, this could also be the remainder of a recirculation zone to the northeast of the marina. Either way, the velocity magnitudes are very weak compared to the previous two days. Another observation is that there is a clockwise circulation throughout nearly the entire survey (lines 4 to 18) with the currents to the northeast at the far offshore end of each survey line and currents to the southwest at the nearshore end of each survey line. The center of the circulation on each line is about 250 meters offshore and moves out and around the marina. A full velocity survey was repeated in the afternoon on June 12 when there was a consistent longshore current to the southwest throughout the survey area (fig. 19). The current was stronger in the afternoon than it was in the morning, and the clockwise circulation is gone. It is notable that there was not a recirculation zone along Villa Angela Beach as was previously observed when the longshore current was in the southwest direction (Jackson, 2013); however, this may be because of much smaller velocities (less than half the magnitude observed by Jackson [2013]) and (or) not enough time for the recirculation zone to get setup. Instead, the currents appear to be steered by the bathymetry around the shoreline structures without flow separation (except locally between the jetties bounding Euclid Creek).

On August 19, 2019, longshore currents were to the southwest at the start of the survey and abruptly reversed at line 9 to the northeast for the remainder of the survey (fig. 20). Recall that during the survey on August 19, wind speeds were moderate throughout while the wind direction shifted from west to north by the end of the survey (fig. 8). A partial velocity survey was repeated in the afternoon on August 19, and the longshore currents continued to be to the northeast throughout the survey (fig. 21). Because of time constraints, some lines were selectively skipped while still covering the full extent of the survey area around Villa Angela Beach. The stronger velocity magnitudes in lines 12–14 (fig. 21) could have been caused by flow acceleration around the piers surrounding Euclid Creek and Wildwood Marina.

On August 20, 2019, longshore currents were to the southwest throughout the survey; however, they were stronger at the end of the survey in the afternoon than at the start of the survey in the morning (fig. 22). This is consistent with the meteorological data indicating that wind speeds increased throughout the survey, but what is not seen is the effect of the abrupt change in wind direction from the south-southwest to the east-northeast about halfway through the survey (fig. 8). Another possible explanation is that the longshore currents were forced to accelerate around the Easterly WWTP because of how the pier structure protrudes out from the shoreline. Again, this is the challenge of trying to separate temporal variation from spatial variation. Additionally, the Easterly WWTP structure seems to shield the nearshore area to the southwest of the WWTP but failed to produce a strong recirculation zone. A partial velocity survey was repeated in the afternoon on August 20, and the longshore currents continued to be to the southwest throughout the survey producing some evidence that a coherent recirculation zone developed to the southwest of the Easterly WWTP and extended northeast to CSO outfall 242 (fig. 23; lines 39–45). Because of time constraints, some lines were selectively skipped while still covering the full extent of the survey area around the Easterly WWTP.

On August 21, 2019, longshore currents were to the northeast throughout the survey (figs. 24–26). Because this was an unexpected extra day of data collection made possible because of favorable conditions during the surveys on the previous two days, additional data were collected with a slightly modified and condensed survey. The morning velocity survey (fig. 24) was concurrent with the AUV, and because of the observed wind and current directions, focus was placed on the area around the mouth of Euclid Creek and to the northeast where the creek plume was expected to be mixing. A small recirculation zone was apparent northeast of the marina within about 200 ft of shore. A partial velocity survey was repeated later in the morning on August 21, and the longshore currents continued to be to the northeast throughout the survey (fig. 25). Because of time constraints, some lines were selectively skipped while still covering the full extent of the survey area around Villa Angela Beach and to the northeast of the mouth of Euclid Creek. The highest depth-averaged velocity (0.58 ft/s) measured during the entire synoptic survey period (June 10–12 and August 19–21) was observed on line 13 near the caissons (dark violet arrows, fig. 25). It is notable that there was not a recirculation zone to the northeast of the marina even though the longshore currents were strong. The wake of the caissons is shown in lines 14 and 15 (blue vectors about 300 ft offshore from Wildwood Marina and inline with the caissons, fig. 25). It is possible that the caissons play a role in flow separation and the formation of recirculation zones, but it is unclear why the weaker of the two flow fields on August 21 caused recirculation (fig. 24). There may be more to learn from depth-averaged velocities or the strength of the currents between the caissons and the marina that may disrupt the formation of a recirculation zone. Slight differences in the angle of attack of currents as they meet the caissons

and marina may also be important. In the time remaining on August 21, three lines were measured near the Easterly WWTP (fig. 26) to determine whether the longshore currents were the same there as they were near Villa Angela Beach that morning. It was observed that the longshore currents also were to the northeast but somewhat weaker than they had been during the morning surveys.

On some days, the longshore currents reversed direction during the survey, but on other days, the longshore currents persisted throughout the survey in spite of changing or opposing winds. Some evidence has been presented that longshore currents measured during the summer 2019 surveys may have been affected by seiche activity in Lake Erie. As noted by Jackson (2013), longshore currents may likely result from a regional circulation setup, and because of the rotation of the Earth and the Coriolis effect, prevailing winds will produce a net transport of water 90 degrees to the right (clockwise) of the direction the wind is blowing; however, it is unclear if this was the driving force behind the summer 2019 data. For example, strong northwesterly winds (20–30 mi/h) observed on September 8, 2012, and continuing from that direction for the next few days at 10–20 mi/h produced longshore currents in the southwesterly direction on September 11–12, 2012 (figs. 8–9 in Jackson, 2013). However, strong northwesterly winds (10–25 mi/h) observed on June 10–11, 2019 (fig. 7), seemed to produce longshore currents in the northeasterly direction in the afternoon on June 10 (fig. 16) and on June 11 (fig. 17), which is opposite the observation from the previous study. This difference may be because of wind characteristics (speed and direction) and event duration that were not exactly comparable between the two studies, different effects from seiche activity, and (or) differences caused by the time of year. The stratification (layers of different water temperature) that forms in Lake Erie during the late summer and fall can change the response of the lake to persistent winds (Rao and Schwab, 2007).

## Using Specific Conductance in Combination with Velocity Mapping

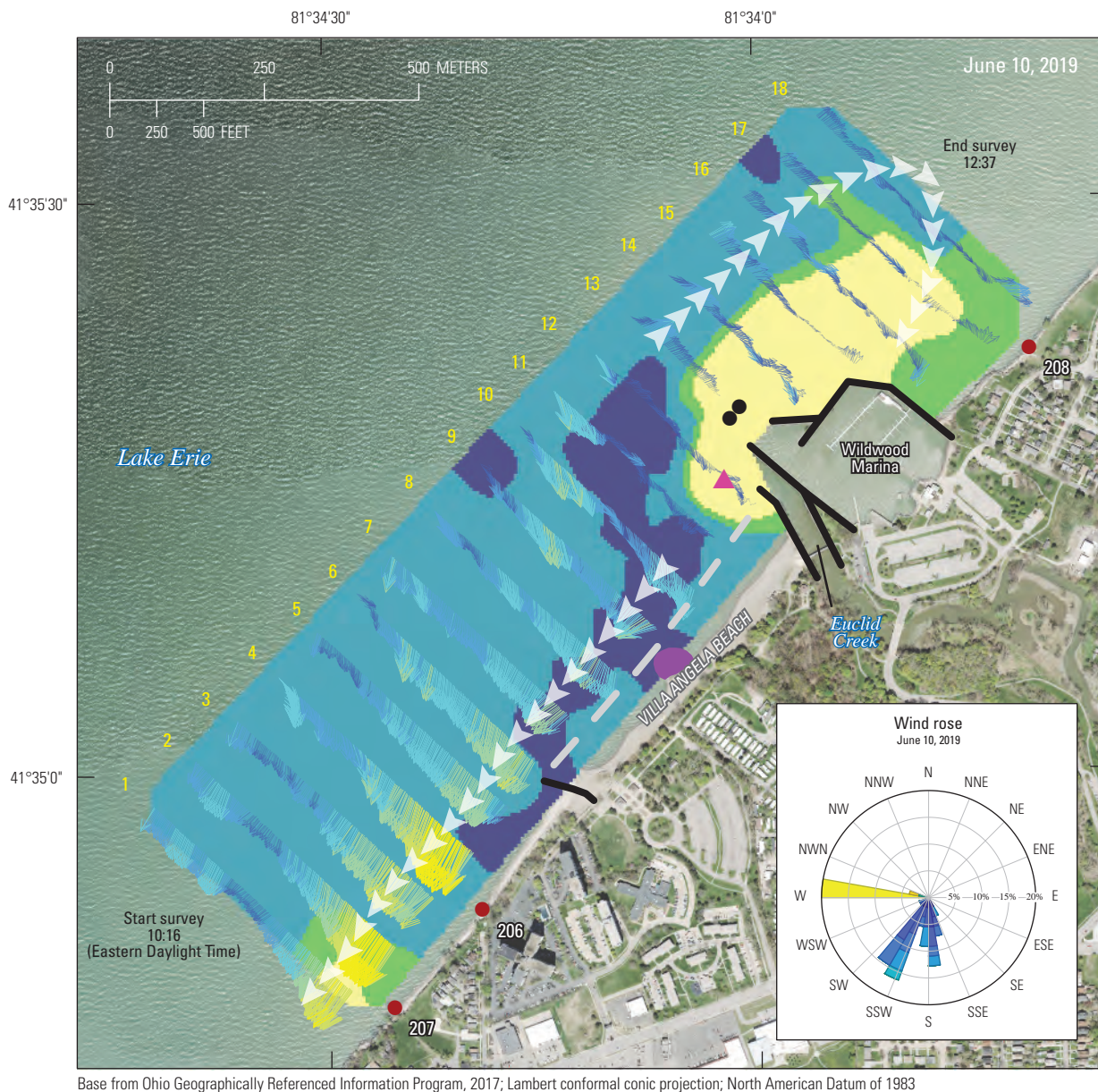
Previous work by Jackson (2013) documented that the high specific conductance water of Euclid Creek relative to water of Lake Erie made it an excellent tracer for visualization of the transport and fate of Euclid Creek water in the nearshore environment. Such visualizations are especially useful when combined with the results of velocity mapping because they provide a more comprehensive picture with which to infer how the Euclid Creek water interacts with nearshore currents. It was assumed that the CSO discharges near the Easterly WWTP would also have higher specific conductance than Lake Erie water and could thus be visualized in the same way.

Recall that only the first survey on each day was a full ADCP velocity survey concurrent with the AUV survey measuring specific conductance, among other constituents. In

the specific conductance and velocity mapping combination plots (figs. 27–32), specific conductance is shown as a background raster and the depth-averaged velocities are overlaid on top. The specific conductance rasters were generated by using the diffusion interpolation with barriers routine in the Geostatistical Analyst Toolbox in ArcMap (Environmental Systems Research Institute, 2020). Absolute barrier features (piers) were not used, and the output raster was trimmed to the data extents. Manually drawn longshore current or recirculation arrows are overlaid on top of the velocity vectors to help summarize the primary patterns in the velocity data. For the specific conductance raster, the data were categorized and colored the same way among plots based on their empirical distribution, with color breaks generally at the first quartile, the third quartile, and the upper adjacent values. The lowest 25 percent of the data are shown by dark blue colors, the middle 50 percent of the data are shown by light blue or cyan colors, the next highest 24 percent of the data (75–99 percent of data) are shown by green colors, and the highest 1 percent of the data are shown by yellow colors. In this way, the yellow areas clearly show where the water from high specific conductance sources (Euclid Creek, CSO locations, and the Easterly WWTP) are transported to after entering Lake Erie. The only exception to this color classification is that a purple color was also used in one of the plots (fig. 27) to highlight a small area with unusually low specific conductance that was only observed on one day.

On June 10, 2019, currents were to the southwest at the start of the survey and to the northeast at the end of the survey (fig. 27). There was also a precipitation event (fig. 7D) that resulted in a sharp increase in the streamflow in Euclid Creek (fig. 9A) and CSO discharges (fig. 7D). An area of elevated specific conductance can be seen near CSO location 207 and being transported to the southwest with the currents (yellow color in fig. 27). Brownish-looking water was also observed in that area by USGS personnel during the survey (see fig. 1–3 in appendix 1). By the afternoon, the streamflow in Euclid Creek had increased and the currents had shifted to the northeast. A large area of elevated specific conductance can be seen at the mouth of Euclid Creek and continuing to the northeast until around line 17 (yellow color in fig. 27). This area included the maximum specific conductance measured on June 10 (0.634 millisiemens per centimeter, more than twice the specific conductance of ambient Lake Erie water), which was just to the west of the end of the southern-most pier along Euclid Creek (fig. 27). There is a sharp concentration-gradient interface along the western and northern edges of the plume, as indicated by the thin green layer, which is likely because of strong winds from the west and currents to the northeast limiting the westward and northward advection of the plume. The calmer area just to the northeast of the marina allowed the plume to expand within the lee of the marina and dilute more gradually through mixing with the Lake Erie water resulting in a larger area of slightly elevated specific conductance (green color nearshore from lines 16 to 18 in fig. 27). Finally, a peculiar low specific conductance anomaly was detected along





### EXPLANATION

[ $w_s$ , wind speed; %, percent]

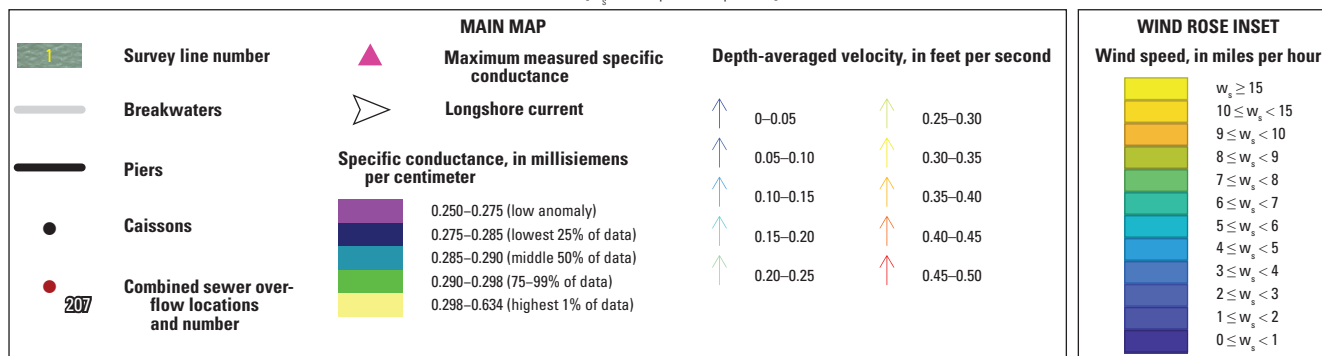
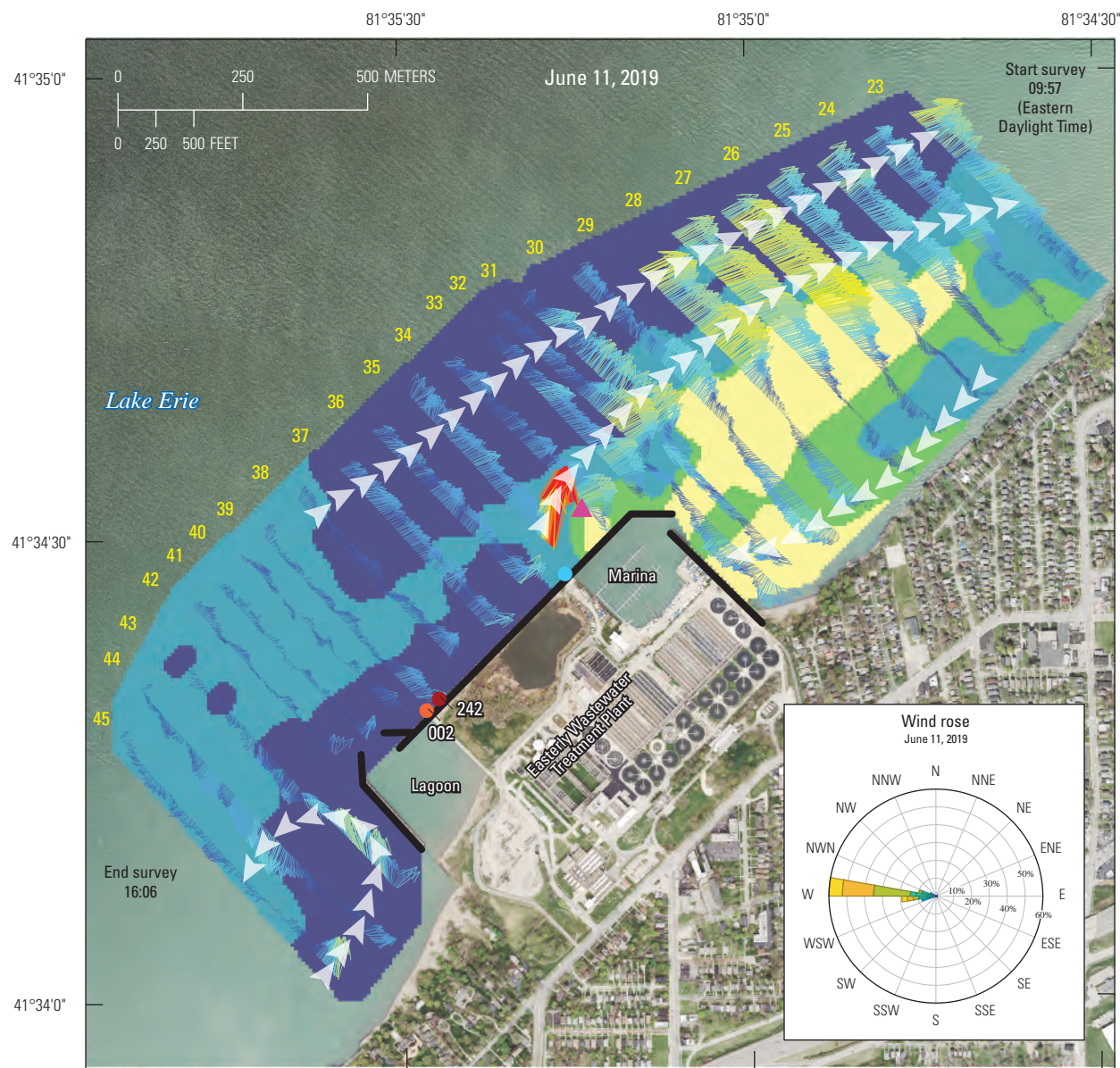


**Figure 27.** Depth-averaged currents and distribution of near-surface specific conductance in coastal Lake Erie in the vicinity of Villa Angela Beach and Euclid Creek, Cleveland, Ohio, June 10, 2019.





Base from Ohio Geographically Referenced Information Program, 2017; Lambert conformal conic projection; North American Datum of 1983

EXPLANATION

[ $w_s$ , wind speed; %, percent]

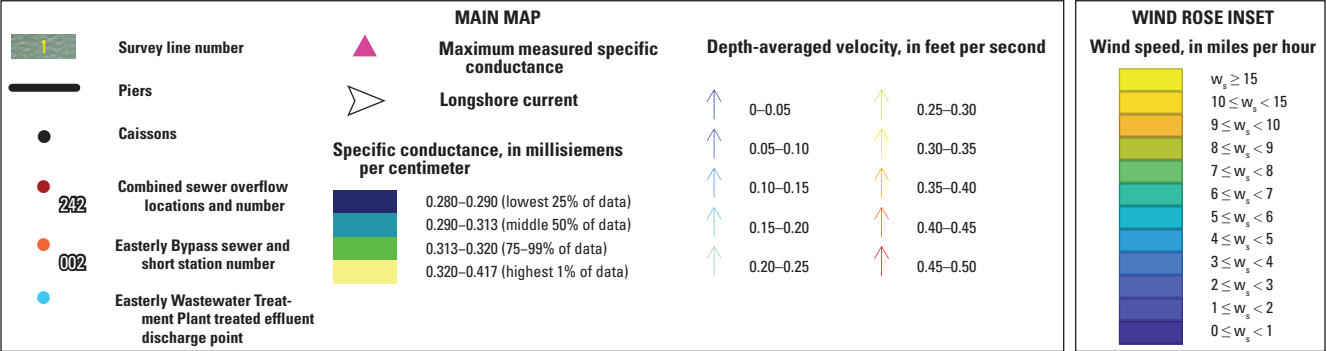
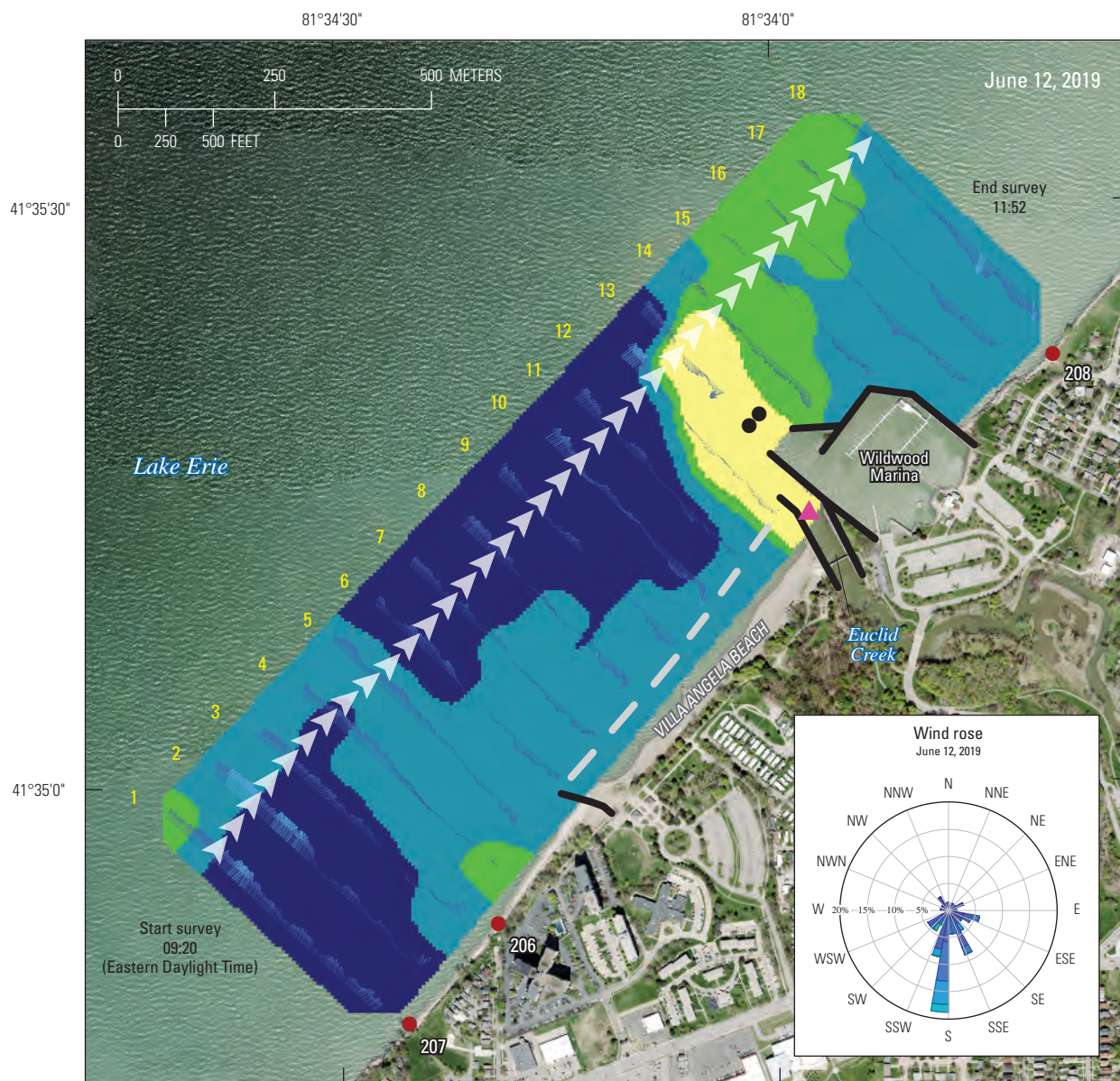


**Figure 28.** Depth-averaged currents and distribution of near-surface specific conductance in coastal Lake Erie in the vicinity of the Easterly Wastewater Treatment Plant, Cleveland, Ohio, June 11, 2019.





Base from Ohio Geographically Referenced Information Program, 2017; Lambert conformal conic projection; North American Datum of 1983

### EXPLANATION

[ $w_s$ , wind speed; %, percent]

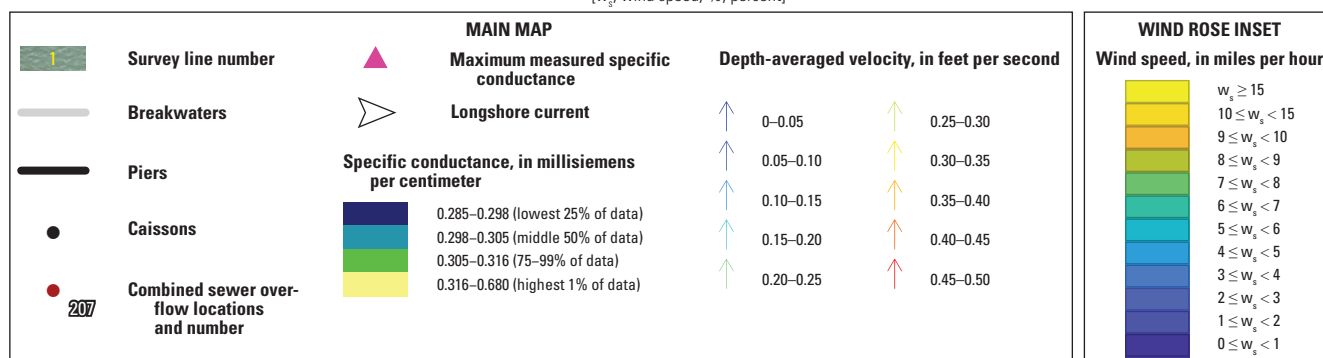
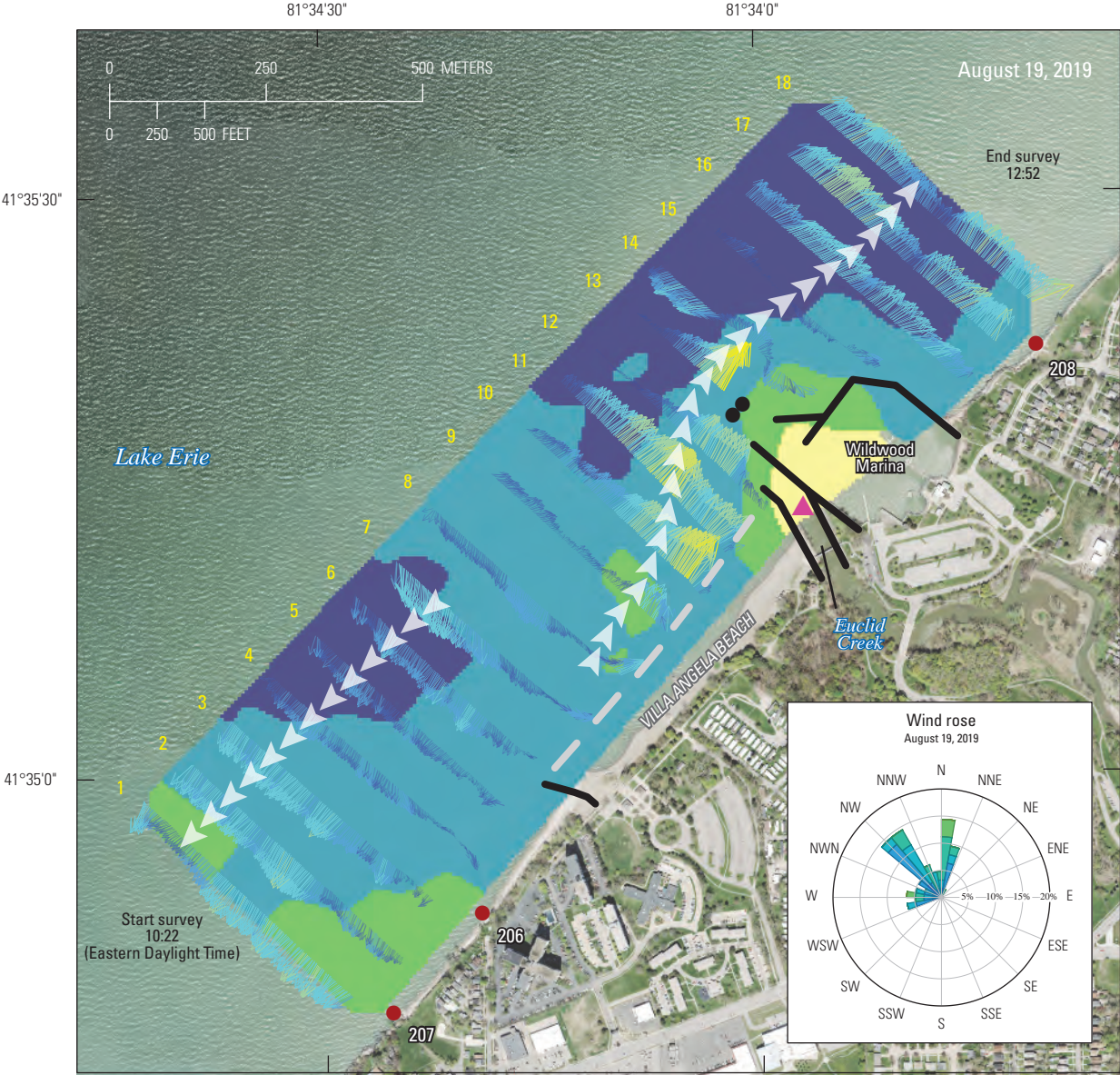


**Figure 29.** Depth-averaged currents and distribution of near-surface specific conductance in coastal Lake Erie in the vicinity of Villa Angela Beach and Euclid Creek, Cleveland, Ohio, June 12, 2019.





Base from Ohio Geographically Referenced Information Program, 2017; Lambert conformal conic projection; North American Datum of 1983

EXPLANATION

[w<sub>s</sub>, wind speed; %, percent]

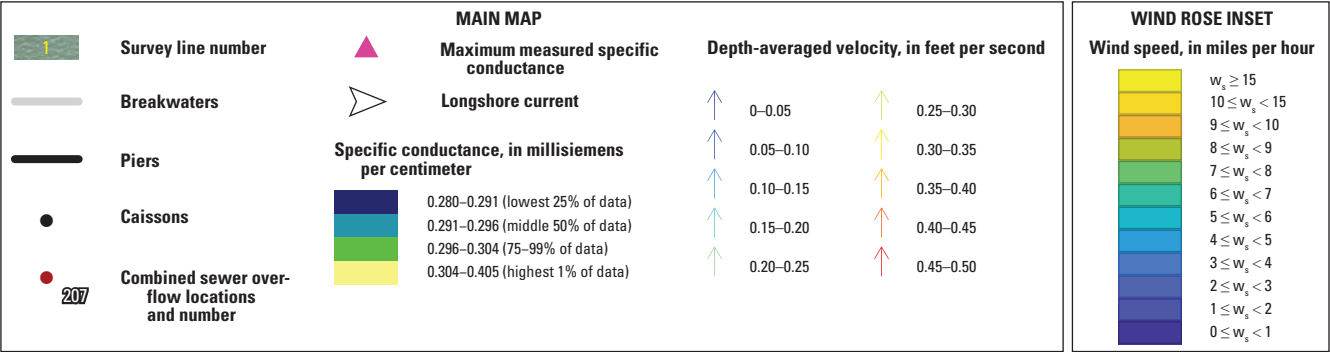
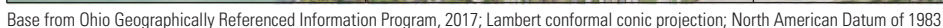


**Figure 30.** Depth-averaged currents and distribution of near-surface specific conductance in coastal Lake Erie in the vicinity of Villa Angela Beach and Euclid Creek, Cleveland, Ohio, August 19, 2019.





### EXPLANATION

[w<sub>s</sub>, wind speed; %, percent]

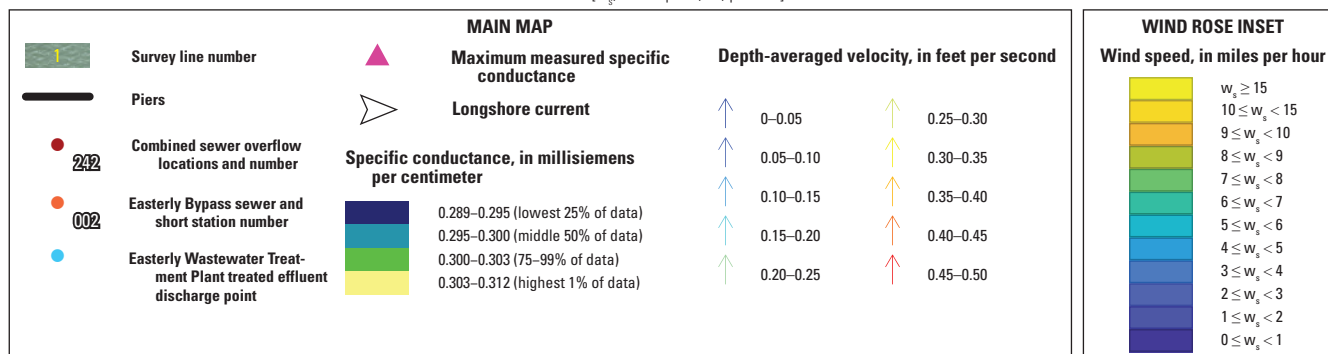


**Figure 31.** Depth-averaged currents and distribution of near-surface specific conductance in coastal Lake Erie in the vicinity of the Easterly Wastewater Treatment Plant, Cleveland, Ohio, August 20, 2019.





Base from Ohio Geographically Referenced Information Program, 2017; Lambert conformal conic projection; North American Datum of 1983

### EXPLANATION

[w<sub>e</sub>, wind speed; %, percent]

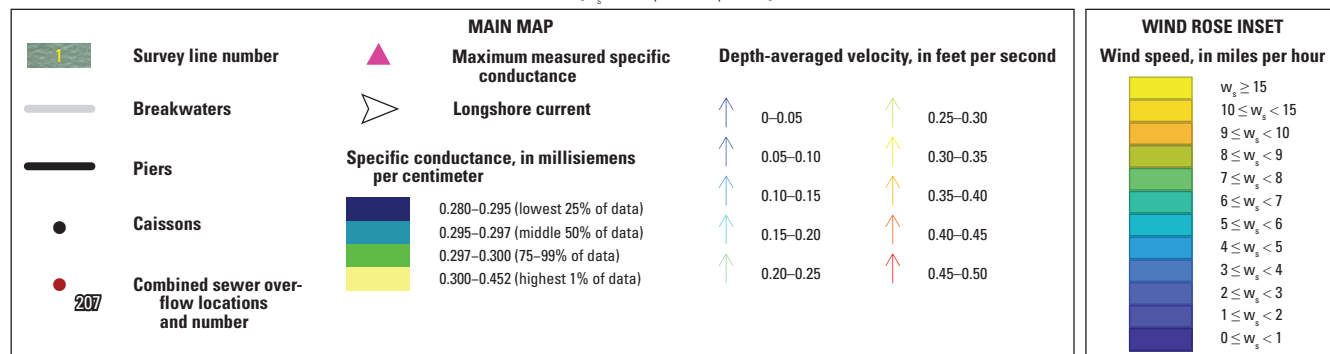


**Figure 32.** Depth-averaged currents and distribution of near-surface specific conductance in coastal Lake Erie in the vicinity of Villa Angela Beach and Euclid Creek, Cleveland, Ohio, August 21, 2019.



Villa Angela Beach inside the breakwaters near line 9 (purple color in [fig. 27](#)). This was also visually observed during the survey as a discoloration in the water (brownish-looking water; see [figs. 1-1](#) and [1-2](#) in appendix 1). The location of the anomaly is near a persistent anomaly observed in the 2011 USGS survey which noted a cold, dense, low pH, low dissolved oxygen anomaly between the second western-most breakwater and the beach (Jackson, 2013), but there was no anomaly in specific conductance. No anomaly was detected in the same location in the 2012 survey. This was the only day of the summer 2019 surveys that the anomaly was detected.

On June 11, 2019, currents were to the northeast throughout the survey and a recirculation zone was present to the northeast of the Easterly WWTP ([fig. 28](#)). This recirculation impeded the ability of nearshore currents to dilute water coming from the Easterly WWTP and led to steering of the Easterly WWTP waters (and CSO-related contaminants such as bacteria) into nearshore areas, as evidenced by the persistence of a large area of elevated specific conductance within the recirculation zone and along the shoreline (yellow color in [fig. 28](#)). It is unclear whether the elevated specific conductance water is coming from the treated effluent discharge point or from the marina or both, but the maximum specific conductance measured on June 11 (0.417 millisiemens per centimeter) occurred just to the northeast of the treated effluent discharge point ([fig. 28](#)). Additional information about the treated effluent (such as the typical specific conductance and the discharge rates) would be helpful in this analysis. The measured specific conductance values on June 11 around the Easterly WWTP were lower than the measured specific conductance values on June 10 around Euclid Creek but were still clearly different from typical Lake Erie water. A discoloration in the water was not observed on June 11.

On June 12, 2019, currents were very weak and to the northeast at the start of the survey and nearly calm by the end of the survey ([fig. 29](#)). Although the streamflow from Euclid Creek was near the tail-end of a recession in the hydrograph ([fig. 9A](#)), it was still higher than normal. Winds were generally out of the south at around 1–5 mi/h throughout the survey ([fig. 7](#)). Under these conditions, the plume from Euclid Creek extends farther into Lake Erie compared to June 10, 2019 ([fig. 27](#)). An area of elevated specific conductance can be seen from the mouth of Euclid Creek and continuing to the north until near the end of the survey domain (yellow color in [fig. 29](#)). This was also visually observed during the survey as a discoloration in the water (brownish-looking water; see [figs. 1-6–1-8](#) in appendix 1). As the plume gets farther offshore, it is diluted through mixing with Lake Erie water—the large green area to the north of the plume indicates increased mixing and transport of Euclid Creek water by the longshore currents ([fig. 29](#)). Unlike the plume on June 10, 2019, that remained attached to the shoreline, the plume on June 12 detached from the shore and was not trapped in the weak recirculation on the northeast side of the marina. The weak currents and offshore wind on June 12 likely helped drive this plume offshore. An effort was

made on that day to get the AUV farther into Euclid Creek, which is why the maximum specific conductance measured on June 12 (0.680 millisiemens per centimeter) occurred along the centerline of Euclid Creek between the two piers ([fig. 29](#)). Two other areas of elevated specific conductance can be seen offshore at line 1, which may be from the Easterly WWTP, and nearshore at line 4, which may be from CSO location 206 (green color in [fig. 29](#)). Data provided by the NEORS D document that CSO location 206 was not active on June 12; however, it discharged 1.34 Mgal on June 10 and a total of 0.93 Mgal from June 13–16. This may indicate that the CSO that discharged from CSO location 206 on June 10 had diluted to some extent with the Lake Erie water and remained within about 500 ft of the CSO discharge point.

On August 19, 2019, currents were to the southwest at the start of the survey and abruptly reversed at line 9 to the northeast for the remainder of the survey ([fig. 30](#)). A small area of elevated specific conductance can be seen but is mostly contained within the piers surrounding Euclid Creek and Wildwood Marina (yellow color in [fig. 30](#)). Although the streamflow from Euclid Creek was slightly higher on that day (daily average flow of 56 ft<sup>3</sup>/s) than it was on June 12, 2019 (daily average flow of 36 ft<sup>3</sup>/s), the plume from the creek did not extend out into Lake Erie as it did on June 12 ([fig. 29](#)); instead, the plume exhibits entrapment within and around the coastal structures (piers around Euclid Creek and Wildwood Marina). This may have been because of moderate winds from the northwest and stronger longshore currents, both of which could result in Euclid Creek water being more contained within the pier structures around Euclid Creek and Wildwood Marina. Similar to June 12, an effort was made on that day to get the AUV farther into Euclid Creek, which is why the maximum specific conductance measured on August 19 (0.405 millisiemens per centimeter) occurred along the centerline of Euclid Creek between the two piers ([fig. 30](#)). The specific conductance in Euclid Creek was notably lower than it was during the June 2019 surveys. One other area of elevated specific conductance can be seen nearshore around lines 1–3 (green color in [fig. 30](#)), which was likely coming from CSO location 206. Data provided by the NEORS D document that CSO location 206 discharged 0.41 Mgal on August 19. During the start of the survey when those lines were measured, currents were in the southwest direction, which is the apparent direction of the plume likely emanating from CSO 206 ([fig. 30](#)).

On August 20, 2019, currents were to the southwest throughout the survey, and the Easterly WWTP structure shielded the nearshore area to the southwest of the Easterly WWTP and created an area of calm water there with possibly weak recirculation ([fig. 31](#)). The areas of elevated specific conductance on August 20 were only slightly greater than the background Lake Erie water, but the data are still able to show distinct spatial patterns. Small areas of elevated specific conductance can be seen but were mostly contained to areas of calm water within the piers surrounding the marina on the eastern side of the Easterly WWTP and along the nearshore

area to the southwest of the Easterly WWTP (yellow color in [fig. 31](#)). An effort was made on that day to get the AUV into the marina on the east side of the Easterly WWTP, and the maximum specific conductance measured on August 20 (0.312 millisiemens per centimeter) occurred in the western corner of the marina near the treated effluent discharge point ([fig. 31](#)). Although the AUV did not measure in the lagoon on the western side of the Easterly WWTP, there is a gap in the pier wall on the nearshore side that may serve as a path of transport of the Easterly WWTP water (specifically from CSO location 242 and Easterly Bypass sewer 002) to the nearshore area southwest of the Easterly WWTP. A photograph taken during the June 2019 surveys showed a clear distinction between the brownish-looking water in the lagoon and the Lake Erie water ([fig. 1-4](#) in appendix 1). A large area of elevated specific conductance can be seen extending off from the piers surrounding the Easterly WWTP around lines 37–42 (green color in [fig. 31](#)), which may be being transported lake-ward by the longshore currents.

On August 21, 2019, when a partial AUV survey was completed around Euclid Creek and Wildwood Marina, currents were to the northeast throughout the survey ([fig. 32](#)). An area of elevated specific conductance can be seen extending from the mouth of Euclid Creek and continuing to the northeast (yellow color in [fig. 32](#)). The thin green area along the western edge of the plume indicates a sharp concentration-gradient interface between Lake Erie water and Euclid Creek water. However, the larger green area to the north of the plume indicates entrainment and transport of Euclid Creek water by the longshore currents ([fig. 32](#)). The wake of the caissons and the marina are likely aiding in the dispersion of the plume here as well. Although the streamflow from Euclid Creek was lower on that day (daily average flow of 12 ft<sup>3</sup>/s) than it was on August 19 (daily average flow of 56 ft<sup>3</sup>/s), the plume of elevated specific conductance water extended farther outside the piers ([fig. 32](#)). This was likely because of a longer duration of nonopposing winds from the west and sustained, well-developed currents to the northeast, both of which would drive the plume to the northeast. Similar to June 12 and August 19, an effort was made on that day to get the AUV farther into Euclid Creek, which is why the maximum specific conductance measured on August 21 (0.452 millisiemens per centimeter) occurred along the centerline of Euclid Creek between the two piers ([fig. 32](#)).

## Spatial Distribution of Water-Quality Constituents

This section discusses the observed spatial distribution of water-quality constituents for June 10–12, 2019, and August 19–21, 2019, near Villa Angela Beach, Euclid Creek,

and the Easterly WWTP. Data are presented in plan view and as cross sections through the survey area to provide the reader with a full three-dimensional picture of the spatial distribution of basic water-quality constituents within the study area. For the plan view plots, the multiparameter sonde data were used because of the larger number and more uniform distribution of measurements. Alternately, the near-surface AUV data could have been used. For the cross-section plots, the AUV data from the undulating profiles were used. Although total chlorophyll and blue-green algae concentrations were measured with the AUV, the data were highly variable (noisy) and did not show any meaningful results. These data are included in the data release associated with this study (Boldt, 2021) but are not presented in the following plots.

## Depth Profiles of Water-Quality Constituents

Depth profiles of basic water-quality constituents were constructed from data collected during undulating AUV missions completed each day ([fig. 33](#)). These profiles represent the median constituent values observed for a given depth. Almost all the profiles are nearly vertical, indicating generally uniform values through the water column; however, daily aggregation obscures the detailed spatial and temporal variations in the water-quality distributions, which are shown in the following sections.

## Water Density Distribution

The water density plan view plots for June 10–12, 2019, and August 19–21, 2019, show nonuniform density distributions throughout the study area ([figs. 34A–39A](#)). The data were categorized and colored the same way among plots based on their empirical distribution, with color breaks at the first quartile and the third quartile. In other words, the lowest 25 percent of the data are shown by light green colors, the middle 50 percent of the data are shown by medium green colors, and the highest 25 percent of the data are shown by dark green colors. In this way, attention is drawn to the areas of lower- or higher-than-typical density. For the summer 2019 surveys, areas of lower density tended to correspond with nearshore areas around Euclid Creek, Wildwood Marina, Villa Angela Beach, and the Easterly WWTP. The overall range in density values for the June 2019 and August 2019 surveys is small (998.30–999.00 and 996.55–997.24 kilograms per cubic meter, respectively). The August 2019 density values are less than the June 2019 density values because the water temperatures were higher in August 2019.

The water density cross-section plots for June 10–12, 2019, and August 19–21, 2019, are shown in similar colors but on a continuous colorbar ([figs. 40A–45A](#)). As expected,

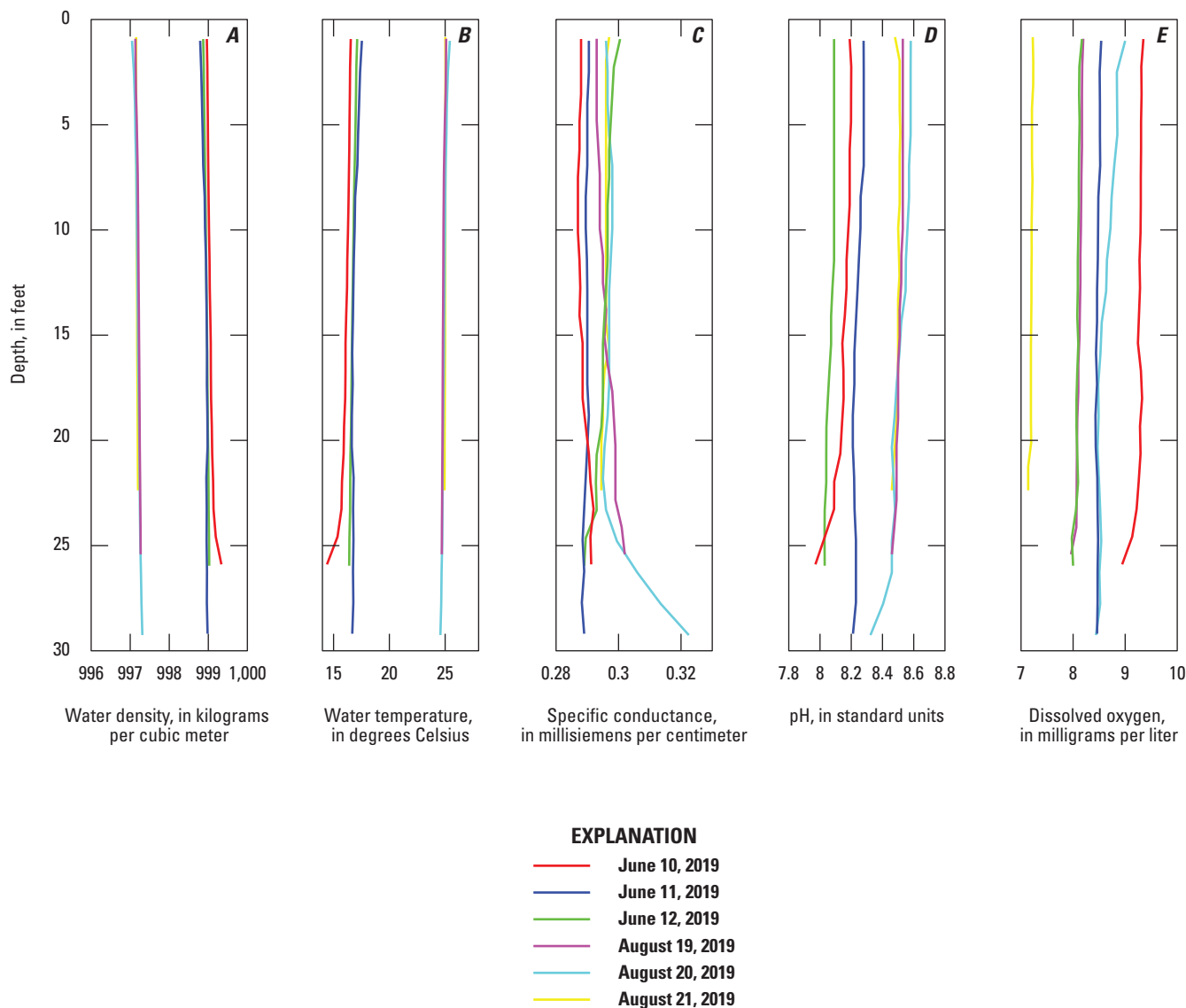


**Figure 33.** Depth profiles of water-quality constituents *A*, water density; *B*, water temperature; *C*, specific conductance; *D*, pH; and *E*, dissolved oxygen compiled from the autonomous underwater vehicle surveys on June 10–12, 2019, and August 19–21, 2019, of coastal Lake Erie in the vicinity of Villa Angela Beach, Euclid Creek, and the Easterly Wastewater Treatment Plant, Cleveland, Ohio. These profiles represent the median constituent values observed for a given depth on indicated days.

denser water is near the lake bottom and less dense water is near the water surface. The overall change in density throughout the depth in nearshore Lake Erie within the study area was 0.30 kilogram per cubic meter during the June 2019 surveys and 0.48 kilogram per cubic meter during the August 2019 surveys. These differences in density indicate the potential for density currents to form along the lake bottom, which are a mechanism for transport and mixing as was thoroughly described in Jackson (2013).

## Water Temperature Distribution

The water temperature plan view plots for June 10–12, 2019, and August 19–21, 2019, show similar patterns of temperature distributions for the same areas among the surveys (figs. 34B–39B). The data were categorized and colored the same way among plots based on their empirical distribution, with color breaks at the median and the third quartile. In other words, the lowest 50 percent of the data are



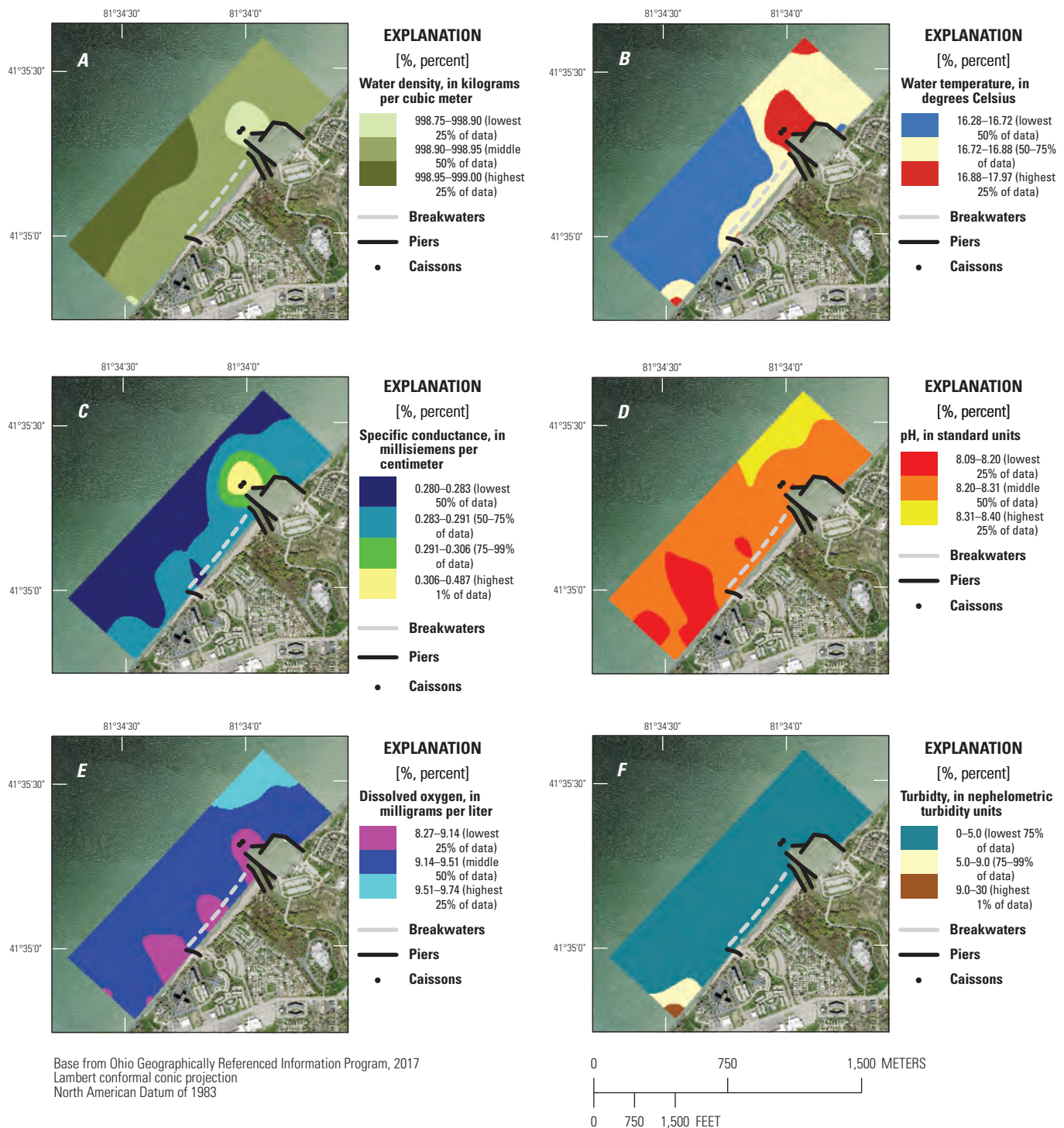


**Figure 34.** Maps showing spatial distributions of near-surface basic water-quality constituents: *A*, water density; *B*, water temperature; *C*, specific conductance; *D*, pH; *E*, dissolved oxygen; and *F*, turbidity for coastal Lake Erie in the vicinity of Villa Angela Beach and Euclid Creek, Cleveland, Ohio, June 10, 2019.

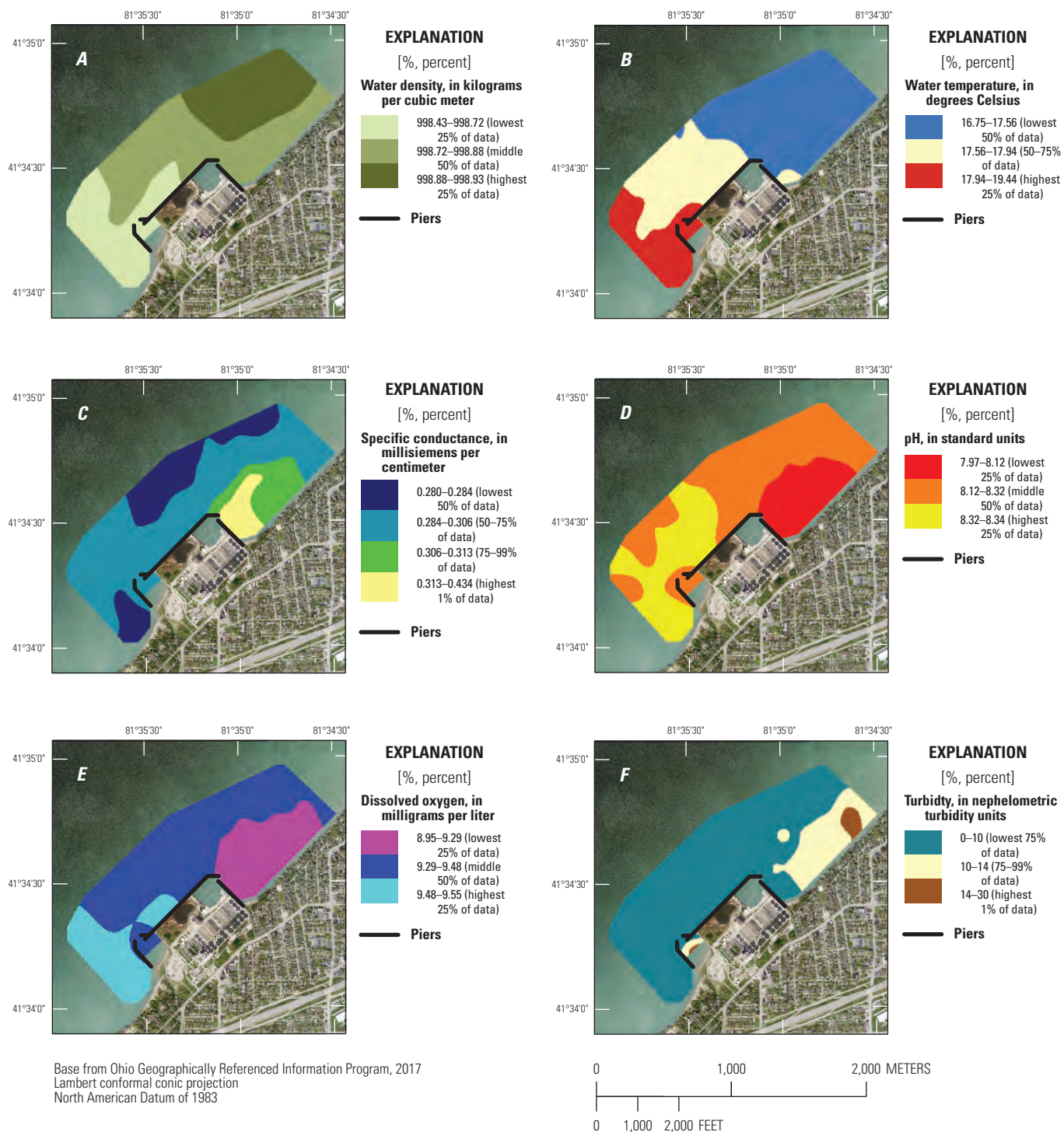


**Figure 35.** Maps showing spatial distributions of near-surface basic water-quality constituents: A, water density; B, water temperature; C, specific conductance; D, pH; E, dissolved oxygen; and F, turbidity for coastal Lake Erie in the vicinity of the Easterly Wastewater Treatment Plant, Cleveland, Ohio, June 11, 2019.



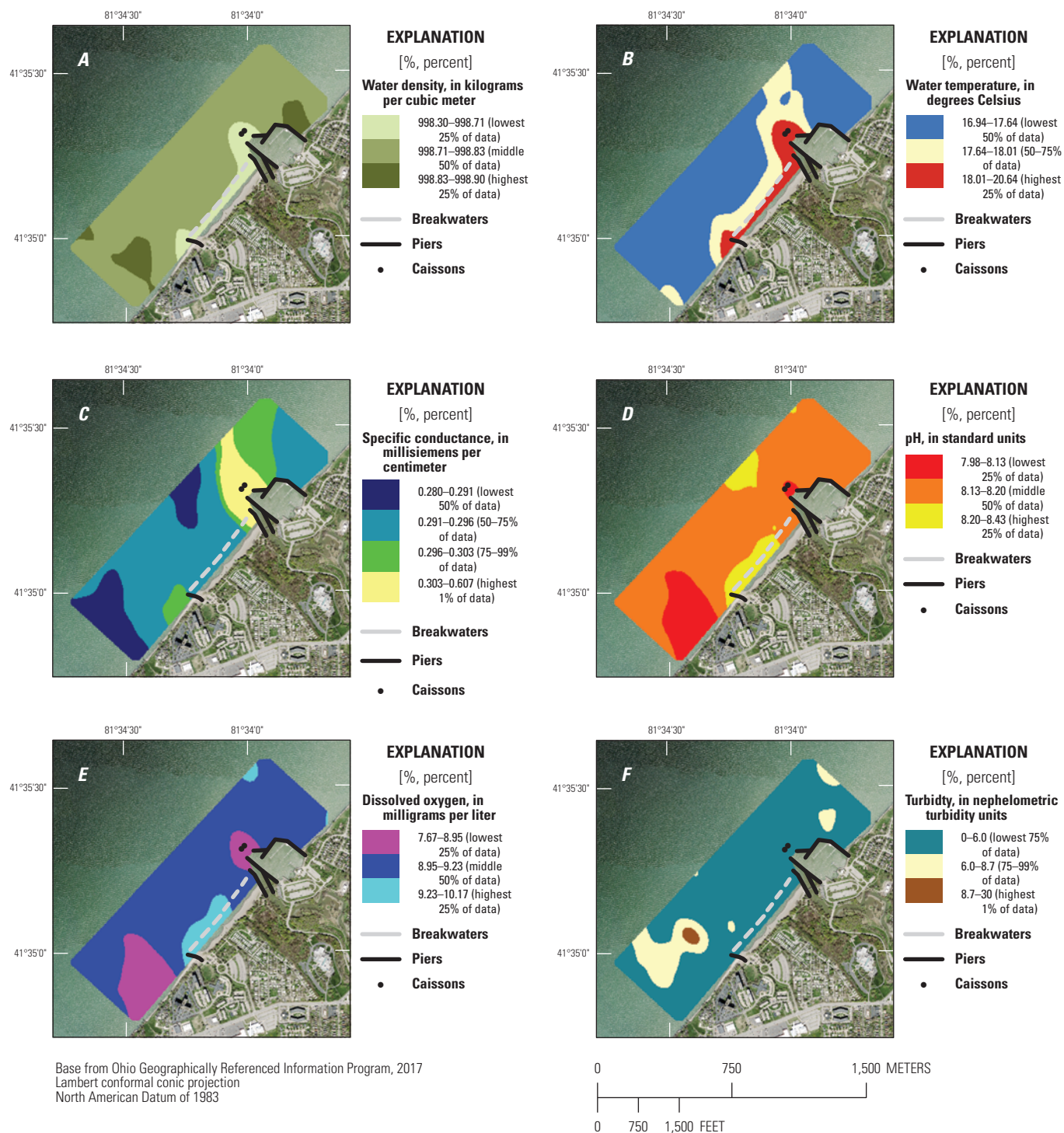


**Figure 36.** Maps showing spatial distributions of near-surface basic water-quality constituents: *A*, water density; *B*, water temperature; *C*, specific conductance; *D*, pH; *E*, dissolved oxygen; and *F*, turbidity for coastal Lake Erie in the vicinity of Villa Angela Beach and Euclid Creek, Cleveland, Ohio, June 12, 2019.



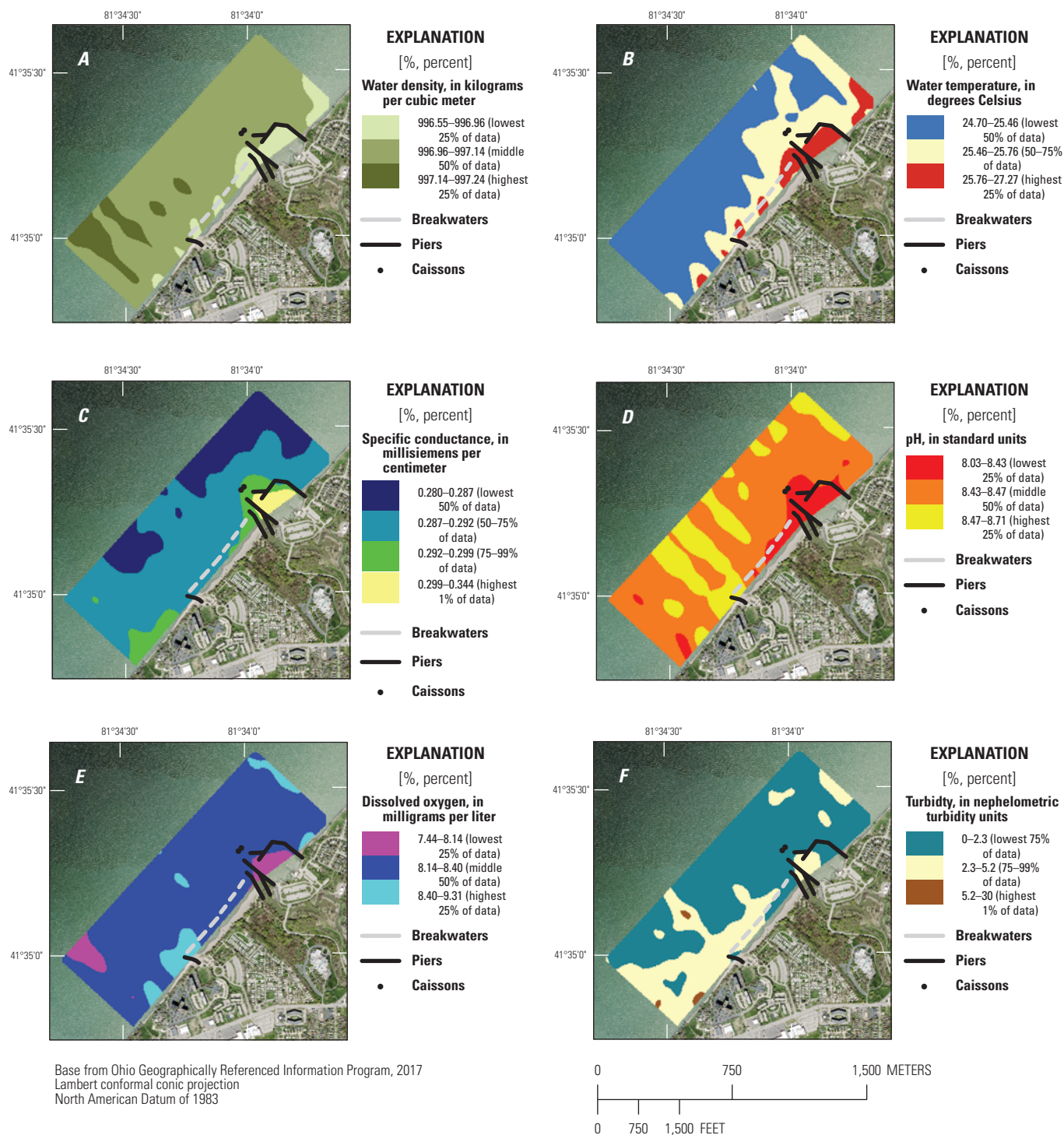


**Figure 37.** Maps showing spatial distributions of near-surface basic water-quality constituents: *A*, water density; *B*, water temperature; *C*, specific conductance; *D*, pH; *E*, dissolved oxygen; and *F*, turbidity for coastal Lake Erie in the vicinity of Villa Angela Beach and Euclid Creek, Cleveland, Ohio, August 19, 2019.

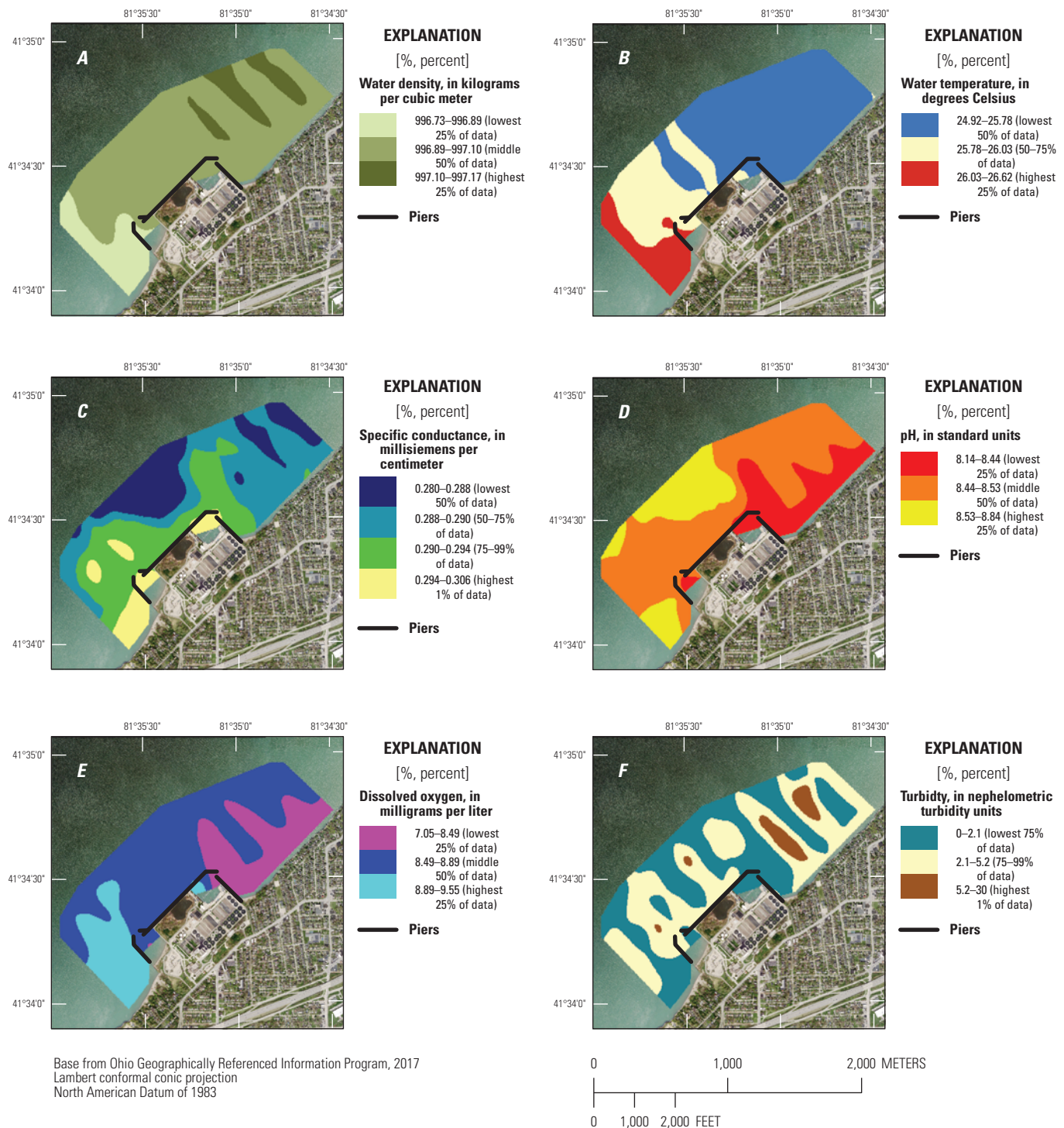


**Figure 38.** Maps showing spatial distributions of near-surface basic water-quality constituents: *A*, water density; *B*, water temperature; *C*, specific conductance; *D*, pH; *E*, dissolved oxygen; and *F*, turbidity for coastal Lake Erie in the vicinity of the Easterly Wastewater Treatment Plant, Cleveland, Ohio, August 20, 2019.



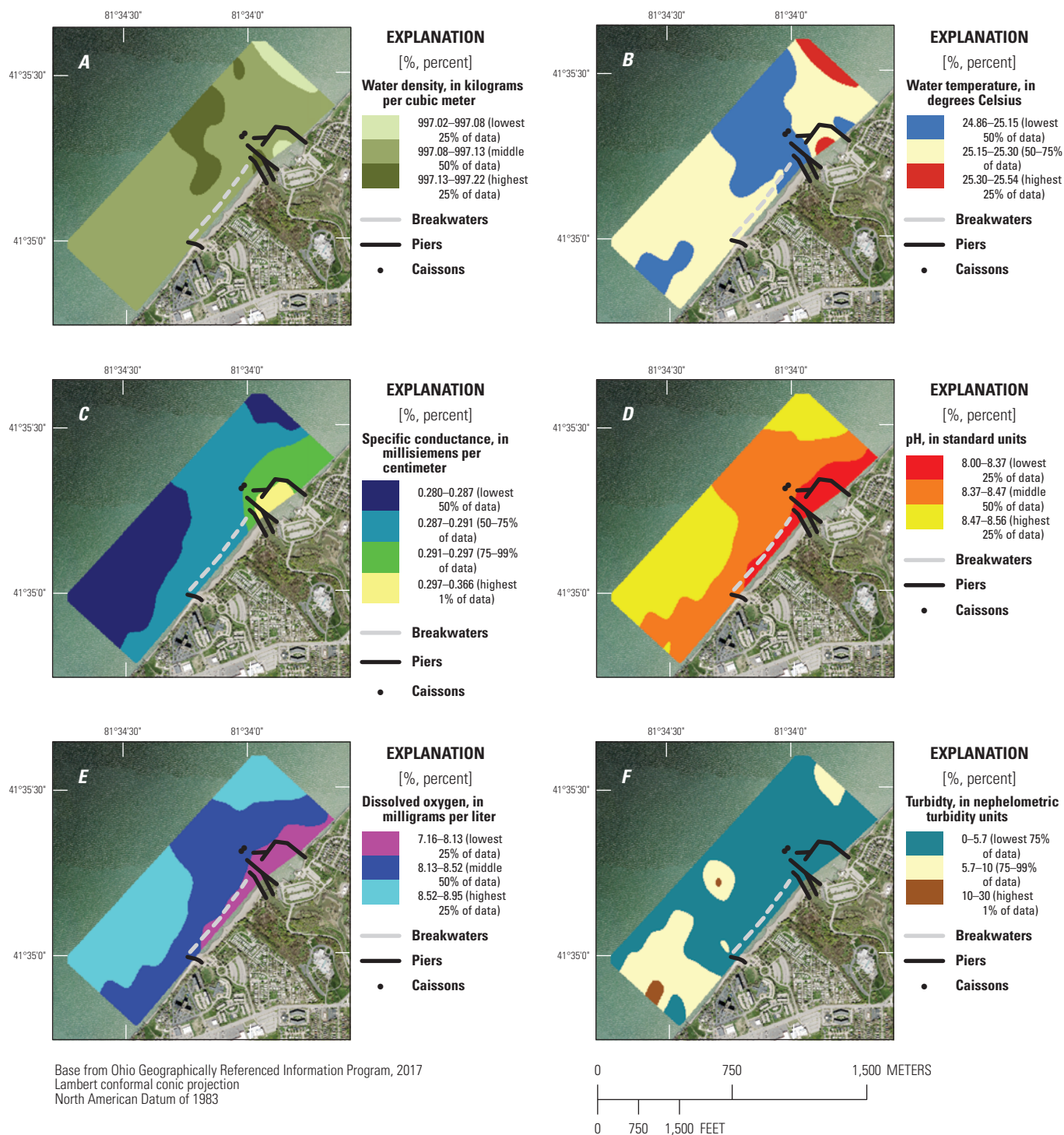


**Figure 39.** Maps showing spatial distributions of near-surface basic water-quality constituents: *A*, water density; *B*, water temperature; *C*, specific conductance; *D*, pH; *E*, dissolved oxygen; and *F*, turbidity for coastal Lake Erie in the vicinity of Villa Angela Beach and Euclid Creek, Cleveland, Ohio, August 21, 2019.



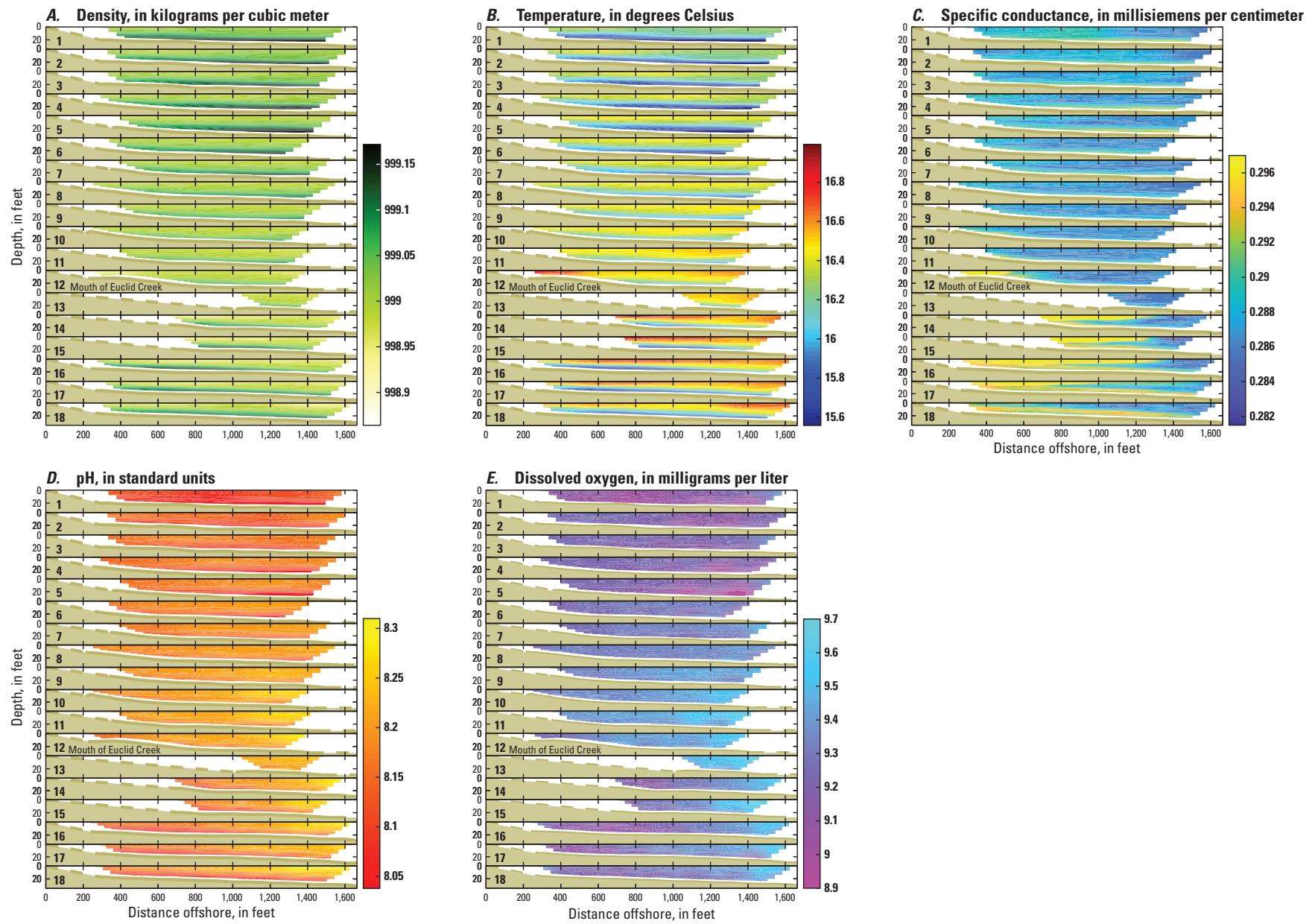


**Figure 40.** Cross sections of basic water-quality constituents: *A*, water density; *B*, water temperature; *C*, specific conductance; *D*, pH; and *E*, dissolved oxygen for 18 sections of coastal Lake Erie in the vicinity of Villa Angela Beach and Euclid Creek, Cleveland, Ohio, June 10, 2019.

shown by blue colors, the next highest 25 percent of the data (50–75 percent of data) are shown by yellow colors, and the highest 25 percent of the data are shown by red colors. In this way, attention is drawn to the areas where the water is much warmer than typical. For the summer 2019 surveys, areas of warmer water tended to correspond with nearshore areas around Euclid Creek, Wildwood Marina, and Villa Angela Beach, which is consistent with the previous observation of lower density water in those areas. Although it seems that the water was warmer on the western side of the Easterly WWTP compared with the eastern side, this is almost certainly an artifact caused by the order in which the survey lines were measured (which started at the northeast extent and ended at the southwest extent) and the solar heating of the water surface throughout the day (figs. 7–8). The overall range in water temperature values for the June 2019 and August 2019 surveys was 16.28–20.64 °C and 24.70–27.27 °C, respectively.

The water temperature cross-section plots for June 10–12, 2019, and August 19–21, 2019, are shown in similar colors but on a continuous colorbar (figs. 40B–45B). Colder water is near the lake bottom and deeper areas and warmer water is near the water surface and shallow areas. The overall change in water temperature throughout the depth in nearshore Lake Erie within the study area was 1.4 °C during the June 2019 surveys and 1.7 °C during the August 2019 surveys.

As water temperature varies during the day because of solar radiation (for example, figs. 35B and 43B) and seasonally due to air temperature and solar radiation variations, and because the lake is not thermally uniform (stratification), use of spatial variations in water temperature would need to be substantiated with other water-quality data to determine the extent of plumes in nearshore areas of Lake Erie.

## Specific Conductance Distribution

With specific conductance in Euclid Creek more than two times higher than Lake Erie (which was relatively uniform away from the creek), specific conductance proved to be an excellent tracer to track the plume of water from Euclid Creek into Lake Erie. Although the water within the Easterly WWTP did not have specific conductance values nearly as high as Euclid Creek, the specific conductance was still higher than the surrounding Lake Erie water and likewise proved to be an excellent tracer to track the water from the Easterly WWTP into Lake Erie.

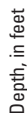
The specific conductance plan view plots for June 10–12, 2019, and August 19–21, 2019, show how water from Euclid Creek and the Easterly WWTP circulate, mix, and transport in nearshore Lake Erie (figs. 34C–39C). The data were categorized and colored the same way among plots based on their empirical distribution, with color breaks generally at the median, the third quartile, and the upper adjacent values. In other words, the lowest 50 percent of the data are shown by dark blue colors, the next highest 25 percent of the data (50–75 percent of data) are shown by light blue or cyan colors, the next highest 24 percent of the data (75–99 percent of

data) are shown by green colors, and the highest 1 percent of the data are shown by yellow colors. In this way, the yellow areas clearly show where the water from high specific conductance sources (Euclid Creek, CSO locations, and the Easterly WWTP) are transported after entering Lake Erie. The plan view plots may look slightly different here than before because of the data source used (towed multiparameter water-quality sonde in figs. 34C–39C compared to AUV in figs. 27–32), the data point density and distribution, and the interpolation algorithms. For the summer 2019 surveys, the circulation, mixing, and transport of plumes of higher specific conductance were strongly affected by longshore currents and nearshore circulation patterns, as was described in the “Using Specific Conductance in Combination with Velocity Mapping” section. The specific conductance cross-section plots for June 10–12, 2019, and August 19–21, 2019, are shown in similar colors but on a continuous colorbar (figs. 40C–45C).

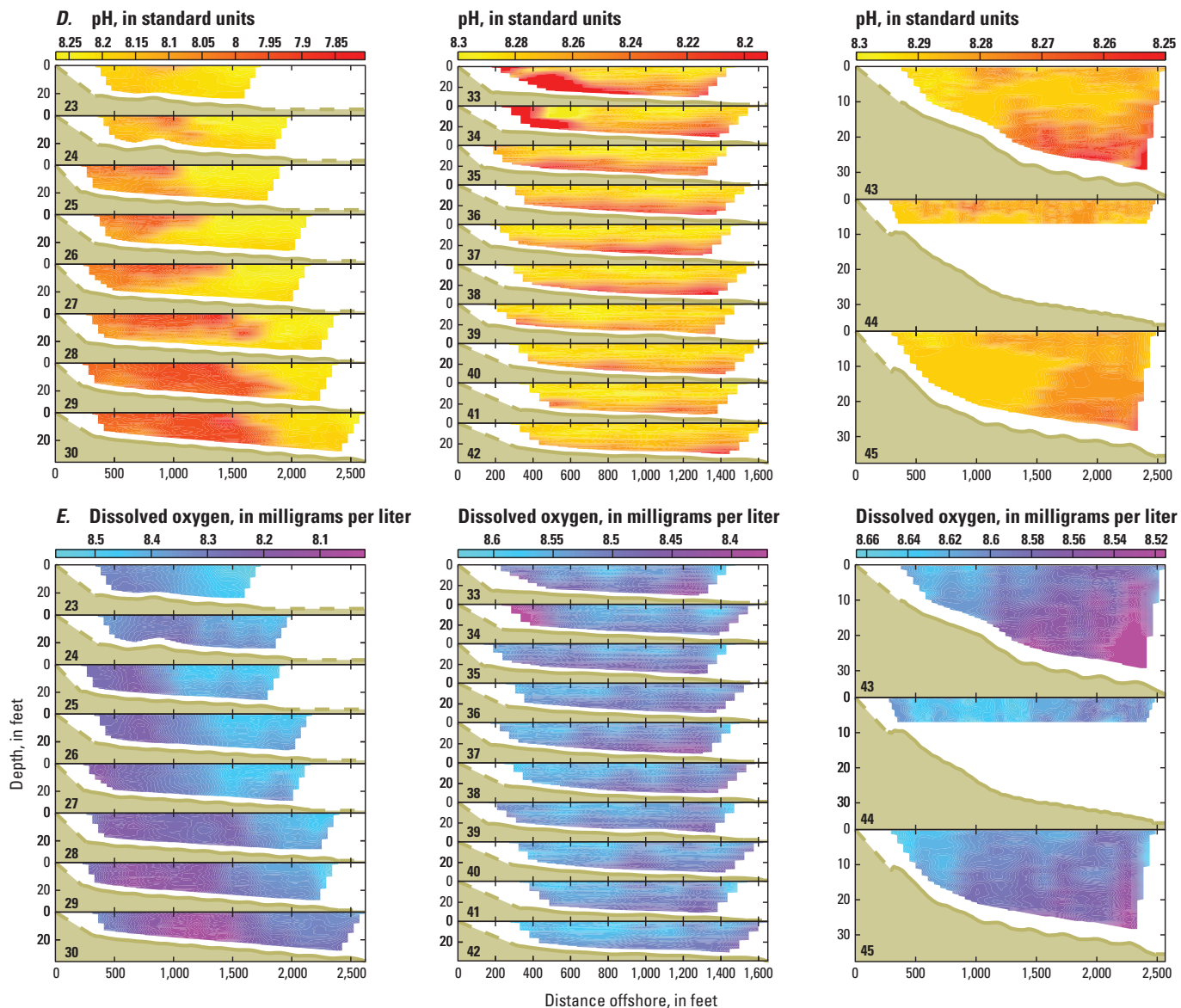
On June 10, a plume of elevated specific conductance water was detected near the surface in nearshore Lake Erie around the mouth of Euclid Creek (figs. 27 and 34C). This area of elevated specific conductance near the surface was also visible in the cross-section plots, particularly at lines 12, 14, 15, and 16 (fig. 40C); however, the AUV also revealed a layer of elevated specific conductance along the lake bottom in lines 14 through 18. Note how this bottom layer of elevated specific conductance extended increasingly farther offshore from lines 14 to 18. When combined with observations of the water density along these lines (fig. 40A), it seems likely that a density current was present and was transporting Euclid Creek water (and possibly CSO-related contaminants such as bacteria) out into Lake Erie along the lake bottom.

On June 11, a plume of elevated specific conductance water was detected near the surface in nearshore Lake Erie to the northeast of the Easterly WWTP (figs. 28 and 35C). This area of elevated specific conductance near the surface was also visible in the cross-section plots, starting at line 34 nearshore and continuing into line 33 (fig. 41C). The dispersion of the plume can be tracked from line 30, where there is still a strong core of elevated specific conductance water, all the way to line 23, where it is almost nondetectable. Although the likely movement of the elevated specific conductance water indicated in lines 34 and 33 seems consistent with a density current, specific conductance was higher primarily near the surface in lines 30 to 23. A possible explanation for this may be that the water coming from the Easterly WWTP treated effluent was warmer (and thus less dense and more buoyant) than the Lake Erie water and so was rising to the surface. The temperature (fig. 41B) and density (fig. 41A) plots support this by showing a thin layer of warmer and less dense water near the surface throughout the survey area.

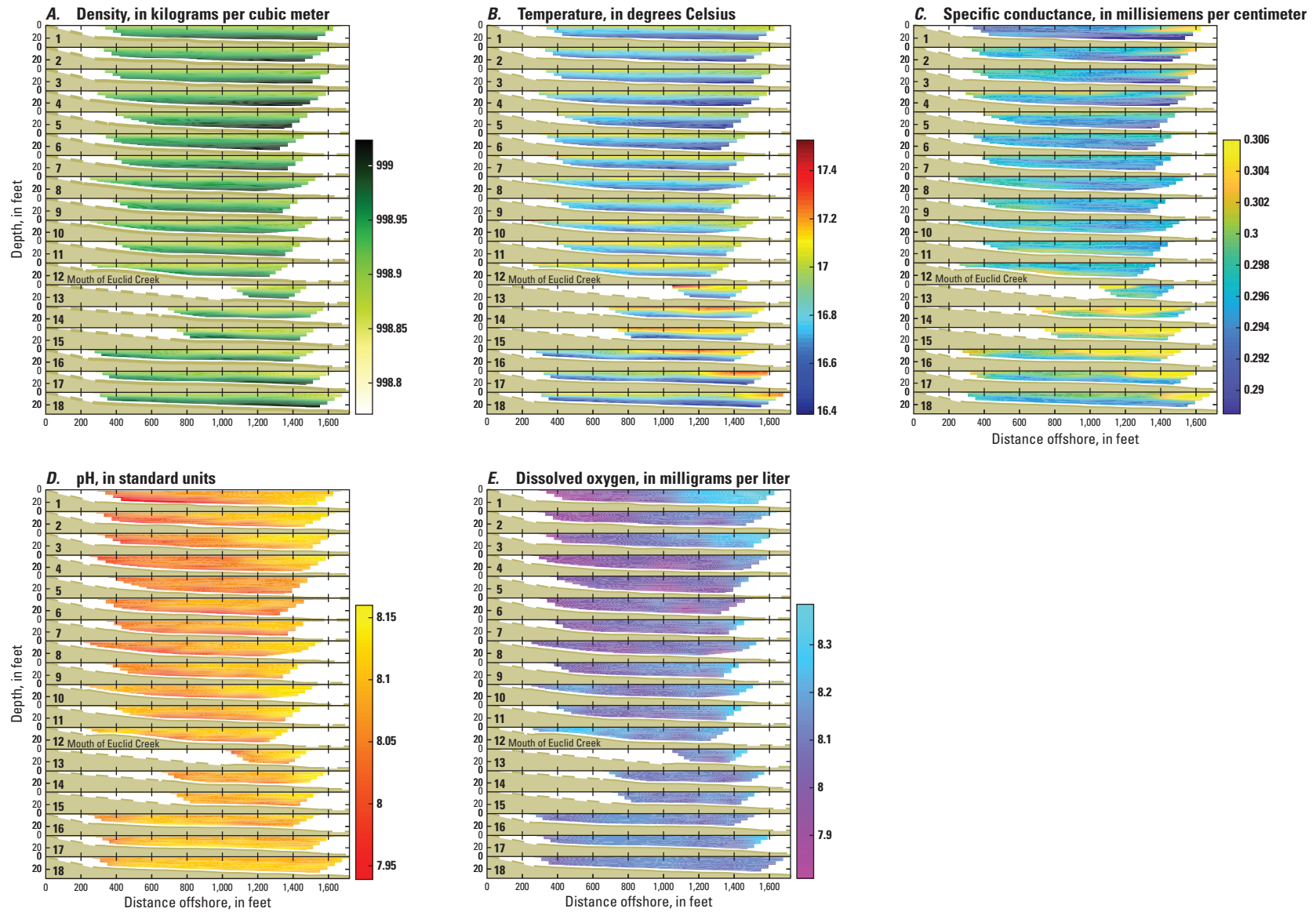
On June 12, a plume of elevated specific conductance water was again detected near the surface in nearshore Lake Erie around the mouth of Euclid Creek and extending out into the lake (figs. 29 and 36C). This area of elevated specific conductance near the surface was also visible in the cross-section plots from line 13 to line 18 (fig. 42C), and the



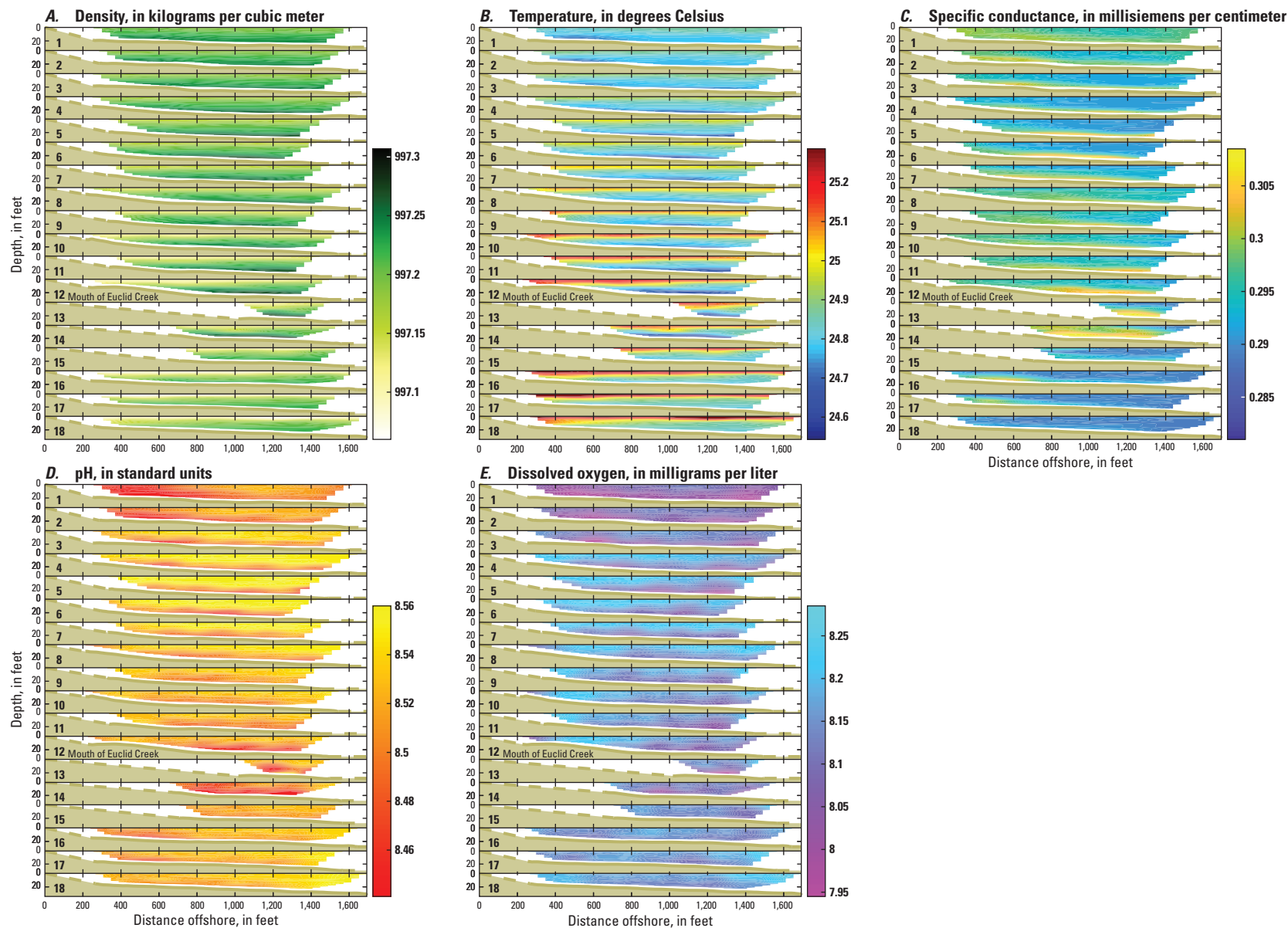




**Figure 41.** Cross sections of basic water-quality constituents: *A*, water density; *B*, water temperature; *C*, specific conductance; *D*, pH; and *E*, dissolved oxygen for 21 sections of coastal Lake Erie in the vicinity of the Easterly Wastewater Treatment Plant, Cleveland, Ohio, June 11, 2019.

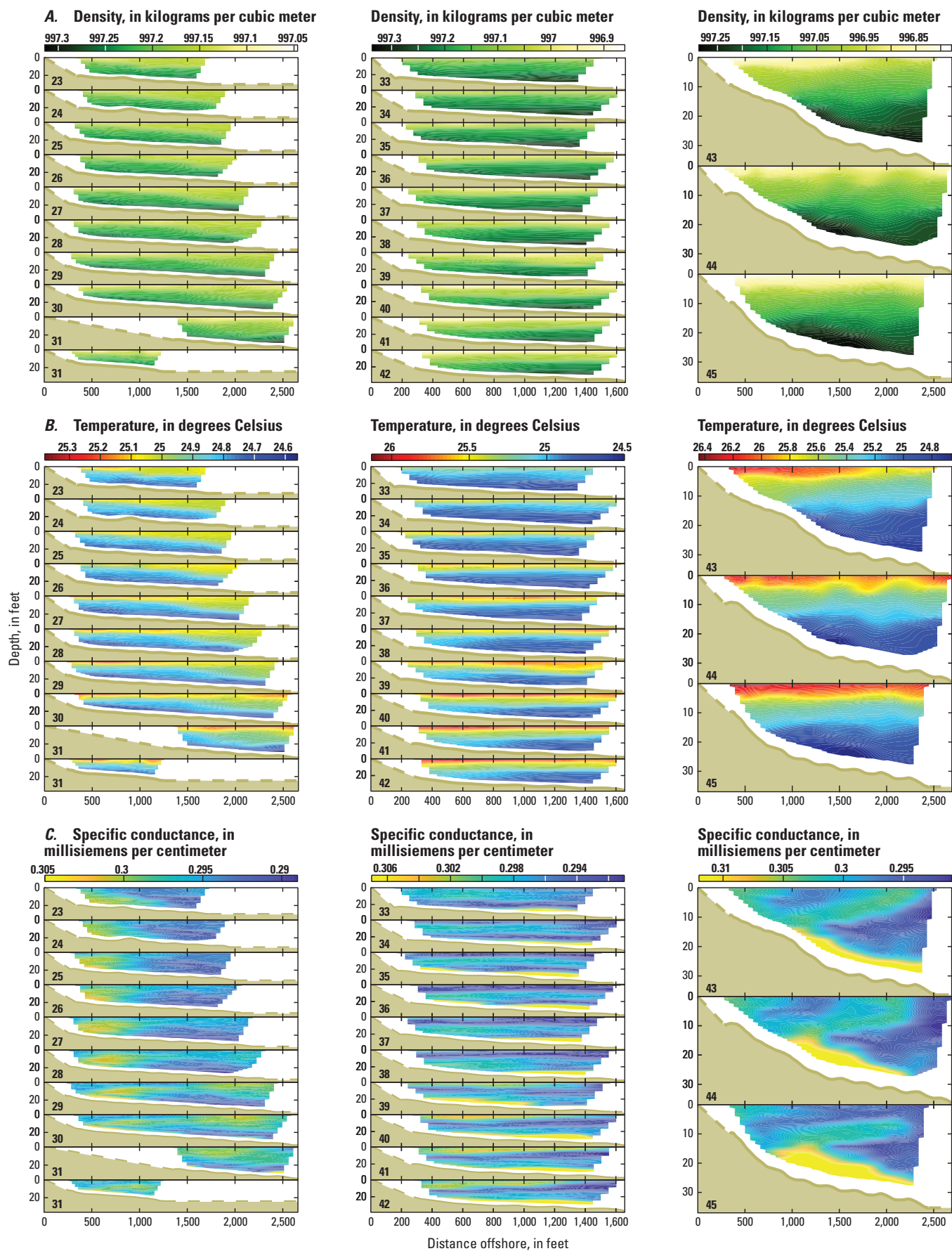


**Figure 42.** Cross sections of basic water-quality constituents: *A*, water density; *B*, water temperature; *C*, specific conductance; *D*, pH; and *E*, dissolved oxygen for 18 sections of coastal Lake Erie in the vicinity of Villa Angela Beach and Euclid Creek, Cleveland, Ohio, June 12, 2019.



**Figure 43.** Cross sections of basic water-quality constituents: *A*, water density; *B*, water temperature; *C*, specific conductance; *D*, pH; and *E*, dissolved oxygen for 18 sections of coastal Lake Erie in the vicinity of Villa Angela Beach and Euclid Creek, Cleveland, Ohio, August 19, 2019.





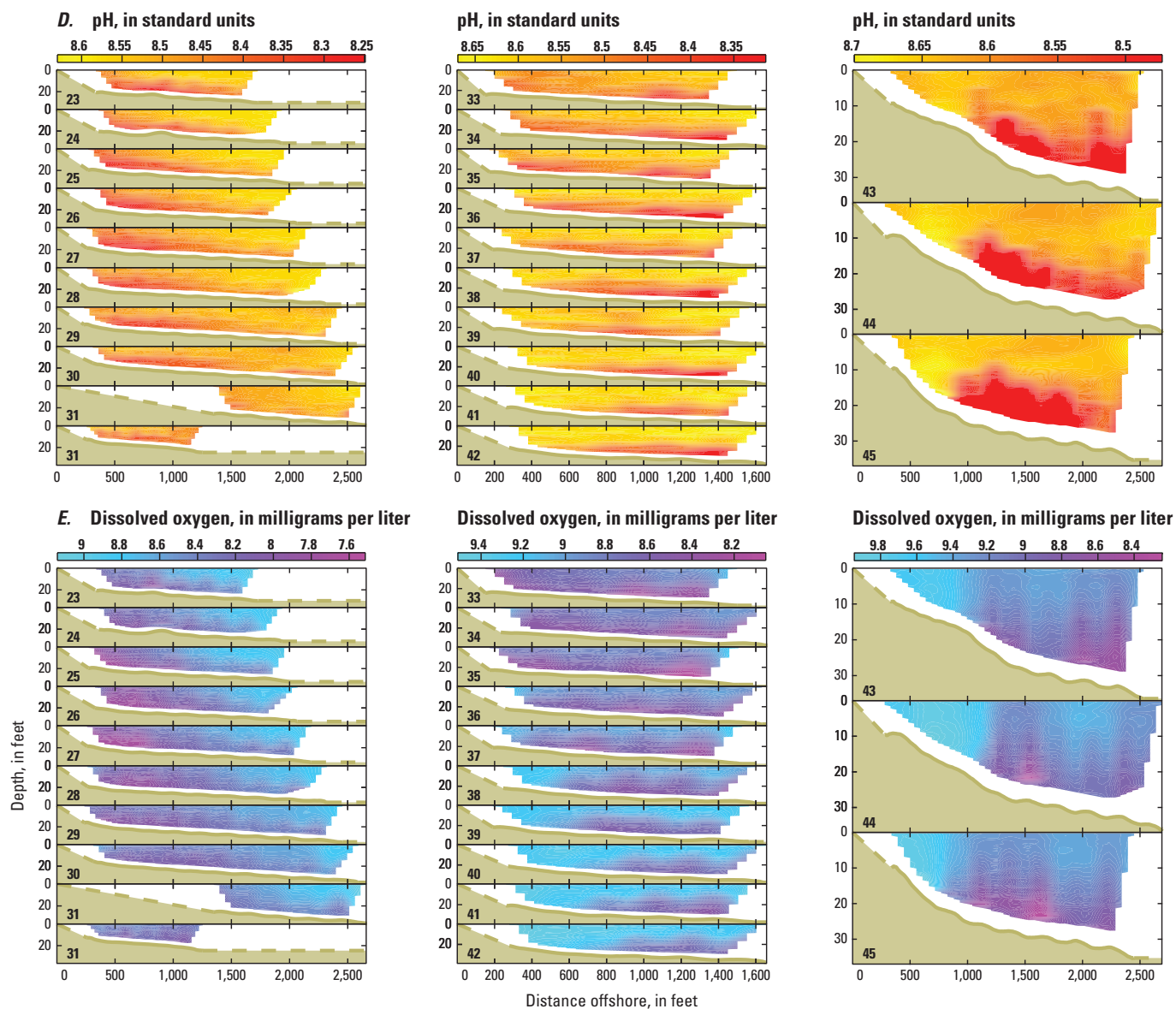


**Figure 44.** Cross sections of basic water-quality constituents: *A*, water density; *B*, water temperature; *C*, specific conductance; *D*, pH; and *E*, dissolved oxygen for 22 sections of coastal Lake Erie in the vicinity of the Easterly Wastewater Treatment Plant, Cleveland, Ohio, August 20, 2019.

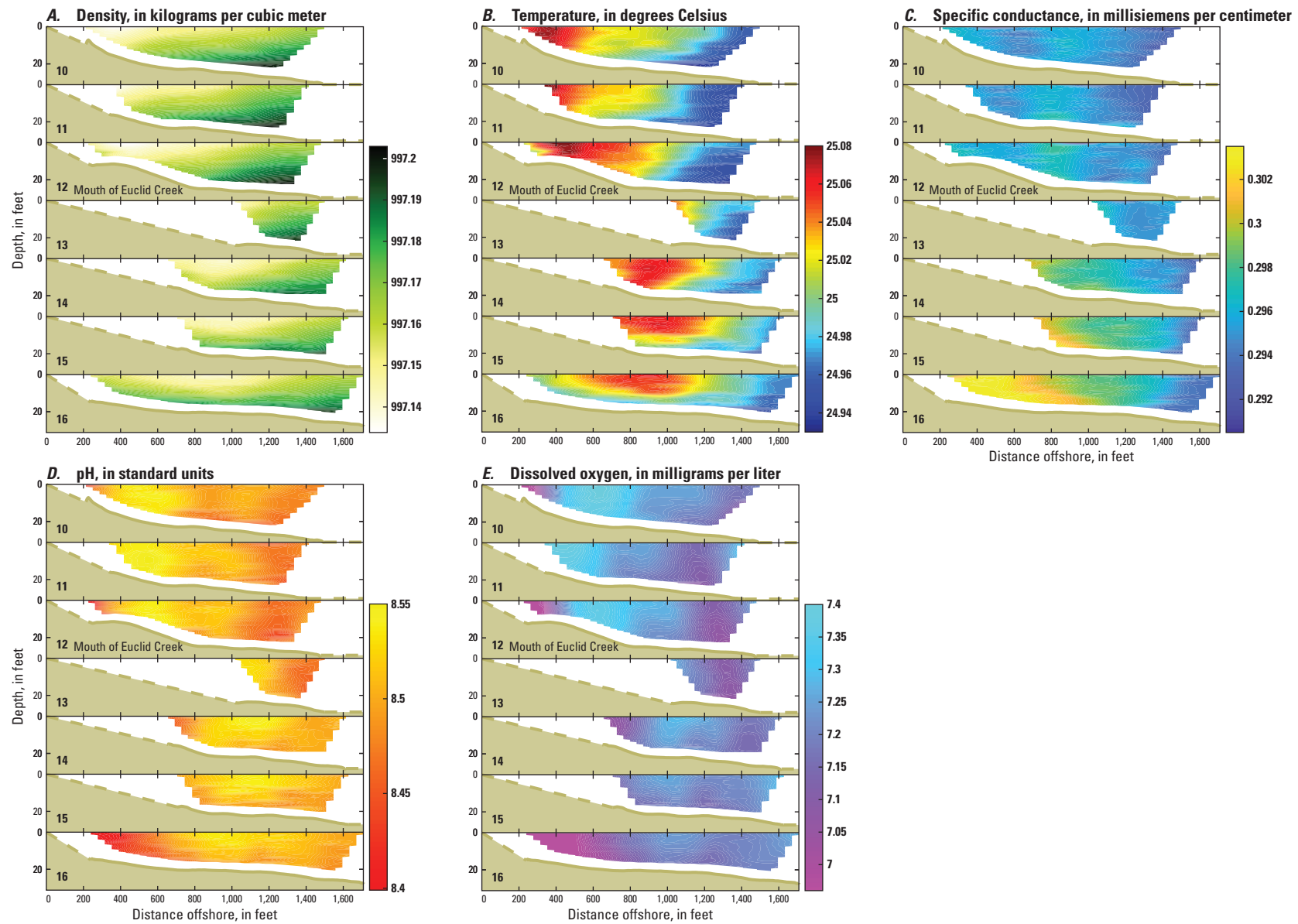


**Figure 45.** Cross sections of basic water-quality constituents: *A*, water density; *B*, water temperature; *C*, specific conductance; *D*, pH; and *E*, dissolved oxygen for 7 sections of coastal Lake Erie in the vicinity of Villa Angela Beach and Euclid Creek, Cleveland, Ohio, August 21, 2019.



AUV surveys revealed that this layer of elevated specific conductance tended to remain at or near the surface. The spatial extent of the elevated specific conductance plume on June 12 corresponds well with areas of warm, less dense water (fig. 42A–B).

On August 19, an area of elevated specific conductance water was within the piers around Euclid Creek and Wildwood Marina (figs. 30 and 37C). Because no undulating missions were done with the AUV within the pier structures, there are no data at depth there; however, it is interesting to note the area of elevated specific conductance along the lake bottom extending far offshore around lines 12 to 14 (fig. 43C). A possible explanation for this may once again be related to water temperature and density. As colder, denser water settles to the bottom of the marina, gravity drives density currents out into the lake along the sloped lake bottom.

On August 20, areas of elevated specific conductance water were primarily within the piers around the Easterly WWTP and to the southwest of the Easterly WWTP (figs. 31 and 38C). Because no undulating missions were done with the AUV within the pier structures, there are no data at depth there; however, it is interesting to note the area of elevated specific conductance along the lake bottom extending from nearshore to lakeward throughout most of the survey area but especially from lines 33 to 45 (fig. 44C). It is possible that any water coming from the Easterly WWTP could be transported along the slope of the lake bottom, possibly as a density current. This near-bottom elevated specific conductance water remains consistently distinct throughout the survey area indicating that there is little vertical mixing occurring. It is interesting to note that in the previous survey of this area on June 11, 2019, the plume of elevated specific conductance water was primarily near the water surface, and on August 20 the elevated specific conductance water was primarily near the lake bottom. Median near-surface water temperatures in Lake Erie were colder on June 11 (17.56 °C) compared to August 20 (25.78 °C), so if the water coming from the Easterly WWTP was between those two water temperatures, that may explain why the plume of elevated specific conductance water stayed near the water surface on June 11 and stayed near the lake bottom on August 20.

On August 21, an area of elevated specific conductance water was near the surface in nearshore Lake Erie around the mouth of Euclid Creek and continuing to the northeast of Wildwood Marina (figs. 32 and 39C). This area of elevated specific conductance was also visible in the cross-section plots from lines 15 to 16 (fig. 45C), and the AUV survey data revealed that the elevated specific conductance water tended to extend throughout the full depth but was more contained to the nearshore area.

## pH Distributions

The pH plan view plots for June 10–12, 2019, and August 19–21, 2019, show some patterns of pH distribution throughout the study area (figs. 34D–39D). The data were

categorized and colored the same way among plots based on their empirical distribution, with color breaks at the first quartile and the third quartile. In other words, the lowest 25 percent of the data are shown by red colors, the middle 50 percent of the data are shown by orange colors, and the highest 25 percent of the data are shown by yellow colors. In this way, attention is drawn to the areas of lower- or higher-than-typical pH. For the summer 2019 surveys, areas of lower pH tended to correspond with areas around the mouth of Euclid Creek, the nearshore area to the northeast of the Easterly WWTP, and for the June 2019 surveys in particular, the area around CSO locations 206 and 207. The overall range in pH values for the June 2019 and August 2019 surveys was 7.97–8.43 and 8.00–8.84 standard units, respectively. The lower end of the range in pH values is about the same for the June 2019 and August 2019 surveys, but the upper end of the range in pH values is higher for the August 2019 surveys. As noted by Jackson (2013), sunny days such as those during the August 2019 surveys promote photosynthesis in the nearshore aquatic vegetation and the plants produce oxygen and use up hydrogen molecules causing a rise in pH.

The pH cross-section plots for June 10–12, 2019, and August 19–21, 2019, are shown in similar colors but on a continuous colorbar (figs. 40D–45D). The overall change in pH throughout the depth in nearshore Lake Erie within the study area was 0.43 standard units during the June 2019 surveys and 0.37 standard units during the August 2019 surveys.

## Dissolved Oxygen Distributions

The dissolved oxygen plan view plots for June 10–12, 2019, and August 19–21, 2019, show some patterns of dissolved oxygen distribution throughout the study area (figs. 34E–39E). The data were categorized and colored the same way among plots based on their empirical distribution, with color breaks at the first quartile and the third quartile. In other words, the lowest 25 percent of the data are shown by pink colors, the middle 50 percent of the data are shown by blue colors, and the highest 25 percent of the data are shown by cyan colors. In this way, attention is drawn to the areas of lower- or higher-than-typical dissolved oxygen. For the summer 2019 surveys, areas of lower dissolved oxygen tended to correspond with areas around the mouth of Euclid Creek, the nearshore area to the northeast of the Easterly WWTP, and for the June 2019 surveys in particular, the area around CSO locations 206 and 207. The areas of lower dissolved oxygen were similar to the areas of lower pH. For the summer 2019 surveys, areas of higher dissolved oxygen tended to correspond with areas measured later in the day, and this may be related to the previous comment about algae and macrophytes in the aquatic environment. Sunny days promote photosynthesis in the nearshore aquatic vegetation and the plants produce oxygen thus increasing dissolved oxygen (Jackson, 2013). The overall range in dissolved oxygen values for the June 2019 and August 2019 surveys was 7.67–10.17 and 7.05–9.55 milligrams per liter, respectively. The June 2019 dissolved oxygen

values tended to be greater than the August 2019 dissolved oxygen values, and this may be because the water temperature was colder in June 2019 (cold water can hold more dissolved oxygen than warm water).

The dissolved oxygen cross-section plots for June 10–12, 2019, and August 19–21, 2019, are shown in similar colors but on a continuous colorbar (figs. 40E–45E). The overall change in dissolved oxygen throughout the depth in nearshore Lake Erie within the study area was 0.8 milligram per liter during the June 2019 surveys and 1.6 milligrams per liter during the August 2019 surveys.

## Turbidity Distributions

The turbidity plan view plots for June 10–12, 2019, and August 19–21, 2019, show nonuniform distributions of turbidity throughout the study area (figs. 34F–39F). Turbidity values were generally less than 10 nephelometric turbidity units. The data were categorized and colored the same way among plots based on their empirical distribution, with color breaks at the third quartile and the upper adjacent value. In other words, the lowest 75 percent of the data are shown by blue colors, the next highest 24 percent of the data (75–99 percent of data) are shown by yellow colors, and the highest 1 percent of the data are shown by brown colors. In this way, the brown areas clearly show where turbidity values are much more elevated than the rest of the lake. Turbidity tends to be a noisy constituent (surface sampling can introduce more noise in the optical probes because of air entrainment), and much spike removal (all readings above 30 nephelometric turbidity units) was needed during the postprocessing of the data, so interpretation is limited. The clearest observation is the area of high turbidity in the nearshore area on June 10 (fig. 34F). This directly corresponds with an observation during the survey of brownish-looking water around CSO location 207 (see fig. 1-3 in appendix 1). Another clear observation is the broader area of elevated turbidity in the nearshore area to the northeast of the Easterly WWTP on June 11 (fig. 35F), which corresponds to the recirculation zone that was present there (fig. 28). There are no turbidity cross-section plots because the turbidity port on the AUV was not operational.

## Summary

Villa Angela Beach, along the Lake Erie lakeshore in Cleveland, Ohio, is adjacent to the mouth of Euclid Creek, a small, flashy stream in which an average of 190 combined

sewer overflows (CSOs) have occurred per year in 2018–2019. Concerns about high concentrations of *Escherichia coli* (*E. coli*) in water samples collected along this beach and a high number of beach closures during the recreational season have led to synoptic sampling of the nearshore mixing zone in an attempt to gain insight into mixing processes, circulation, and potential for transport of CSO-related contaminants, such as bacteria, from nearby sources to the beach. Synoptic surveys of the nearshore mixing zone were completed on June 10–12, 2019, and August 19–21, 2019, by the U.S. Geological Survey. Sampling methods included deployment of an autonomous underwater vehicle (AUV) and use of a manned boat equipped with an acoustic Doppler current profiler and a multiparameter sonde to measure currents and basic water-quality distributions (temperature, specific conductance, pH, dissolved oxygen, and turbidity). Spatial distributions of specific conductance and nearshore currents indicate the mixing zones in the vicinity of Euclid Creek, Villa Angela Beach, and the Easterly Wastewater Treatment Plant (WWTP) are dynamic and highly variable but can exhibit large and persistent coherent structures, which is consistent with previous findings in a 2012 study.

A 2012 study notes that the observation of currents that are decoupled from local wind forcing (in the summer 2012 study) contradicts the observations from the 2011 study in which local currents appeared to be driven primarily by local winds. The summer 2019 study provided examples of both observations, which seems to confirm a conclusion in the 2012 study that large-scale circulation patterns within Lake Erie generated by regional wind patterns, inertial waves, and seiche activity, can, at times, oppose local wind patterns for at least a period of days. Therefore, any prediction of nearshore currents near Villa Angela Beach based on local wind observations should also take into account recent regional wind patterns and the associated large-scale circulation patterns within the entire Lake Erie Basin.

This study documented that the high specific conductance water of Euclid Creek relative to water of Lake Erie made it an excellent tracer for visualization of the transport and fate of Euclid Creek water in the nearshore environment. Although the water coming from the Easterly WWTP did not have nearly as high specific conductance values as Euclid Creek, the water coming from the Easterly WWTP was still able to be tracked in this same way. Other constituents such as temperature, pH, dissolved oxygen, and turbidity proved less useful for tracking Euclid Creek and Easterly WWTP water.

Observed circulation patterns from the summer 2019 surveys indicate that Euclid Creek water and water discharged from nearby CSO discharge points along the shoreline (and

the bacteria therein) interact with nearshore currents and shoreline structures. During the four synoptic surveys of the area around Euclid Creek and Villa Angela Beach on June 10 and 12, 2019, and August 19 and 21, 2019, longshore currents were of various strengths but were all in the northeasterly direction. As a result, different patterns of the transport and fate of Euclid Creek water (as traced by measurements of specific conductance) were observed, but none indicated that Euclid Creek water was reaching Villa Angela Beach except for close to the southwestern pier at the mouth of Euclid Creek. It is unfortunate that a persistent longshore current to the southwest did not occur during the 2019 surveys because in the previous 2012 study that was the condition that contributed to the recirculation zone off Villa Angela Beach that trapped contaminants in Euclid Creek water along the beachfront. Although it would have been informative to confirm the existence of and document a recirculation zone off Villa Angela Beach again, this study documents several different patterns of how Euclid Creek water moves to the northeast under certain conditions. Analysis of continuous current measurements near the Wildwood Marina entrance indicated that currents with a northeasterly longshore component occurred nearly 65 percent of the time during summer 2019, so it is not unlikely that all four of those days exhibited conditions with a longshore current to the northeast.

One of the observations from the 2012 study was that because currents with a northeasterly longshore component were dominant during summer 2012 (and also during summer 2019), a mechanism exists for longshore transport of bacteria to Villa Angela Beach from sources to the southwest including effluent from the Easterly WWTP and lakefront CSO discharge points. Although elevated specific conductance water was observed on most of the survey days that were likely from these sources, none of the elevated specific conductance water was observed along Villa Angela Beach. Additionally, observations from the summer 2019 surveys indicated that the discharge from the lakefront CSO discharge points either remained localized around the CSO location or were transported to the southwest by currents. Unfortunately, there were not strong currents to the northeast around the lakefront CSO discharge points during a discharge event to observe what would happen. Although the longshore currents to the northeast did not create a recirculation zone off Villa Angela Beach, the water inside the breakwaters is generally calm and there are gaps between the breakwaters, so it is unclear how contaminated water may enter or exit the protected Villa Angela Beach area when currents are to the northeast. Therefore, the lakefront CSO locations are still a potential source of bacteria to Villa Angela Beach.

Observed circulation patterns from the summer 2019 surveys indicate that Easterly WWTP water and water discharged from nearby CSO discharge points along the WWTP, and the bacteria therein, also interact with nearshore currents and shoreline structures. During the two synoptic surveys of the area around the Easterly WWTP on June 11, 2019, and August 20, 2019, longshore currents varied in magnitude throughout each day and were observed in both directions (to the northeast on June 11 and to the southwest on August 20). As a result, different patterns of the transport and fate of Easterly WWTP water (as traced by measurements of specific conductance) were observed. A large recirculation zone was observed to the northeast of the WWTP on June 11 and the nearshore area exhibited elevated specific conductance water. The plume appeared to disperse in the northeast direction, and the extent of the recirculation zone and the plume appear to be near the edge of the survey extent, which was about halfway between the Easterly WWTP and Villa Angela Beach. Consequently, it seems unlikely that water from the Easterly WWTP was being transported to Villa Angela Beach that day. The area of elevated specific conductance water observed offshore at the southwest survey extent during the next day's survey on June 12 may be the remainder or the farthest extent of the plume from the previous day, which again is still far removed from Villa Angela Beach. However, this observation indicates the mechanism for transport does exist and farther transport may be possible with stronger longshore currents. The primary area that exhibited elevated specific conductance water on August 20 was the nearshore area to the southwest of the WWTP. This is an area of private beaches, and a few recreational boaters were observed in the area. The elevated specific conductance water tended to be near the surface on June 11 and near the lake bottom on August 20, which may be because of water temperature and density differences.

This study provides data to help improve the understanding of flow dynamics and water quality in and around Euclid Creek, Villa Angela Beach, and the Easterly WWTP. The data collected in this study can be used by the Northeast Ohio Regional Sewer District to reevaluate potential sources and transport of *E. coli* near Villa Angela Beach. Additional monitoring would be beneficial for continued understanding of circulation, mixing, and transport in nearshore Lake Erie in the vicinity of Villa Angela Beach, particularly adding a second boat to get a more instantaneous snapshot of conditions (reducing the temporal changes because of changing environmental conditions), synoptic surveys targeted during specific wind and current conditions of interest, and continuous monitoring of specific conductance and other water-quality constituents at discrete points along Villa Angela Beach.



## References Cited

- Boldt, J.A., 2021, Velocity surveys and three-dimensional point measurements of basic water-quality constituents in nearshore Lake Erie in the vicinity of Villa Angela Beach and Euclid Creek, Cleveland, Ohio, June 10–12, 2019, and August 19–21, 2019: U.S. Geological Survey data release, <https://doi.org/10.5066/P963OH6M>.
- Bushon, R.N., Stelzer, E.A., and Stoeckel, D.M., 2009, Results from a microbial source-tracking study at Villa Angela Beach, Cleveland, Ohio, 2007: U.S. Geological Survey Open-File Report 2009–1160, 9 p., <https://doi.org/10.3133/ofr20091160>.
- Environmental Systems Research Institute, 2020, ArcGIS: Esri, Inc., software release, accessed August 2021, at <https://www.esri.com/en-us/arcgis/about-arcgis/overview>.
- Gibs, J., Wilde, F.D., and Heckathorn, H.A., 2012, Use of multiparameter instruments for routine field measurements: U.S. Geological Survey Techniques of Water-Resources Investigations, book 9, chap. A6, <https://doi.org/10.3133/twri09A6.8>.
- HYPACK, Inc., 2019, HYPACK hydrographic survey software user manual: HYPACK, Inc., software release, accessed March 2020, at <https://www.hypack.com/File%20Library/Resource%20Library/Manuals/2019/2019-HYPACK-User-Manual.pdf>.
- Jackson, P.R., 2013, Circulation, mixing, and transport in nearshore Lake Erie in the vicinity of Villa Angela Beach and Euclid Creek, Cleveland, Ohio, September 11–12, 2012: U.S. Geological Survey Scientific Investigations Report 2013–5198, 34 p., <https://doi.org/10.3133/sir20135198>.
- Jackson, P.R., and Reneau, P.C., 2014, Integrated synoptic surveys of the hydrodynamics and water-quality distributions in two Lake Michigan river mouth mixing zones using an autonomous underwater vehicle and a manned boat: U.S. Geological Survey Scientific Investigations Report 2014–5043, 33 p., <https://doi.org/10.3133/sir20145043>.
- Lalor, M., and Pitt, R., 1999, Use of tracers to identify sources of contamination in dry weather flow: Watershed Protection Techniques, v. 3, no. 1, p. 585–592.
- Mueller, D.S., Wagner, C.R., Rehmel, M.S., Oberg, K.A., and Rainville, F., 2013, Measuring discharge with acoustic Doppler current profilers from a moving boat (ver. 2.0, December 2013): U.S. Geological Survey Techniques and Methods, book 3, chap. A22, 95 p., <https://doi.org/10.3133/tm3A22>.
- Ohio Department of Health, 2021, Bathing beach monitoring: Ohio Department of Health webpage, accessed March 12, 2021, at <https://odh.ohio.gov/wps/portal/gov/odh/know-our-programs/bathing-beach-monitoring>.
- Parsons, D.R., Jackson, P.R., Czuba, J.A., Engel, F.L., Rhoads, B.L., Oberg, K.A., Best, J.L., Mueller, D.S., Johnson, K.K., and Riley, J.D., 2013, Velocity Mapping Toolbox (VMT)—A processing and visualization suite for moving-vessel ADCP measurements: Earth Surface Processes and Landforms, v. 38, no. 11, p. 1244–1260 [<https://doi.org/10.1002/esp.3367>].
- Platzman, G.W., and Rao, D.B., 1964, Spectra of Lake Erie water levels: Journal of Geophysical Research, v. 69, no. 12, p. 2525–2535.
- Rao, Y.R., and Schwab, D.J., 2007, Transport and mixing between the coastal and offshore waters in the Great Lakes, a review: Journal of Great Lakes Research, v. 33, no. 1, p. 202–218 [[https://doi.org/10.3394/0380-1330\(2007\)33\[202:TAMBTC\]2.0.CO;2](https://doi.org/10.3394/0380-1330(2007)33[202:TAMBTC]2.0.CO;2)].
- U.S. Geological Survey, 2020, USGS 04208700 Euclid Creek at Cleveland, OH, in USGS water data for the Nation: U.S. Geological Survey National Water Information System database, accessed August 2020, at <https://doi.org/10.5066/F7P55KJN>. [Site information directly accessible at [https://waterdata.usgs.gov/nwis/inventory/?site\\_no=04208700](https://waterdata.usgs.gov/nwis/inventory/?site_no=04208700)].

## Appendix 1. Supplemental Photographs

---

During the synoptic surveys, visibly discolored water was often observed near the mouth of Euclid Creek and combined sewer overflow discharge points. Photographs were taken to document these observations ([figs. 1-1-1-8](#)). The discolored water was usually a brownish color compared to the surrounding Lake Erie water.



**Figure 1-1.** Discolored water inside the breakwaters along Villa Angela Beach on June 10, 2019, at 13:48 Eastern Daylight Time. Photograph by Justin Boldt, U.S. Geological Survey.





**Figure 1-2.** Discolored water inside the breakwaters along Villa Angela Beach on June 10, 2019, at 13:48 Eastern Daylight Time. Photograph by Justin Boldt, U.S. Geological Survey.



**Figure 1-3.** Discolored water around combined sewer overflow location 207 on June 10, 2019, at 15:01 Eastern Daylight Time. Photograph by Justin Boldt, U.S. Geological Survey.





**Figure 1-4.** Discolored water inside the lagoon at the Easterly Wastewater Treatment Plant on June 11, 2019, at 14:07 Eastern Daylight Time. Photograph by Justin Boldt, U.S. Geological Survey.





**Figure 1-5.** Discolored water around combined sewer overflow location 206 on June 12, 2019, at 09:46 Eastern Daylight Time. Photograph by Justin Boldt, U.S. Geological Survey.



**Figure 1-6.** Discolored water near the mouth of Euclid Creek on June 12, 2019, at 12:48 Eastern Daylight Time. Photograph by Justin Boldt, U.S. Geological Survey.





**Figure 1-7.** Discolored water near the mouth of Euclid Creek on June 12, 2019, at 12:49 Eastern Daylight Time. Photograph by Justin Boldt, U.S. Geological Survey.





**Figure 1-8.** Discolored water near the mouth of Euclid Creek on June 12, 2019, at 13:07 Eastern Daylight Time. Photograph by Justin Boldt, U.S. Geological Survey.



For additional information contact:

[Director](#), USGS Ohio-Kentucky-Indiana Water Science Center  
U.S. Geological Survey  
9818 Bluegrass Parkway  
Louisville, KY 40299  
502-493-1900

For additional information, visit:  
<https://www.usgs.gov/centers/oki-water>



